VŠB – Technical University of Ostrava
Faculty of Mechanical Engineering
Department of Applied Mechanics

Modeling of Mechanical Tests on Composite Specimens Produced By 3D Printing

Modelování mechanických zkoušek na kompozitních vzorcích vyrobených 3D tiskem

Student: **JOYSON SAM DEVAPAUL PENIEL PAULDOSS**
Personal number: **PEN0055**
Supervisor: **prof. Ing. RADIM HALAMA, Ph.D.**

Ostrava, 2021

VSB – Technical University of Ostrava
Faculty of Mechanical Engineering
Department of Applied Mechanics

Diploma Thesis Assignment

Student: **Joyson Sam Devapaul Peniel Pauldoss**

Study Programme: N2301 Mechanical Engineering

Study Branch: 3901T003 Applied Mechanics

Title: Modeling of Mechanical Tests on Composite Specimens Produced by 3D Printing
Modelování mechanických zkoušek na kompozitních vzorcích vyrobených 3D tiskem

The thesis language: English

Description:

1) Literature survey - testing/modeling of Onyx with Carbon Fibers
2) Design of specimens
3) Experiments realization
4) FE modeling
5) Discussion and conclusions

References:

Rajkumar Arokiaraj James Akshay Nicholas, Investigation of stress-strain behaviour in ONYX material and its modelling. Ostrava: VŠB Technical University of Ostrava, Faculty of Mechanical Engineering, Department of Applied Mechanics, 2020, (57) p. Supervisor: prof. Ing. Radim Halama, Ph.D.
L. G. Blok, M. L. Longana, H. Yu, B. K. S. Woods. An investigation into 3D printing of fibre reinforced thermoplastic composites, Additive Manufacturing 22, 176 (2018). DOI: https://doi.org/10.1016/j.addma.2018.04.039.
Markforged. https://markforged.com/x7/. [Online]

Extent and terms of a thesis are specified in directions for its elaboration that are opened to the public on the web sites of the faculty.

Supervisor: **prof. Ing. Radim Halama, Ph.D.**

Date of issue: 18.12.2020

Date of submission: 17.05.2021

doc. Ing. Martin Fusek, Ph.D.
Head of Department

prof. Ing. Robert Čep, Ph.D.
Dean

Student’s affidavit

I declare that I have prepared the whole diploma thesis including appendices independently under the leadership of the diploma thesis supervisor, and I stated all the documents and literature used.

In Ostrava on May 17, 2021.

……………………………………………..

Signature of Student

I declare that:

- I am aware that Act No. 121/2000 Coll, Act on copyright, rights related to copyright and amending some laws (the copyright Act), in particular, section 35(Use of a work in the civil or religious ceremonies or official events organized by public authorities, in the context of university performance and use of university work) and Section 60(university work) shall apply to my final Diploma thesis
- I understand that VŠB- Technical University of Ostrava (hereinafter referred to as "VŠBTUO") has the right to use this final Diploma thesis non-commercially for its internal use (Section 35 Subsection 3 of the Copyright Act)
- If requested, a copy of this Diploma thesis will be deposited with the thesis supervisor,
- If VŠB-TUO is interested, I will make a licensing agreement with it permitting to use the thesis within the scope of Section 12 Subsection 4 of the Copyright Act,
- I can only use my thesis, or grant a license to use it with the consent of VŠB-TUO, which is authorized in such a case to demand an appropriate contribution to the costs that were incurred by VŠB-TUO to create the thesis (up to the actual amount),
- I understand that - according to Act No. 111/1998 Coll., on higher education institutions and changes and amendments to other acts (Higher Education Act), as amended - that this Diploma thesis will be available for the public before the defense at the thesis supervisor's workplace, and electronically stored and published after the defense at the Central Library of VŠB-TUO, regardless of the outcome of its defense.

In Ostrava on May 17, 2021.

P. Joyson

…………………………………………..

Signature of Author

Name and surname of the thesis author: Joyson Sam Devapaul Peniel Pauldoss,

Permanent address of the thesis author: Tuticorin, Tamil Nadu, India.

ANNOTATION OF MASTER THESIS

Joyson Sam Devapaul Peniel Pauldoss, Modeling of Mechanical Tests on Composite Specimens Produced By 3d Printing. Ostrava: VŠB - Technical University of Ostrava, Faculty of Mechanical Engineering, Department of Applied Mechanics, 2021, 68 p. Supervisor: Prof. Ing. Radim Halama, Ph.D.

ANOTACE DIPLOMOVÉ PRÁCE

Joyson Sam Devapaul Peniel Pauldoss, Modelování mechanických zkoušek na kompozitních vzorcích vyrobených 3D tiskem. Ostrava: VŠB-Technická univerzita Ostrava, Fakulta strojní, Katedra aplikované mechaniky, 2021, 68 p. Supervisor: Prof. Ing. Radim Halama, Ph.D.

ABSTRACT

The thesis is focused on the modelling of mechanical tests on a composite specimen produced by 3D printing. The experimental, numerical and analytical techniques were utilized to compare the different composite specimens with different volumetric fractions of Carbon fiber filaments. The reinforcement by long fibers is provided to the ONYX matrix by layer-by-layer diffusion. This study contains the investigation of three separate specimen design i.e., - Rectangular specimen with longitudinal loading, transversal loading and the testing specimen with two contour lines of carbon fibers loaded in tensile, shear and combined modes. All these tests were performed under room temperature and uniaxial testing was done under strain-controlled loading. These tests are very useful to determine the reliability of the composite materials, especially produced by 3D printing. The numerical simulations were performed under consideration of reduced geometry with symmetrical consideration and with a suitable choice of finite elements. This study allows to predict the stiffness of elastic structure of the composite with carbon fibers. A proper filament orientation and density can be obtained by the proposed methodology.

Keywords: Additive manufacturing, composites, carbon fibers, MKP, FEM.

ABSTRAKT

Diplomová práce je zaměřena na modelování mechanických zkoušek na kompozitním vzorku vyrobeném 3D tiskem. Experimentální, numerické a analytické metody byly využity k porovnání různých kompozitních vzorků s různými objemovými frakcemi uhlíkových vláken. Výztuž dlouhými vlákny je pro matrici ONYX realizována difúzí vrstvu po vrstvě. Tato studie obsahuje vyšetřování tří samostatných návrhů vzorků, tj. obdélníkového vzorku s podélným zatížením, příčným zatížením a zkušebním vzorkem s dvěma konturami karbonových vláken namáhaný tahem, smykem a kombinací. Všechny tyto testy byly prováděny při pokojové teplotě a v deformačním režimu řízení. Tyto testy jsou velmi užitečné pro zjištění spolehlivosti kompozitních materiálů, zejména vyrobených 3D tiskem. Numerické simulace byly provedeny s využitím redukované geometrie uvažováním symetrie a také s využitím vhodných konečných prvků. Tato studie umožňuje predikci tuhosti elastických struktur kompozitu s dlouhými karbonovými vlákny. Navržená metodika vede k nalezení vhodné orientace a hustoty výztuže.

Klíčová slova: Aditivní výroba, kompozity, karbonová vlákna, MKP, FEM.

LIST OF CONTENTS

LIST OF FIGURES

LIST OF TABLES

LIST OF SYMBOLS

SYMBOL	DESCRIPTION	UNITS
t	Time	s
E	Young's Modulus	MPa
σ	Stress	MPa
ε	Strain	-
σ_{y}	Yield limit	MPa
μ	Poisson's ratio	-
V_F	Volumetric Fraction	%
δ	Deflection	mm
F	Force	N
σ_{ult}	Ultimate stress	MPa
ε_{ult}	Ultimate Strain	-
σ_C	Stress acting on Composite material	MPa
σ_M	Stress acting on Onyx Layer	MPa
σ_F	Stress acting on CF Filament	MPa
E_C	Young's Modulus on Composite material	MPa
E_M	Young's Modulus on Onyx Layer	MPa
E_F	Young's Modulus on CF Filament	MPa
ε_C	Strain acting on Composite material	-
ε_M	Strain acting on Onyx Layer	-
ε_F	Strain acting on CF Filament	-
F_C	Force acting on Composite material	N
F_M	Force acting on Matrix (Onyx)	N
F_F	Force acting on CF Filament (fiber)	N
v_F	Volume of fibers	mm^3
v_C	Volume of whole composite	mm^3

1 INTRODUCTION

Mechanical testing is the approach used to carry out the testing of several materials to determine the material response due to the externally applied load factors, internal reactions and also to investigate the properties of the materials. Nowadays, the testing is conducted particularly in composite materials as those materials are replacing the natural metallic materials with its better performance, mechanical properties, and its less weight. The composite materials are made up of at least two or more visually separable different materials which are having different microscopic structure and different physical or chemical properties. The goal of the modelling of a composite material is to obtain a more desirable combination of properties by the principle of combined action. There are various types of composite materials based on engineering applications. The Composite Materials are playing a significant role in Aerospace Industry for several reasons.

The composite materials are having mechanical properties which depend on the volumetric fraction of the fiber. The anisotropic property will cause the composite materials to behave strangely to that of the different orientation of fiber and matrix. Most of the composites are man-made and have multiple phases. The Continuous Fiber Reinforced polymer is having the ability to increase the strength of the composites compared to other fibers. The carbon fiber reinforced Nylon filament (35% CF & rest PA6) provides heat resistance and has adhesive property between the layers and has good stiffness. The polyamide (PA6) is having the moisture absorbing ability.

Based on the requirement of materials with different properties under different conditions, the 3D printed composite materials are going to be analyzed and optimized to deliver the mechanical properties and functionalities under different combinations and proportions. It will create a detailed idea about the behavior of the composite materials. Additive Manufacturing (AM) is an alternative approach to that traditional approach which minimizes the labor cast and reduces the tooling and fixture needs. The technical advancement which utilizes the conversion of analogue to digital processing in industrial manufacturing creates the possibility of making use of CAD models or 3D scanned object with further improvisation in their geometry to manufacture the required parts even with complicated geometries. The design is then transferred to the hardware and then the material is getting deposited layer by layer based on the specifications. The layers are fused to form a solid object based on the geometrical aspects. Markforged x7 3D printer is having two nozzles and it increases the stability of the object pointed by it. The advantage is that the fiber is printed without discontinuation. The surface finish is high when printing the Onyx with Markforged x7 3D printer. The Eiger software is used to specify the interior section of the design along with the application of supports. As the Onyx is made up of chopped carbon fiber and nylon, it gives more stiffness when fused with other high strength fiber like carbon fiber to achieve more strength to the composite. The combination of Onyx and carbon fiber reinforced matrix materials printed by Markforged printers provide interesting results if there are tested with different orientation of fibers and with a different volumetric fraction of carbon fiber.

The mechanical properties are influenced by the orientation of the fiber and the concentration of the fiber. Tensile tests are carried out to determine the deviation in the stress-strain curve which directly depicts the durability, strength, and toughness of the composites. The fatigue test under constant loading, i.e., constant strain rate, will provide valid information regarding the fatigue life of the composites. The shear testing is used to find the in-plane stress and strain of the composites and the notch effect. V notch rails are used for shear testing to perform tensile, shear and combined loading.

The study deals with the modelling of the tested composite specimen based on the standards along with the creation of a file and implements it in the 3D printing by Markforged X7 printer to create the specimen by the utilization of Eiger software to set up the orientation and internal specification of the composite specimen. The mechanical testing results and various properties for the set of specimens are produced by 3D printer and the comparisons are done utilizing the experimental, numerical and analytical determination to determine the behavior under proportional loading conditions. The motivation of this study is to introduce numerical simulations and analytical methods and compare the experimental results for composite material with ONYX and different volumetric fraction of CF filaments. The whole testing is done under strain-controlled process. The specimen used are rectangular specimen with transversal (loading in the perpendicular direction of continuous fiber), the longitudinal loading (loading in the perpendicular direction of continuous fiber) of fibers and also shear testing specimen with tensile, shear and combined loading of fiber in the direction of concentric fills of fiber near the edges of the material. The ultimate aim is to test the tensile strength and stiffness of the composite with different VF of Carbon fiber to evaluate the response of the material and also the shear, combined and tensile load influence on the stiffness of the shear testing specimen.

2 DESCRIPTION OF TECHNOLOGY

2.1 MODELLING

Manual drafting is replaced by Computer-Aided Design (CAD). It will help us to visualize the 3D model graphically and it is having user-friendly options to design whatever object based on the idea of thinking. The vector-based graphics are used to create the object and the shape. The dimension, tolerance and the definition of the material of the model can be depicted. It creates the ability to do calculations to solve problems in the engineering environment. The advanced level of 3D visualization and rendering techniques make the CAD more effective. Even the simulation and visualization of the animation of the calculation with various material assignments can be also possible nowadays in CAD commercial software, which makes the software more interesting.

On the other hand, the CAD files and models are used to simulate and visualize the static, dynamic characteristics and other mechanical problems of the system with the algorithm of using energy equations and partial derivatives. The quality of the design is kept on increasing day by day due to engineering development and optimized techniques. Computer-Aided Three-Dimensional Interactive Application (CATIA) developed by Dassault System is used here to design the specimen and it is saved as an STP file. The STP file is then imported to the Eiger software. Eiger software can be helpful to 3D print any part based on their needs.

2.2 3D SCANNING

The 3D printer needs the CAD file to process the data to do the printing of the object based on the geometry and tolerance limits. However, in some cases, it is hard to design some complicated geometries or else in some cases where the modifications have to be done, particularly in the domain of the object. Thus, in these cases, the actual creation of CAD design will not be a suitable way of approach. 3D scanners can minimize this kind of tasks. It can analyze the object and collects the data based on the reference of the object. 3D scanning is also used in reverse engineering applications to modify particular specifications. The Figure 1 shows how the scanning is performed in ice hockey stick and how the visualization of the part is done to help the creation of CAD design which will be useful for reverse engineering and optimization.

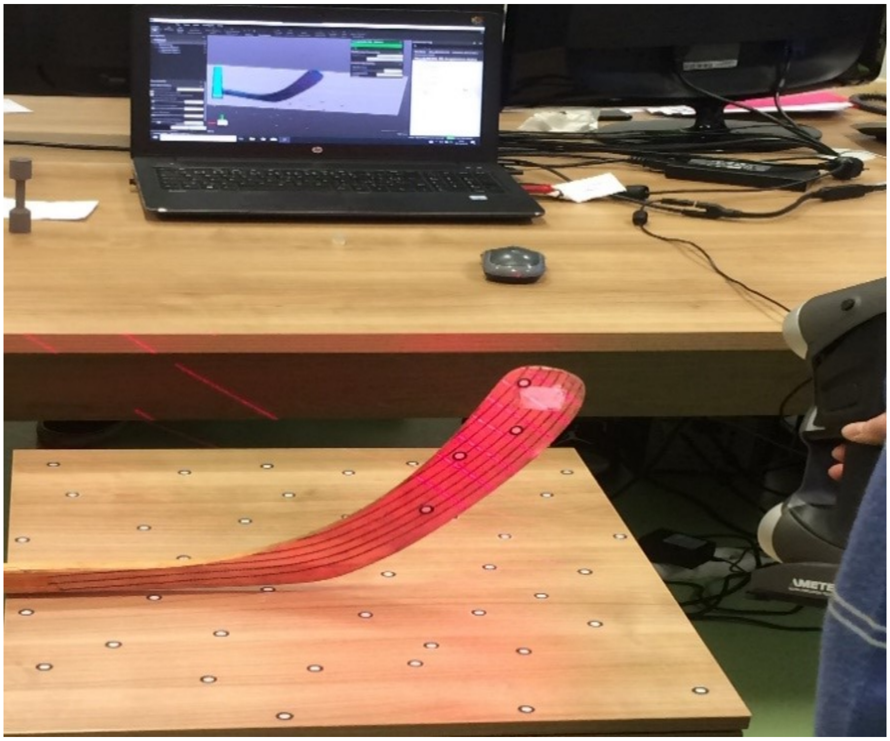

Figure 1: 3D Scanning of Ice Hockey Stick

The 3D printer slicer software (Eiger) also utilizes the STL file of the 3D scanning technique to implement corrections and print. However, the scanning has to be done several times to get the precise shape and angle of the exact object. The scanned images are integrated by fixing the common reference and merged.

2.3 3D PRINTING

The additive manufacturing technique and the rapid prototyping makes the 3D printing a more significant method in the production. Additive manufacturing is the layer-by-layer fusion of one or more materials to form a material with different composition to achieve the relevant mechanical and chemical properties based on the requirement and customer needs. Even more complicated geometries can be produced by 3D printer easily, which is a very tedious process when it is machined by conventional methods. The cost of the printer is getting minimized in recent years is an advantage of this technique in future considerations. The Figure 2 shows the systematic function of the additive manufacturing technique particularly for fiber reinforced composites.

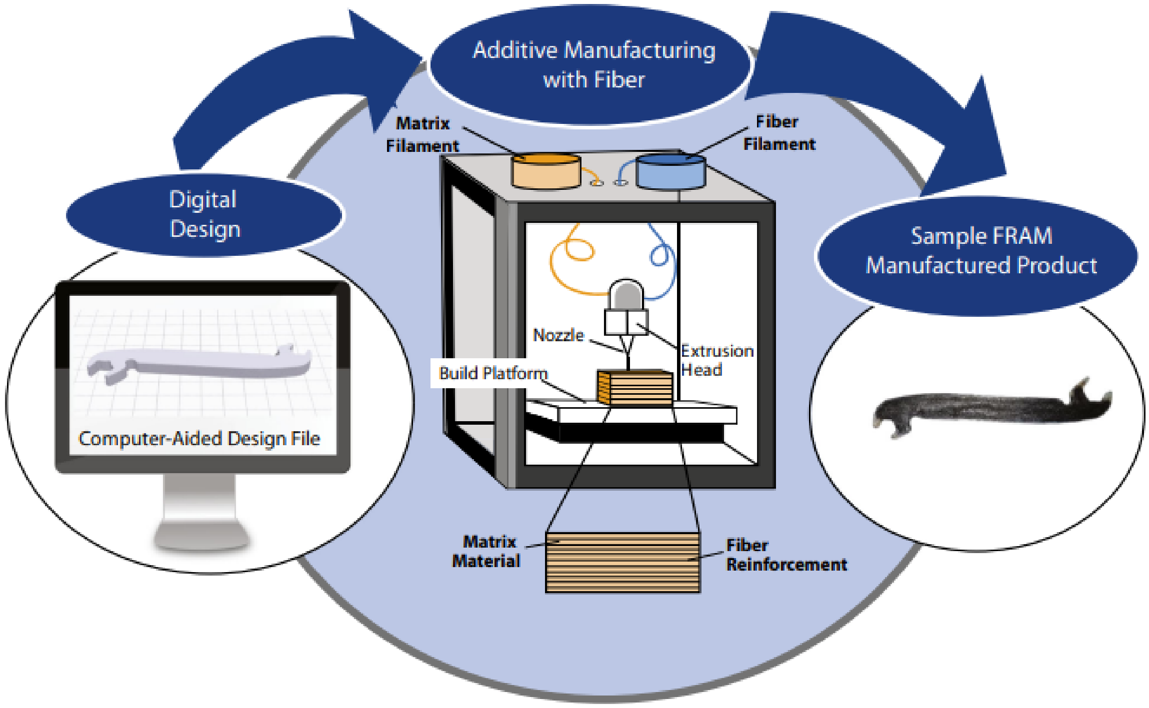

Figure 2: Additive Manufacturing Layout of FRAM [7]

Fiber Reinforced Additive Manufacturing (FRAM) is the method of printing composite materials by fusion of polymer, i.e., Nylon as a matrix along with the fibers. In this case, the material property is influenced by the orientation, density and type of fiber. It utilizes the CAD model to create G codes to print layer by layer. The advantage is that the composite material along with AM techniques can be most useful to create complicated geometries with different material combinations and properties [7].

Fusion Deposition Modelling (FDM) techniques are mostly used in thermoplastics. The products are very strong, stabilized and high durable products. This technique was proposed by Stratasys and his company is leading the field with its tremendous improvement and inventions. As this technique is not too complicated and the process of production is clean, it can be used in the office environment and easy to handle. The supports used in this printing process can be easily removed and it can be helpful to print more complicated parts without any complications. This technique can produce the product comparably stronger in comparison with other production techniques like molding, forming etc.

The Figure 3 shows the mechanism behind the fusion of filaments and the thermocouple principle. It uses the material extrusion technique to print the filament using rollers, gears, and stepper motors. The gears and rollers are the mechanical systems used to pull the filament from the spool which is at the cold end. The stepper motor is used to feed the filament at a constant rate. The heating chamber and the nozzle are situated in the hot end. The hot end is maintained by the thermo-coupling reaction. The filament then gets melted due to the pressure when it is fed into the hot chamber and gets liquified to pass through the nozzle. Every filament will be having different viscous properties and based on that property the feed rate is maintained by the force-controlled process. The liquified thin layer of plastic gets deposited on the already printed layer by the adhesive property. There are various types of printers used in recent times [1].

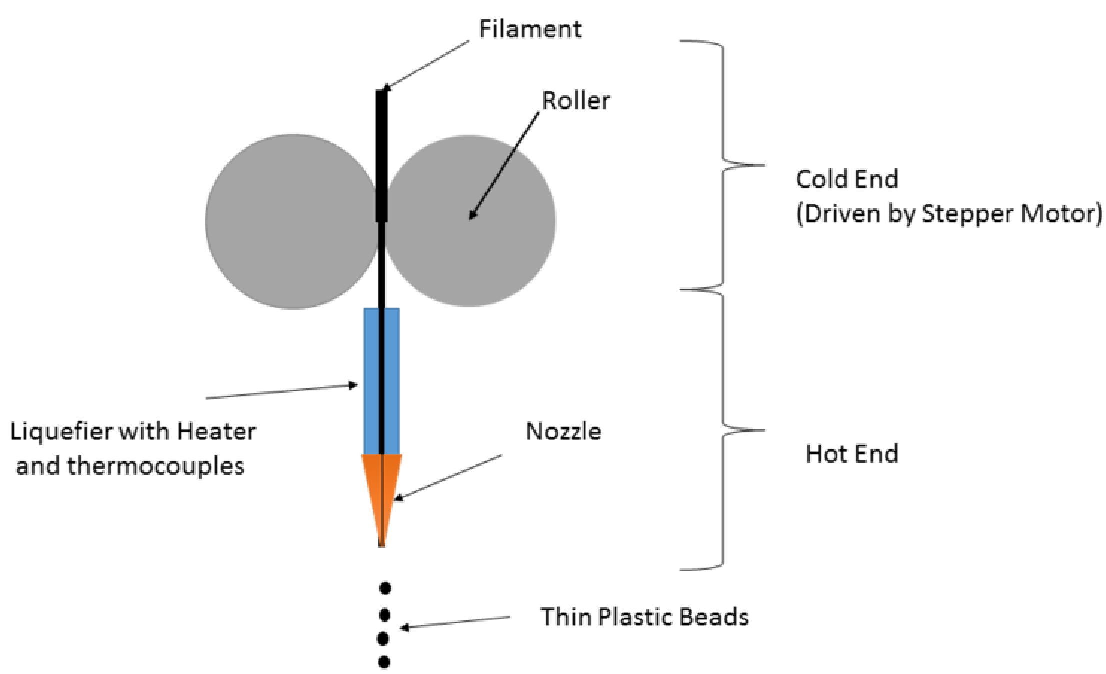

Figure 3: 3D Printer Extruder-FDM Technique [1]

2.3.1 MARKFORGED X7 PRINTER

Markforged x7 printer is the latest version 3D printer. The advantage of using the Markforged x7 printer in composite material manufacturing is that the dual nozzle system can utilize different nozzles for printing the Onyx and carbon fiber, and it helps the printing materials to increase its strength by introducing continuous fibers. The components present in this printer are demonstrated in the Figure *4*.

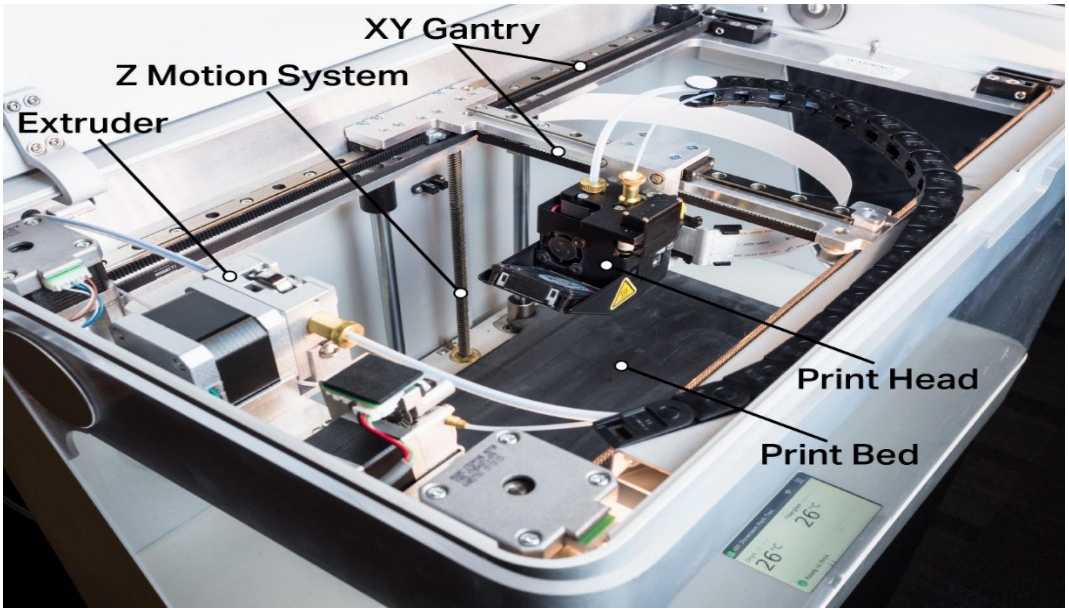

Figure 4: Markforged x7 printer interior parts [2]

The components are as follows:

- The printer head is responsible for the thermal coupling reaction to heat up the filament. Then the filament gets melted to form a molten state.
- The print bed is the place where the object is getting printed layer by layer to hold the final object.
- Z motion system moves and places the print bed to the position according to the nozzle based on the orientation of the print which will be programmed.
- The extrusion system will be having a servo motor to control the feed rate based on the individual fiber properties.
- XY Gantry motion system controls the movement of the print head based on x and y direction as the movement in the z-direction is controlled by the Z motion system [2].

The interesting thing about the Markforged x7 printer is that the layer height of 0.05mm can be printed. The volume is high compared to the previous version as this printer can print more mechatronic components. This printer can be easily controlled by LAN cable and USB devices.

2.3.2 EIGER SOFTWARE

In Markforged printers, the controlling of the motion of the tool and the extrusion part is carried out by Eiger Software. In the composite material manufacturing process, the slicing of the design is done by this software to define the material and its composition. This software is having the advantage that the CAD files can be stored in the cloud and the software can be used in the website platform by simply browsing. The only thing is to sign up before using it for the first time. The advantage is that the scheduling process and can be processed when we are not the exact place to operate. The below Figure *5* shows how the Eiger software looks like and the 2D view of the uploaded CAD geometry and material assignment.

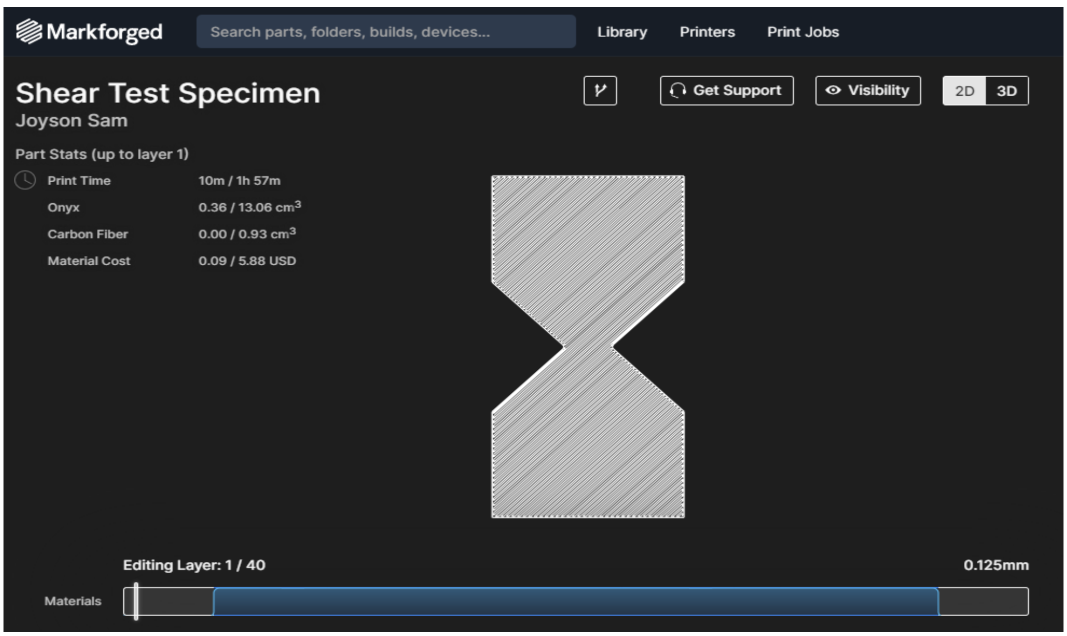

Figure 5: Eiger Software Visualization

After installing the latest version of the Eiger setup file or else getting signed on the online Eiger website, the tutorial section is available to view as it is helpful to follow the instruction to do the changes in the internal CAD design which is uploaded to the STL file. The print icon depicts whether the printer is engaged in any other printing or it is ready to work. After uploading the STL file, the part view appears and it displays the design part in the print bed and allows to modify the material assignment along with the reinforcement matrix of the fiber, the direction and orientation of the fiber get fixed in the general menu. Then the support can be assigned for the printing in the setting menu if it is a complicated geometry. The most important assignment is the infill which defines the volumetric fraction of the fiber to be printed along with structure of the fill, i.e., solid, triangular, hexagonal etc. The part can be saved in the library file for further use. The part view is shown below in Figure *6* and it shows how user-friendly the working of this software is.

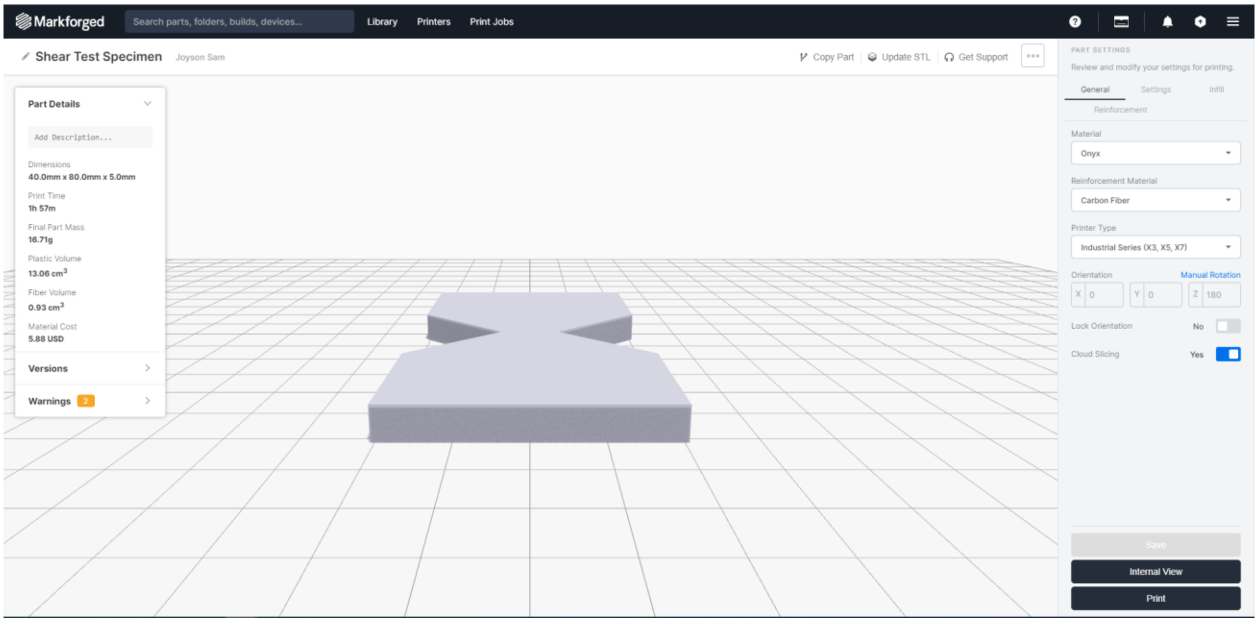

Figure 6: Eiger Software part view

The internal view is having the option to set the fiber angle and the options like isotropic and concentric fills to appear in the part which depends on the material property. And we can see the exact dimension of the part along with the material cost based on the assignment of every property. The warning section gives explanations regarding the recommendations to modify for further improvements.

2.4 EXPERIMENTAL SETUP

2.4.1 UNIVERSAL TESTING MACHINE

Universal Testing Machine is the testing machine used to perform the experimental tensile and compressive test of the specimen to determine its mechanical strength of the material. These results provide the basis which will be useful to study the materials and about the failure and using other techniques to improve the material further on. In recent years, the results from the testing machine can be reproduced and can be compared with analytical as well as numerical iterative solutions. The conventional universal testing machine used along with camera and lighting system for DIC optical measurement purpose is shown in Figure *7*.

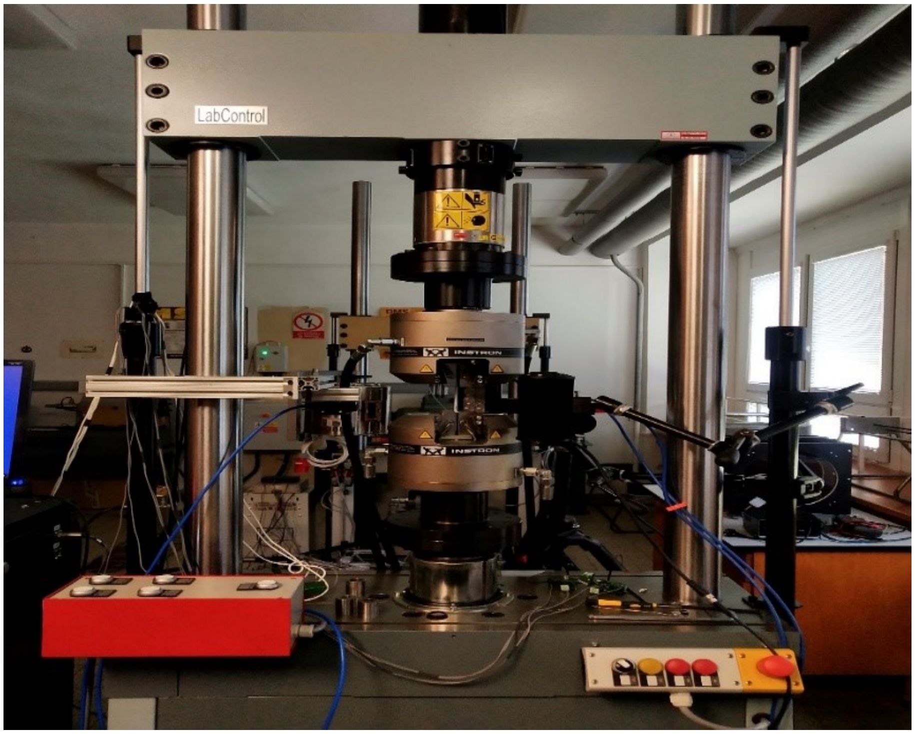

Figure 7: Universal Testing Machine with DIC Measurement

The accuracy and repeatability of the machine is helping the researches to focus on the calculations to evaluate the stress-strain behavior of the material. Various testing with different loading rates, speed and force can be performed by this machine. Lab Control 100 KN/1000 Nm Universal testing machine is used to perform this operation. For using this machine to calibrate the readings, it has to follow certain standards in testing specimen geometry, i.e., Dog Bone specimen, shear testing specimen, rectangular specimen. Once the testing part is done, the calculations regarding the yield strength, ultimate strength, modulus of elasticity, elongation, durability, and other properties like strain hardening can be determined [6]. The servo motor is used to control the overall testing process by the multifunctional remote controlling handset located on the frame is shown in Figure *7*.

The universal testing machine consists of an upper cross head, lower cross head, and the hydraulic valve is used to drive the cross head up and down based on the algorithm. The software access to the testing machine can easily control the operation. The extensometers are used to determine the strain as per the loading. Some UTM are having temperature chamber considering the temperature effect. The grips of different types are used in both the sides of the head to restrict the movement. Based on the boundary conditions and material properties, the grip design may vary to perform the experiment without defects.

2.4.2 V-NOTCHED RAIL SHEAR TESTING APPARATUS

The V- notched rail shear method is widely used for testing in-plane shear, which applies an asymmetric four-point bending load to the notched sample. In this testing, mono camera of 5 Megapixel is used in DIC measurement along with manual regime of loading in the testing machine but the correlation is done manually by taking notes of the forces and displacement value with DIC measurement. The Figure *8* shows the combined testing mode of the shear testing specimen which is locked in the V-notched rail.

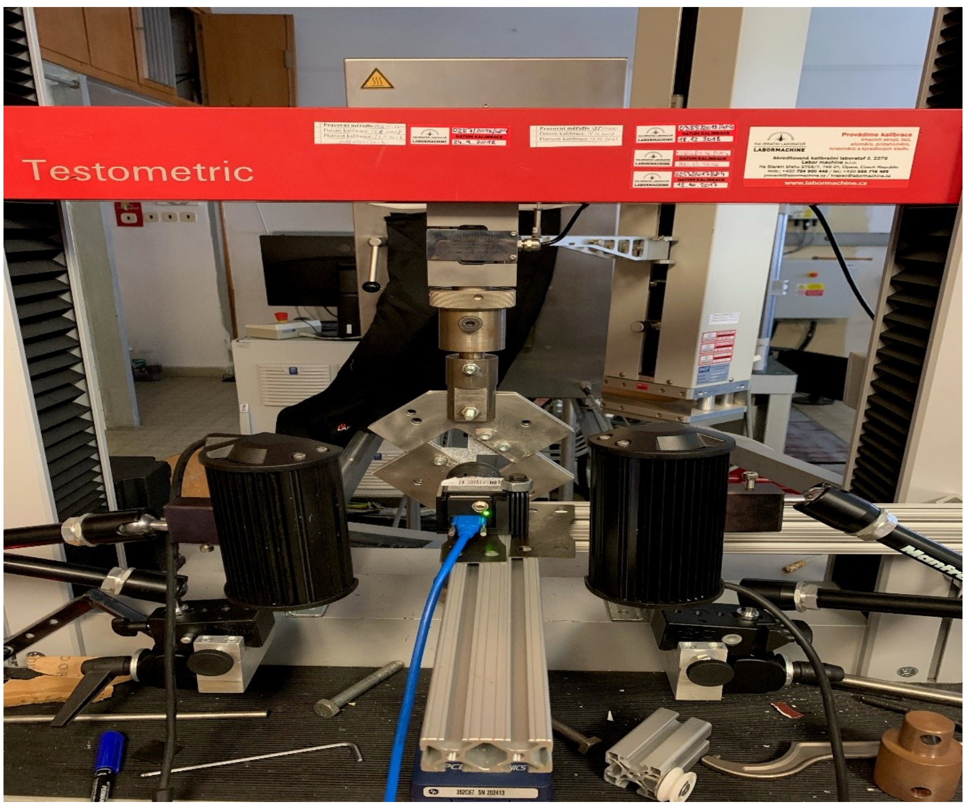

Figure 8: Shear testing apparatus with Fixture

The testing was performed at the speed of 0.5 mm/min. The Figure *9* shows the mechanism behind the placement of fixture with the specimen.

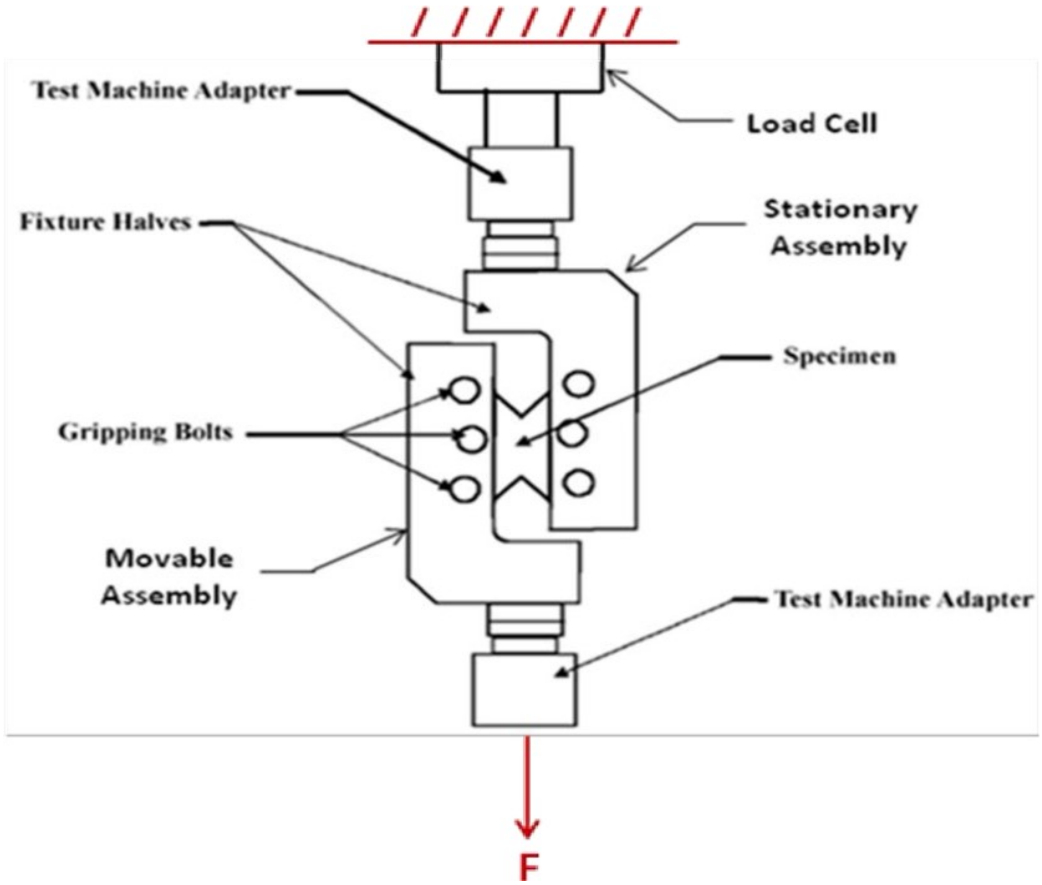

Figure 9: Shear testing fixture description [15]

The shear testing specimens in composite materials are used for shear testing specially to determine the notch effect due to loading as per the ASTM D7078 standard [16]. The in-plane shear modulus can be determined from this method of testing [16]. For composite materials, it is very difficult to predict the parameters. Therefore, that we will be using the V-notched rail shear fixture to perform tensile, shear, and combined tensile & shear testing. To increase the load capacity for testing very high strength composites, some modifications of the standard fixture have been proposed [17]. The apparatus consists of two halves of fixtures which will be fitted to the specimen with gripping bolts and nuts. The fixtures are having holes in different directions so that the testing can be done by simply rotating the fixture without doing any modifications in the specimen and testing machine. Different number of possibilities are provided by the fixture which will be very useful for the composite material testing. However, the numerical simulation has to consider the particular point of application of the load so that the stiffness will not cause error in comparison with the experimental results. The DIC Optical measurements are used to capture the change in displacement of the specimen for chosen points. The detailed working principles and method of DIC measurement will be discussed in the following section.

2.4.3 OPTICAL MEASUREMENT

The Digital Image Correlation Technique is the optical method used in experimental testing to measure the deformation of the specimen when the load is applied to it. The deformation will be measured by the digital correlation of the images before and after the interval. This measurement is better compared to the other optical measurements. It is the calibration without any contacts and fast data assets. In mechanical testing, DIC measurements are the best way of measurement to measure the material properties in elastic as well as plastic region. The high-resolution cameras are used to calibrate the static as well as dynamic cases. Mono camera is enough for a small planar specimen but the multiple cameras are used for capturing complex structures [4]. The Mercury RT system provided by Sobriety Company was used in DIC measurements. In DIC measurement calibration, capturing images needs some tracking reference on the specimen to clearly calibrate the specimen deformation. The pattern has to be covered the area of interest and it should be in gray scale contrast as it will be more visible. Spray paints are used in the case and in particularly black and white paints are highly visible and recommendable. The above Figure *10* shows how the speckle pattern looks like. In some cases, powdered particles are used instead of paint sprays when the specimen is having a sticky nature. The DIC algorithm used in calculation of the dimensions of displacement or using pattern matching technique [5].

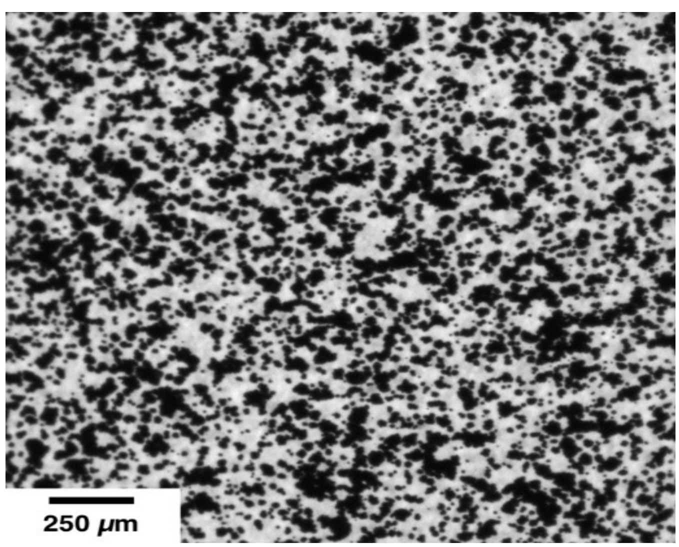

Figure 10: Speckle Pattern [5]

2.5 NUMERICAL METHODS

There are several numerical methods present to solve the engineering problems. Finite Difference method (FDM) and Finite Element Analysis (FEM) are the most preferable methods in the current engineering applications. FDM is solving the problems based on the differential along the coordinate axis, whereas FEM is solving it in a way by discretization of elements by using shape function, but the advantage is that it can solve even dynamic simulations and large strain applications.

2.5.1 FINITE ELEMENT ANALYSIS

The finite element analysis method was introduced by Turner in 1956 and uses approximation techniques to find out the solution. There are three approaches in finding the approximate solution. They are direct approach, weight Residual & Variational approach.

The steps involved in FEM analysis are as follows [8]:

- Division of body or object into finite number of subdivisions as nodes and elements.
- Selection of interpolation function.
- Derivation of local stiffness or mass matrix.
- Assembling the local matrix into global matrix.
- Applying boundary conditions.
- Finding solution of set of equations.
- Calculation of additional results based on the analysis results.

The finite element analysis is having the advantage to easily model whatever the complicated structure it may be and give the accurate solution. The visualization of solutions in time-dependent simulations is simple. The assumptions in the models are affordable to get accurate results. Therefore, we are considering FEM analysis by the application of Ansys APDL for further simulation in this study work. Ansys APDL is having the advantage of using macros to do the repetition of modelling conveniently.

2.6 ANALYTICAL METHOD

Analytical approach is an easy and quick way of calculation, when the solution is available. However, for more complicated structures, the formulas are not very well defined or the solution is not known. In those cases, we cannot perform the calculation by this approach. We need to have appropriate knowledge about fibers and matrices to perform the calculation.

2.6.1 EXPRESSION FOR LONGITUDINAL LOADING

We are applying the tensile load of F_c acting along the vertical direction in the longitudinal fiber direction as shown in the Figure *11*. The Figure *11* shows the blue region which is the carbon fiber orientation direction, and the white region is the Onyx region. Because of the application of the tensile load, the composite tends to elongate with the distance of δL as shown in the figure. The interesting thing is that both the fibers and the matrix are experiencing the same elongation along the loading direction, which leads to establish the relation as follows.

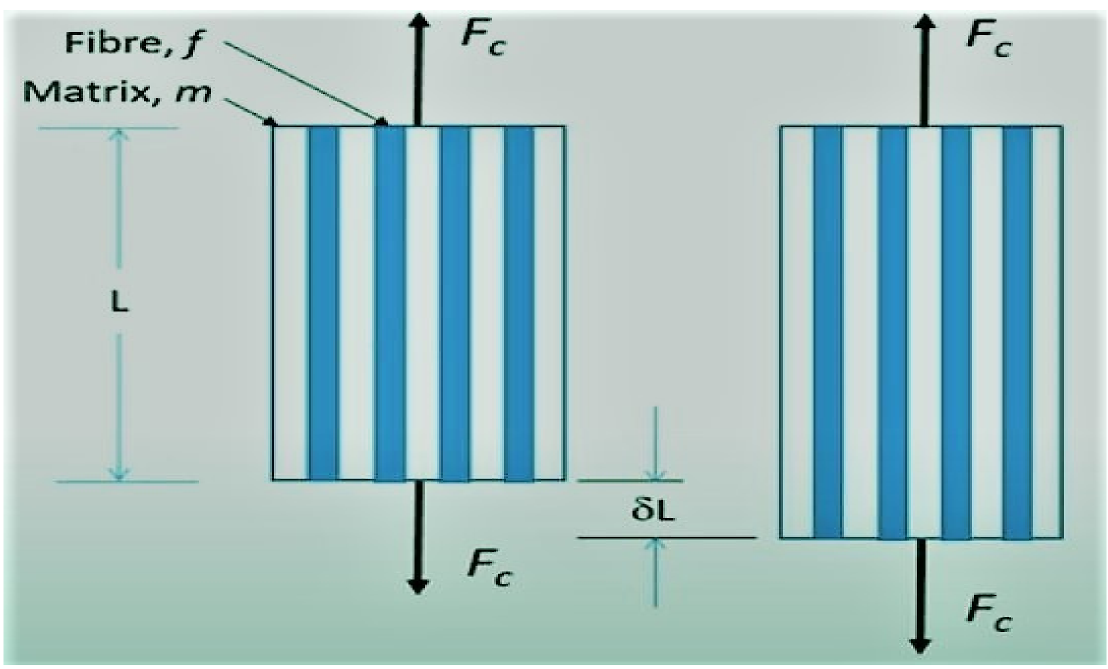

Figure 11 : Unidirectional fiber in longitudinal direction [19]

Equilibrium of the forces is described by the equation

$$F_C = F_F + F_M, \tag{2.1}$$

where F_C, F_F and F_M are the total force in composite, the force in carbon fibers, and the force in the matrix, respectively.

After substituting the relationship between an axial stress and corresponding cross-sectional area

$$\sigma_C A_C = \sigma_F A_F + \sigma_M A_M, \tag{2.2}$$

where $\sigma_M, \sigma_F, \sigma_c$ are stresses acting in matrix, fiber and composite respectively, and A_C, A_F, A_M are cross-sectional areas of composite, long fibers and matrix, respectively.

Due to the geometrical constraints total strain in the composite ε_C is the same as in fibers ε_F and matrix ε_M, i.e.

$$\varepsilon_C = \varepsilon_F = \varepsilon_M. \tag{2.3}$$

The stress-strain relationship is given by

$$\sigma_C = E_C \varepsilon_C \tag{2.4}$$

$$\sigma_F = E_F \varepsilon_F \tag{2.5}$$

$$\sigma_M = E_M \varepsilon_M \tag{2.6}$$

where E_M, E_F, E_c is Young's modulus obtained in matrix, fiber and composite respectively.

By combining the equations (2.4 to 2.6) with the equation (2.2), we get

$$E_C \varepsilon_C A_C = E_F \varepsilon_F A_F + E_M \varepsilon_M A_M. \tag{2.7}$$

We know that

$$\frac{A_F}{A_C} = \frac{A_F}{Ac}\frac{L}{L} = \frac{v_F}{v_C} = V_F \tag{2.8}$$

where v_F, v_C are volumes of fibers and the whole composite respectively. The volume fraction of matrix V_M could be expressed analogously considering the volume of matrix v_M.

Then, considering V_M, V_F as volume fractions of matrix and fibers respectively, the rule of mixture can be stated

$$E_C = E_F V_F + E_M V_M \tag{2.9}$$

Similarly, strength equation

$$\sigma_C = \sigma_F V_F + \sigma_M V_M \tag{2.10}$$

For finding ultimate strength

$$\sigma_{C,\text{ult}} = \sigma_{F,\text{ult}} V_F + \sigma_{M,\text{ult}} V_M \tag{2.11}$$

where $\sigma_{\text{M,ult}}$, $\sigma_{\text{F,ult}}$, $\sigma_{\text{C,ult}}$ are the ultimate stresses obtained in matrix, fiber and composite respectively.

2.6.2 EXPRESSION FOR TRANSVERSE LOADING

We are applying the tensile load of F_C acting along the vertical direction perpendicular to that of the fiber direction (Transverse direction) as shown in the Figure *12*. The Figure *12* shows the blue region which characterizes the carbon fiber orientation direction, and the white region is the Onyx region. The interesting thing is that both the fibers and the matrix are experiencing the same force and stress along the loading direction, which leads to establish the relation analogously as for the longitudinal direction.

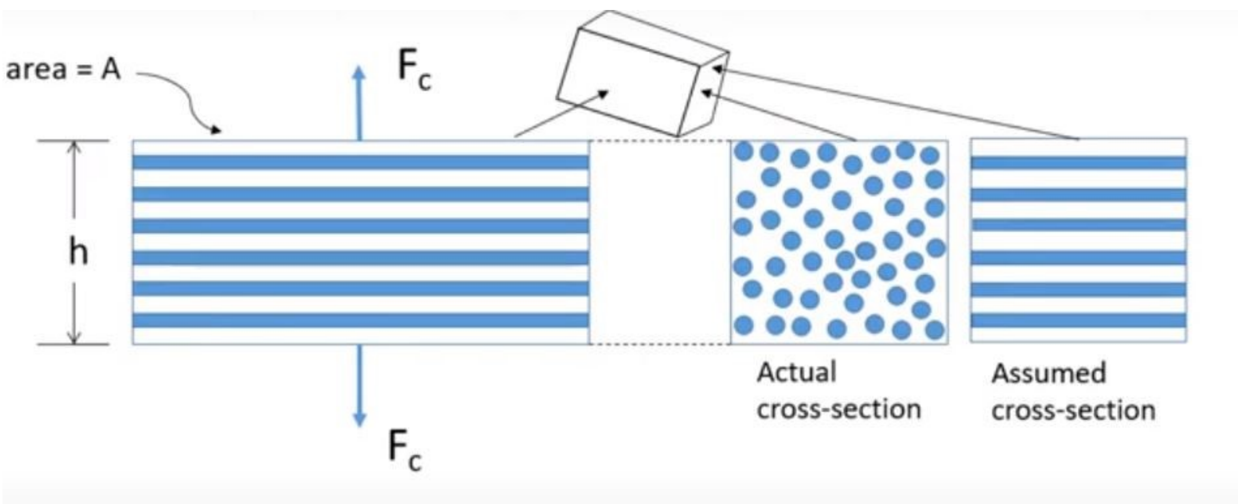

Figure 12 *:* Unidirectional fiber in Transversal direction [20]

Equilibrium of the forces:

$$F_C = F_F = F_M \tag{2.12}$$

$$\sigma_C = \sigma_F = \sigma_M \tag{2.13}$$

Geometry of deformation: Total strain in the composite can be written as

$$\varepsilon_C = V_F \varepsilon_F = V_M \varepsilon_M \tag{2.14}$$

The stress-strain relationships are given by

$$\sigma_C = E_C \varepsilon_C \tag{2.15}$$

$$\sigma_F = E_F \varepsilon_F \tag{2.16}$$

$$\sigma_M = E_M \varepsilon_M \tag{2.17}$$

where,

$\varepsilon_M, \varepsilon_F, \varepsilon_C$ are strains obtained in Matrix, Fiber and composite respectively.

$\sigma_M, \sigma_F, \sigma_C$ are stresses obtained in Matrix, Fiber and composite respectively.

E_M, E_F, E_C is Young's modulus obtained in Matrix, Fiber and composite respectively.

V_M, V_F, V_C are volume fractions obtained in Matrix, Fiber and composite respectively.

Combining the above equation, we get

$$\frac{\sigma_C}{E_C} = \frac{\sigma_F V_F}{E_F} + \frac{\sigma_M V_M}{E_M} \tag{2.18}$$

We know that

$$\sigma_C = \sigma_F = \sigma_M \tag{2.19}$$

Therefore, the rule of mixture

$$E_C = \frac{E_F E_M}{V_M E_F + V_F E_M} \tag{2.20}$$

The above equations are used to perform the analytical prediction of the composite material particularly for unidirectional fibre reinforced composite.

3 DESIGN AND PRINTING SPECIFICATION OF THE MATERIAL

Unidirectional continuous fiber provides the maximum strengthening or reinforcement to the composites. Therefore, we are using unidirectional continuous carbon fiber along with Onyx. Continuous fiber composite provides more strength and stiffness compared to short fibers and others. Onyx is the thermoplastic in the combination of carbon fiber in chopped form and can be easily reinforced with other fibers. The stiffness of the onyx will be high if it is 3D printed. The onyx is twice as hard as ABS and has high toughness and wear resistance. It can be combined with high strength fiber to increase the strength further on. Thus, the Onyx along with carbon fiber at the composition of (35% CF and rest PA6) will produce more strength material along with good surface finished part. The specimen is made with Onyx in the outer layers. The middle layer and the intermediate layers are filled with carbon fiber matrix. Composite materials are having anisotropic behavior of materials. However, by applying the fiber in different orientation at each layer, an isotropic property can be achieved. The fiber provides maximum strength when the load is applied in the direction of the fiber, whereas the loads applied perpendicular to the fiber mostly depend on the weak matrix phase [9]. For numerical simulations, the structural analysis of test is conducted in Ansys APDL to determine the stress-strain behavior.

In this work, the composite materials with various geometries and with different volumetric fraction of carbon fiber along with Onyx are tested. The design of the composites is shown below.

- Longitudinal loading – Rectangular Specimen - 5 specimen
- Transversal Loading – Rectangular Specimen - 5 Specimen
- Tensile, shear, combined loading – Shear testing Specimen – 1 specimen

Every specimen is designed and loaded as STL file in Eiger software and the material definition is done manually as per the requirement and can be printed.

3.1 LONGITUDINAL LOADING - RECTANGULAR SPECIMEN

The composite rectangular specimen is suitable for the particular testing as per the ASTM-D3039 standards for longitudinal loading as shown in Figure *13* below with only one sample longitudinal layer in the dark black line. The rectangular specimens made up of eight layers combination of Onyx and CF with dimensions (250mm * 15mm * 1mm) having different densities of CF (21.3%, 31.7%, 42.4%, 53.1%, 63.7%) are designed and sliced in the direction of application of load by using Eiger software. Subsequently, specimens were 3D printed by Markforged X7 printer. The particular design and other layer details are shown in Appendix 1 , Appendix 2 , Appendix 3 , Appendix 4 and Appendix 5 , respectively.

Table 1 and Table 2 shows the specification of the five different specimens and the same specimen is printed. The same geometry with reduced structure is used to evaluate numerical approach.

Table 1 : Longitudinal loading - Rectangular specimen - Eiger printing Specification

Material	Onyx
Reinforcement	Carbon fiber
Printer type	Markforged X7
Layer Thickness [mm]	0.125
Total Thickness [mm]	1
Concentric fiber rings	7
Fill Pattern	Rectangular fill
Fill density [%]	92
Roof and floor layer	1
Fiber orientation angle [°]	0
Wall layer	1

Table 2: Longitudinal loading – Rectangular specimen - Specification for different volume fraction

Parameters	Specification of different specimen				
Volumetric Fraction of CF Filament [%]	21.3	31.7	42.4	53	63.7
Total Layers	8	8	8	8	8
Infill layers [CF]	3, 6	3, 5, 6	3 - 6	3 - 7	2 - 7
Reinforced layers [ONYX]	1, 2, 4, 5, 7, 8	1, 2, 4, 7, 8	1, 2, 7, 8	1, 2, 8	1, 8

3.2 TRANSVERSAL LOADING - RECTANGULAR SPECIMEN

The composite rectangular specimen is suitable for the particular testing of transversal loading as per the ASTM-D3039 standard as shown above in Figure 13 below with only one sample transversal layer in the dark black line. The rectangular specimen is made up of sixteen layers combination of Onyx and CF with dimensions (175mm * 25mm * 2mm) having different densities of CF (21.4%, 32%, 42.9%, 53.6%, 64.2%) as designed and sliced in the direction normal to the direction of the load application using Eiger and 3D printed by Markforged X7 printer. The particular design and other layer details are shown below in the Appendix 6 , Appendix 7 , Appendix 8 , Appendix 9 , Appendix 10 .

Table 3 and Table 4 show the specification of the five different specimens. The same specimens were printed. The isotropic fill provides the fiber in a zig – zag pattern to simulate the individual layers of the unidirectional composite. It resists the bending in XY plane [3].

Table 3 : Transversal loading – Rectangular specimen -Eiger printing Specification

Parameters	Specification of different specimen				
Volumetric Fraction of CF Filament [%]	21.4	32	42.9	53.6	64.2
Total Layers	16	16	16	16	16
Infill layers [CF]	4,7,10,13	4,5,7,10,12,13	5 - 12	4 – 13	1, 2, 15, 16.
Reinforced layers [ONYX]	1 – 3, 5, 6, 8, 9, 11,12,14 -16.	1 – 3, 6, 8, 9, 11, 14 – 16.	1 – 4, 13 – 16.	1 – 3, 14 - 16	3 - 14

Table 4 : Transversal loading – Rectangular specimen - Specification for different VF

Material	Onyx
Reinforcement	Carbon fiber
Printer type	Mark forged X7
Layer Thickness [mm]	0.125
Total Thickness [mm]	2
fiber fill	Isotropic
Fill Pattern	Rectangular fill
Fill density [%]	92
Roof and floor layer	1
Fiber orientation angle [°]	90
Wall layer	1

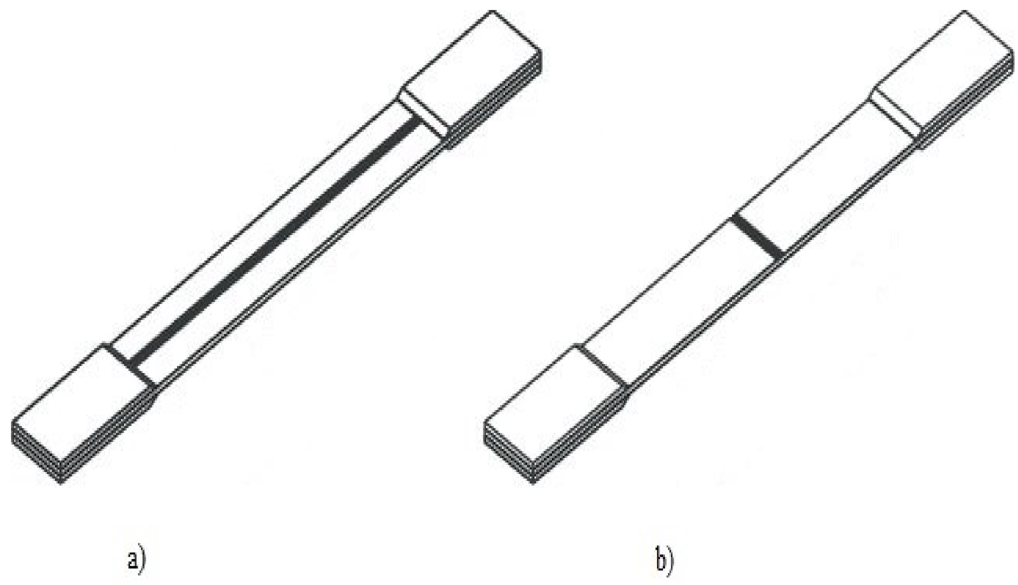

Figure 13 : a) Longitudinal Loading of (CF) Composite layer b) Transverse Loading of CF Composite layer

3.3 SHEAR TESTING SPECIMEN – TENSILE, SHEAR AND COMBINED TESTING

The particular design and other layer details are shown in Figure 14. The Eiger software visualization of the specimen is shown in Appendix 11 . The material consumption is less in the case of concentric fill. We are using 2 concentric fills for this particular shear testing specimen for the tensile, shear, and combined loading as an application. The concentric fill lays fiber around the perimeter of the walls. It helps to resist the bending about z axis and it strengthens the walls against deformation. We are considering a concentric fiber ring on all walls [3]. Table 5 and Table 6 show the specification of the specimen with 2 concentric fill of CF filament and the same specimen was printed.

Table 5 : Tensile, shear, combined loading – Shear Testing specimen Specification for different volume fraction

Parameters	Specification of specimen
Volumetric Fraction of CF Filament [%]	0.05
Total Layers	24
Infill layers [CF]	4,7,10,13
Reinforced layers [ONYX]	1 - 3, 5, 6, 8, 9, 11, 12, 14 -16.

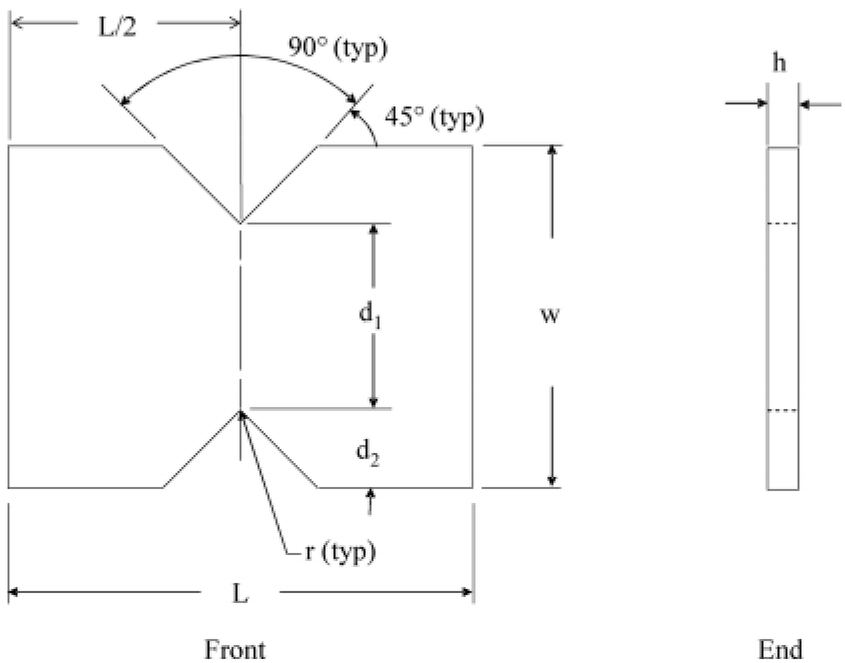

Specimen dimension

L = 80 mm

W = 40 mm

r = 0.5 mm

d_1=10 mm

h = 3 mm

Figure 14: Eiger Software-Internal View of 2 concentric CF Fill -Shear Testing Specimen [14]

Table 6 : Tensile, shear, combined loading – Shear Testing specimen - Eiger printing Specification

Material	Onyx
Reinforcement	Carbon fiber
Printer type	Mark forged X7
Layer Thickness [mm]	0.125
Total Thickness [mm]	3
fiber fill	Concentric
Fill Pattern	Solid fill
Fill density [%]	92
Roof and floor layer	1
Reinforce	All Walls
Concentric fiber ring	2

4 EXPERIMENTS

The experimental approach has to be considered for a verification of reliability of the production technology of the material because there may occur imperfections in different manufacturing processes. However, in the case of composite materials, experimental methods do not need much knowledge about the fibers and matrix and its properties. The experimental test is realized using the universal testing machine and is calibrated by DIC measurement using a mono camera. The various experimentation is realized with Onyx and CF layered composite materials of different volumetric fractions. The fibers are loaded in the longitudinal and transversal direction to investigate the strength. The dog bone shaped specimen was considered previously to measure CF reinforced composites printed by 3D printing but due to the continuous failure at the grip section needs the alternative of rectangular specimen with ASTM D3039 Standard [11]. The testing is done under room temperature. In general, the composite materials are tested particularly applying loads in the direction of the fiber or in the normal to the direction of the fiber so that the strength and stiffness of the fiber are determined from the process. And, the orientation of the fibers is changed or else the composite density is varied and tested so that the particular property of the specimen will be identified to be used in particular applications in future. These studies are also useful to realize different experiments by modifying the properties or load conditions to achieve the results in the future. In our case, the density of the composite (CF) in terms of volumetric fraction is modified to realize the experiment in the universal testing machine. As per the ASTM standards, the dimensions of the longitudinal and transversal specimens are shown in Figure *15*.

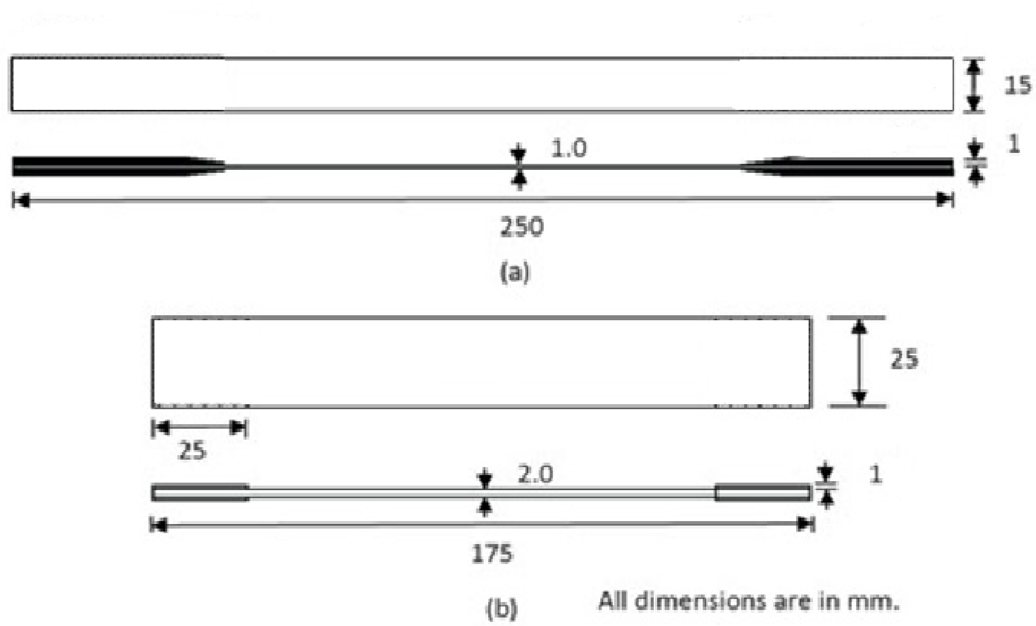

Figure 15 a) Rectangular specimen dimensions for Longitudinal loading b) Rectangular specimen dimensions for Transversal loading [12]

4.1 LONGITUDINAL LOADING OF RECTANGULAR SPECIMEN

4.1.1 EXPERIMENTAL RESULTS - STRAIN CONTROLLED TEST

The uniaxial testing of the five specimens were done under room temperature with the influence of strain rate using universal testing machine in the laboratory. The experimental results of force response due to strain-controlled tensile testing for five different volumetric fractions of carbon fiber (with the Position rate is 2 mm/min for all the specimen as shown in the Figure *16*) are depicted below in Figure *17*. The Figure *17* and Table *7* show interesting results as the Young's modulus and strength of the composite (Onyx & CF) increase when the volumetric fraction of the CF gets increases, but in the case of Poisson's ratio, the peak value is obtained for the specimen with 31.7% of VF then the value goes on decreasing for further increase in the density of CF. Another notable fact is that the influence of carbon fiber increases the tensile strength and ductility of the composites under same position rate of 2 mm/min as shown in the Figure *17*.

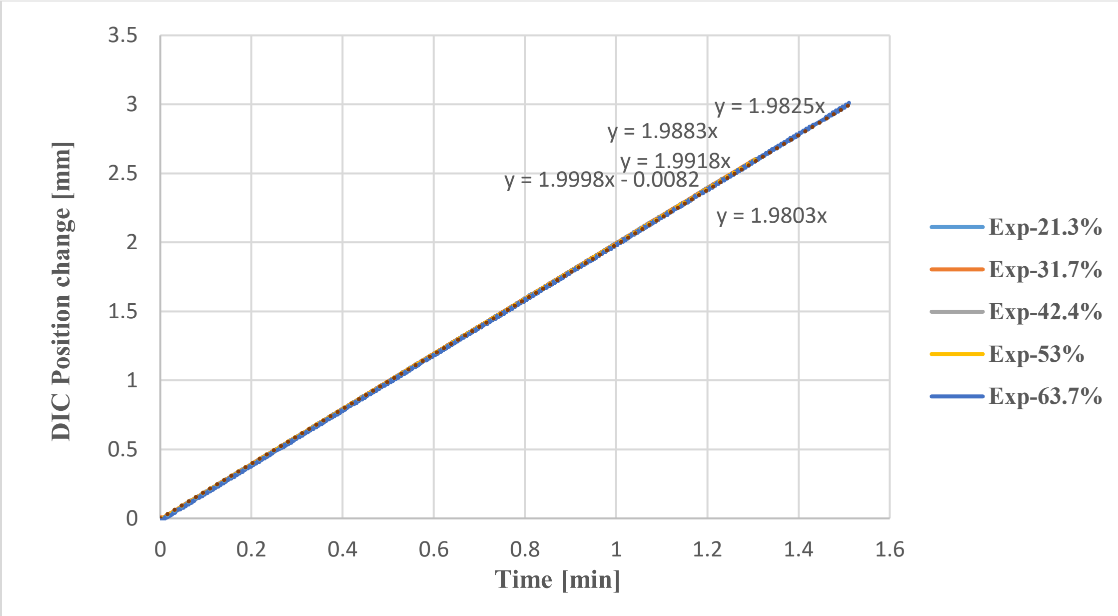

Figure 16 : Position rate for different specimen - Longitudinal loading

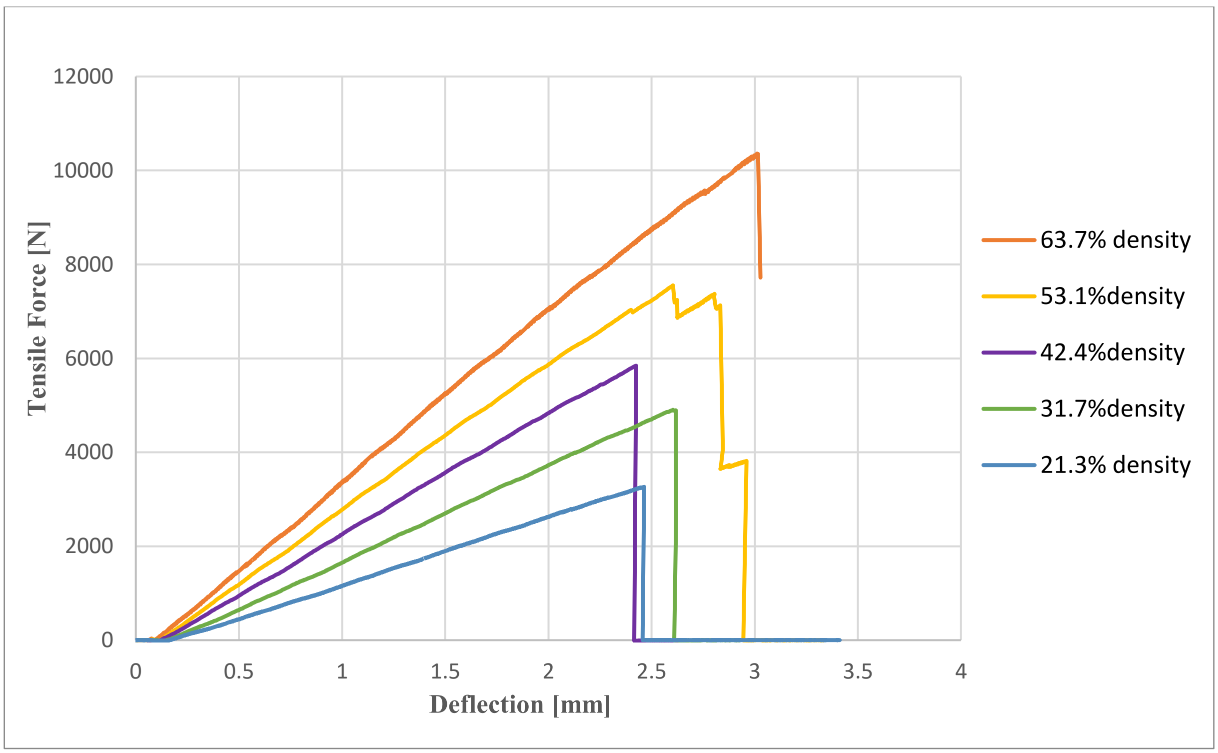

Figure 17 : Force vs Deflection Graph for composite specimen (Onyx & CF) with different density of CF loading in the longitudinal direction.

Table 7 : Mechanical Properties of specimen for Longitudinal loading

Specimen with CF (%)	Poisson's Ratio [-]	Young's Modulus [MPa]	Ultimate Strength [MPa]
21.3	0.621	18350	207.50
31.7	0.703	29853	226.72
42.4	0.628	34809	389.47
53.1	0.506	40783	503.61
63.7	0.491	50842	690.60

The Figure 18 and Figure 19 shows the averaged experimental results of the different specimen tested under each volumetric fraction of CF filaments under two position rate. The averaged results of young's modulus and ultimate strength for longitudinal loading is depicted below.

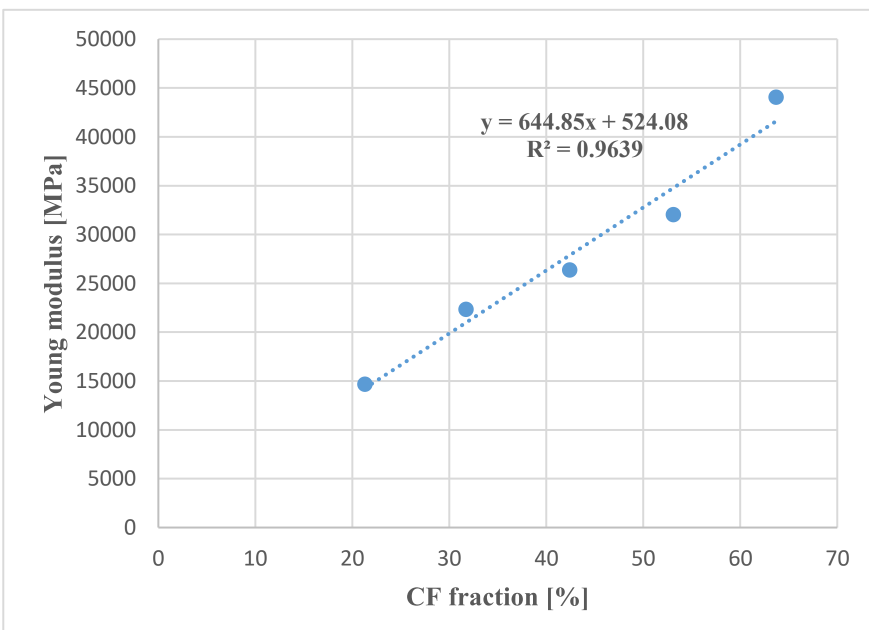

Figure 18 : Young's Modulus averaged value for each volumetric fraction of CF filament

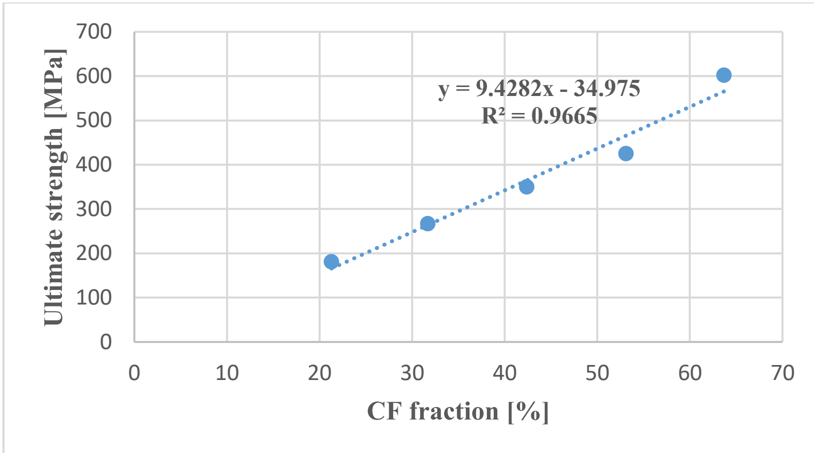

Figure 19 : Ultimate strength averaged value for each volumetric fraction of CF filament

4.2 TRANSVERSAL LOADING OF RECTANGULAR SPECIMEN

4.2.1 EXPERIMENTAL RESULTS – STRAIN CONTROLLED TEST

Figure 20 and Figure 21 show the experimental results of the same volumetric fraction composite specimen with more realization, which gives a significant uncertainty in response. The uniaxial testing of the specimens was done under room temperature with the influence of strain rate using universal testing machine in the laboratory. Specimens sp1, sp5 and sp6 are tested at the position rate of 2 mm/min and specimens sp2, sp3 and sp4 are tested at the position rate of 0.5 mm/min (this is the rule for all the transversal loading cases). The results are depicted below in Table 8.

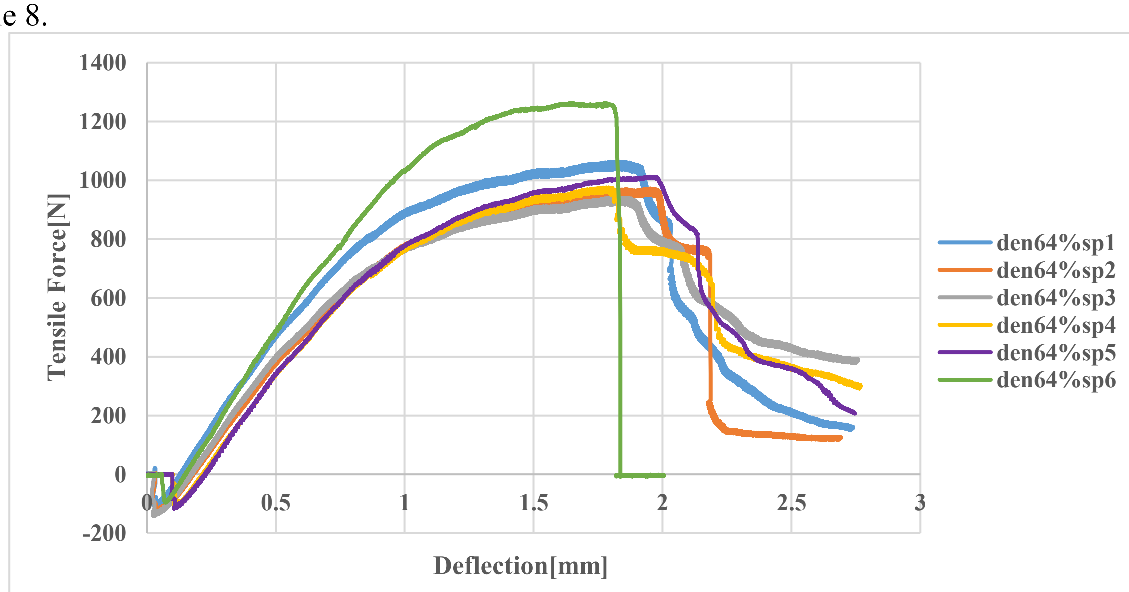

Figure 20: Force VS Deflection Curve for specimen with 64% CF in transverse Direction

The interesting results obtained in the case of the transversal loading are that the strength and Young's modulus of the composite material is getting decreased in the specimen having 42.9 % VF of carbon fiber and then gradually increasing as the density of CF increases. The reason is not clear. The deviation in obtained results was similar for all cases of CF density. The notable part is that the transversal loading of composite specimen (Onyx & CF) is having less strength compared to the longitudinal loading as the continuous long fibers and its reinforced composites are having less strength in the direction normal to the direction of applied load. The speed of loading is also causing more influence as the deviations are shown in the Table 8.

The same position rate is used to compare the readings with the numerical simulations as shown in the Figure 45. Figure 20 and Figure 21 show that there is a slight influence of position rate. The uncertainty of resulting maximal tensile force in the curve is probably due to the delamination of the layer between CF and ONYX.

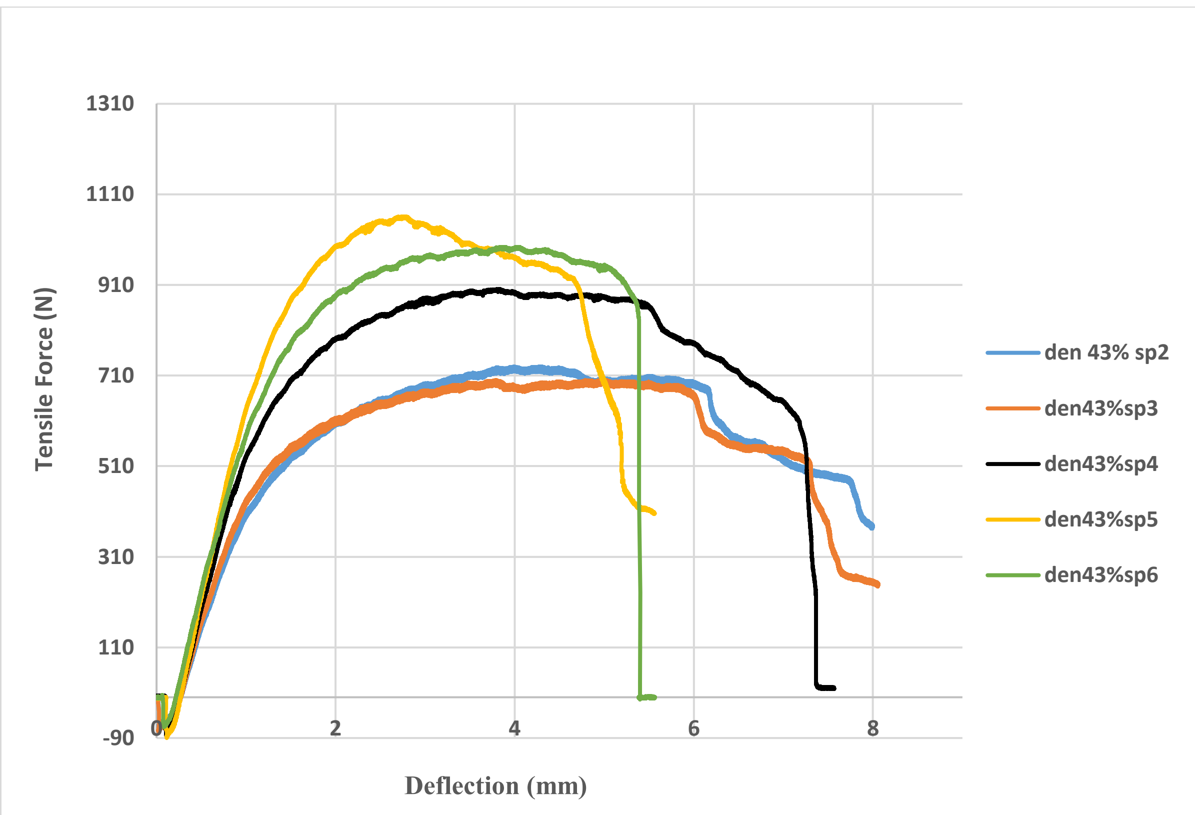

Figure 21: Force VS Deflection for different specimen with 43% VF of CF in transverse Direction

Table 8 : Mechanical Properties of specimen for Transverse loading

Specimen with CF%	Position rate [mm/min]	Young's Modulus [MPa]	Ultimate Strength [MPa]
21.4	2	1528.5	22.53
32	2	1297.7	21.53
42.9	2	1136.4	19.87
53.6	2	1240.3	21.2
64.2	2	2206.9	19.51

The Figure *22* also shows that the resistivity of the composite increases as the volumetric fraction of carbon fiber increases but the allowable deformation of the composite is decreasing as the CF density increases. These results are very useful in the case of further study and practical consideration of materials with similar properties for different purposes.

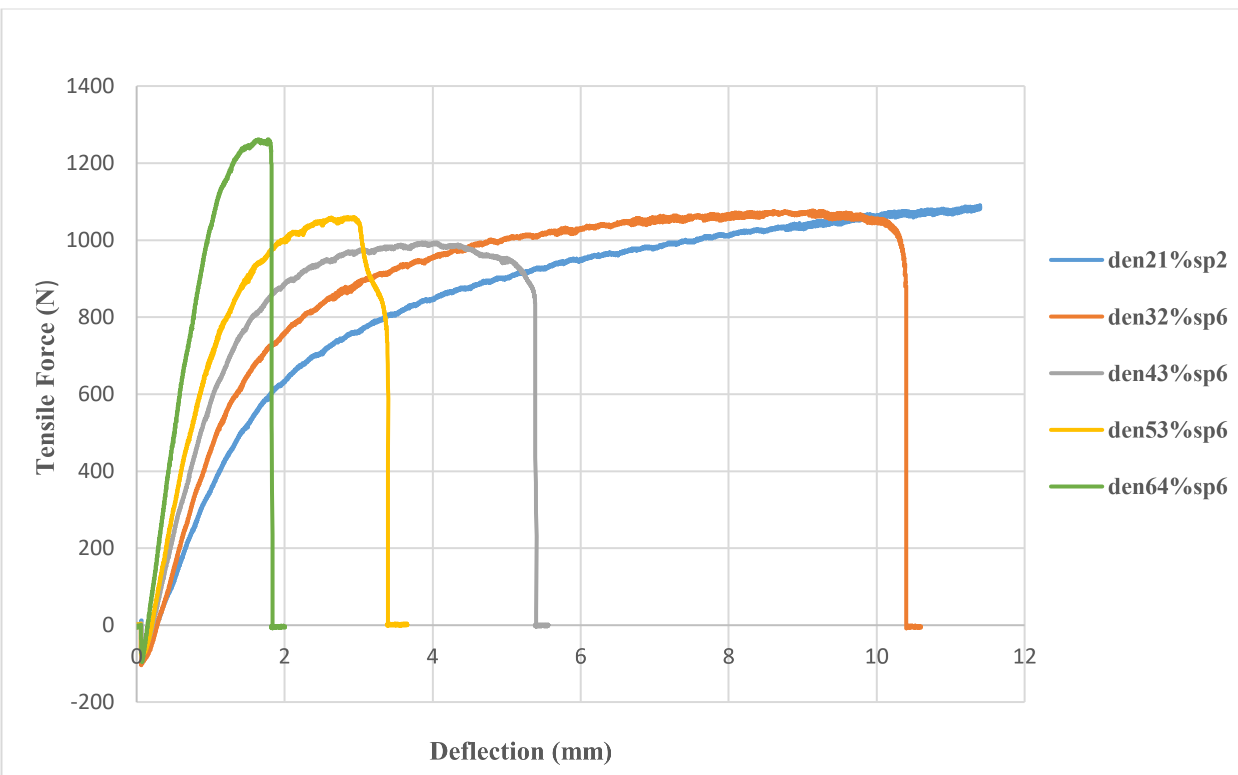

Figure 22: Force VS Deflection for specimen with different density of CF in Transverse direction

4.3 SHEAR TESTING SPECIMEN WITH TWO CONCENTRIC CF FILLS

The testing of the shear specimen was realized on the Testometric M500-50CT testing machine considering three different loading regimes. The same specimen was used in all three experiments. The loading was very low to do not generate any irreversible strain.

4.3.1 TENSILE LOADING

The tensile stiffness of the composite with two concentric fills of CF filament is found by tensile loading the Shear testing specimen. The shear testing specimen is placed vertically in the fixture shown in the Figure *23*. The specimen is made up of Onyx along with two concentric fills of carbon fiber filaments printed by Markforged X7 3D printer. The tensile load is applied at the speed of 0.1mm/min to determine the tensile properties of the specimen with the fiber acting along the boundaries of the specimen as two concentric contour fills as the application for the previous concepts.

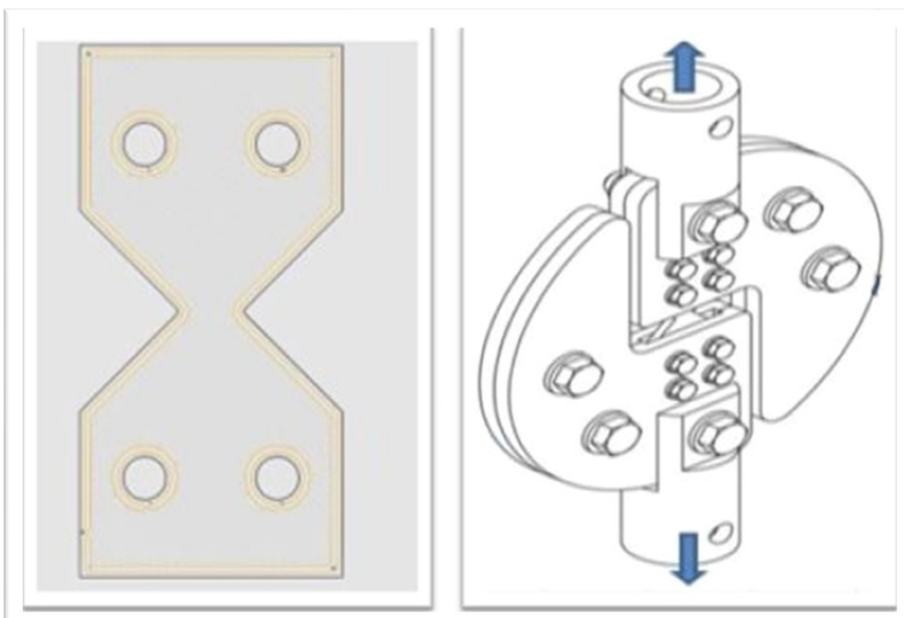

Figure 23: Tensile loading Fixture orientation vertically for tensile loading case

The Figure *24* shows the contours of displacement in the axial direction obtained using mono camera capturing. The experimental curves are discussed in the following chapter along with the numerical comparison.

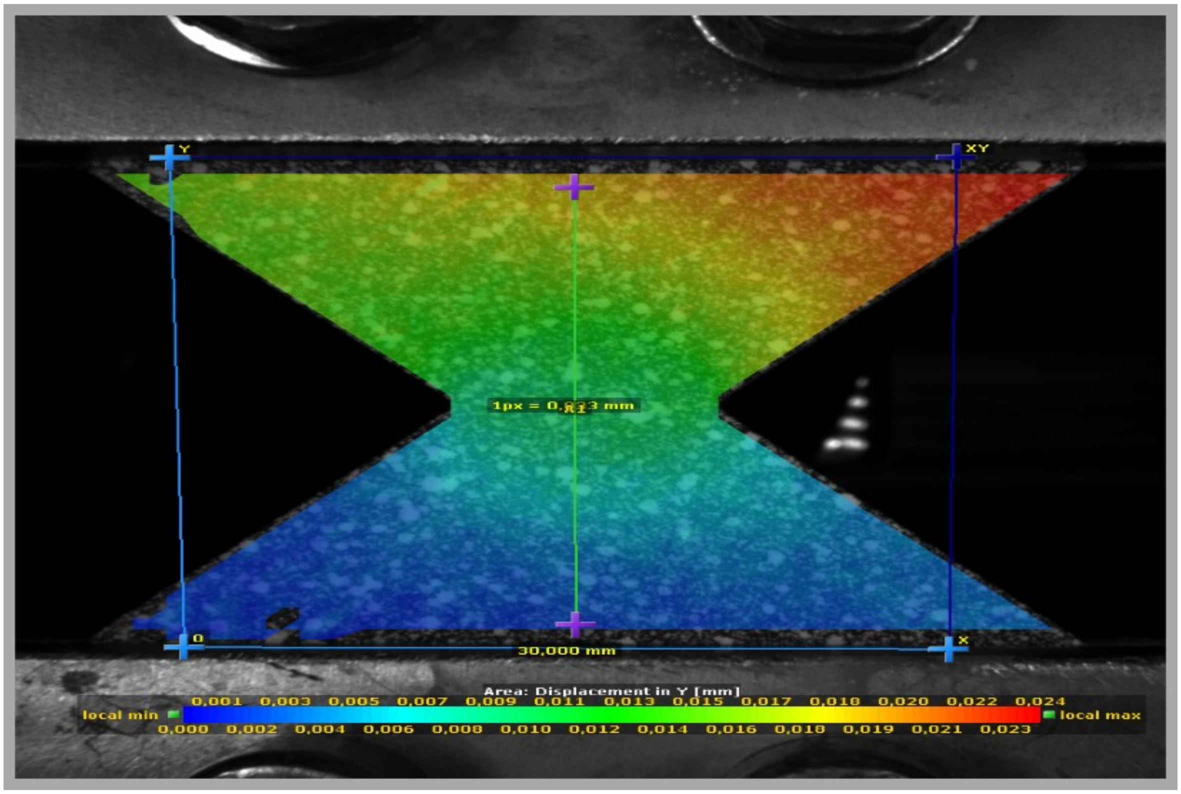

Figure 24: Experimental displacement contour in the direction of application of load

4.3.2 SHEAR LOADING

The shear testing is performed to investigate the in-plane shear properties. The loading of the specimen at the speed of 0.1 mm/min is according to the mechanism shown in Figure *25*, Figure *26*.

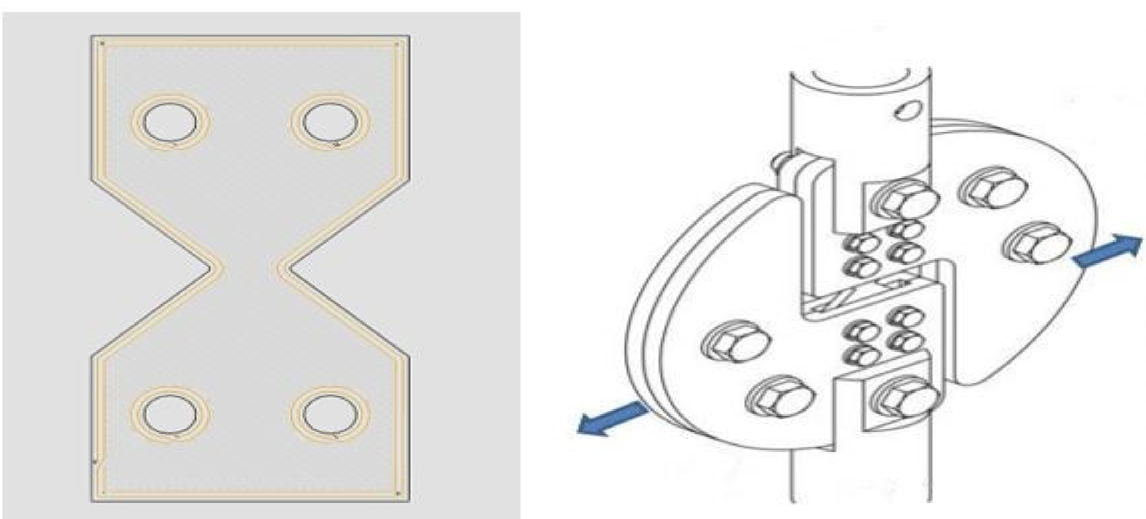

Figure 25 : Shear Loading visualization

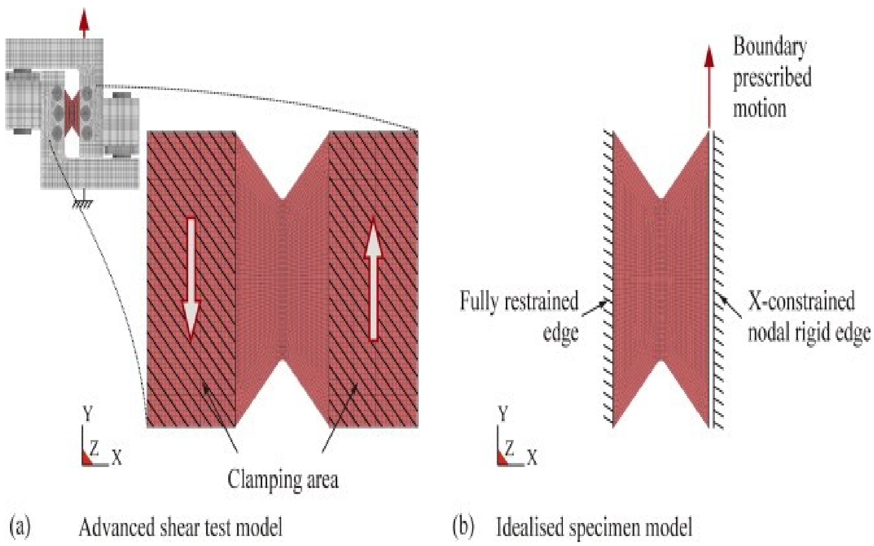

Figure 26 : Shear Loading mechanism in V Notched rail [18]

The Figure *27* shows the contours of displacement in direction to the application of load obtained using mono camera capturing. The experimental curves are discussed in the following chapter along with the numerical comparison.

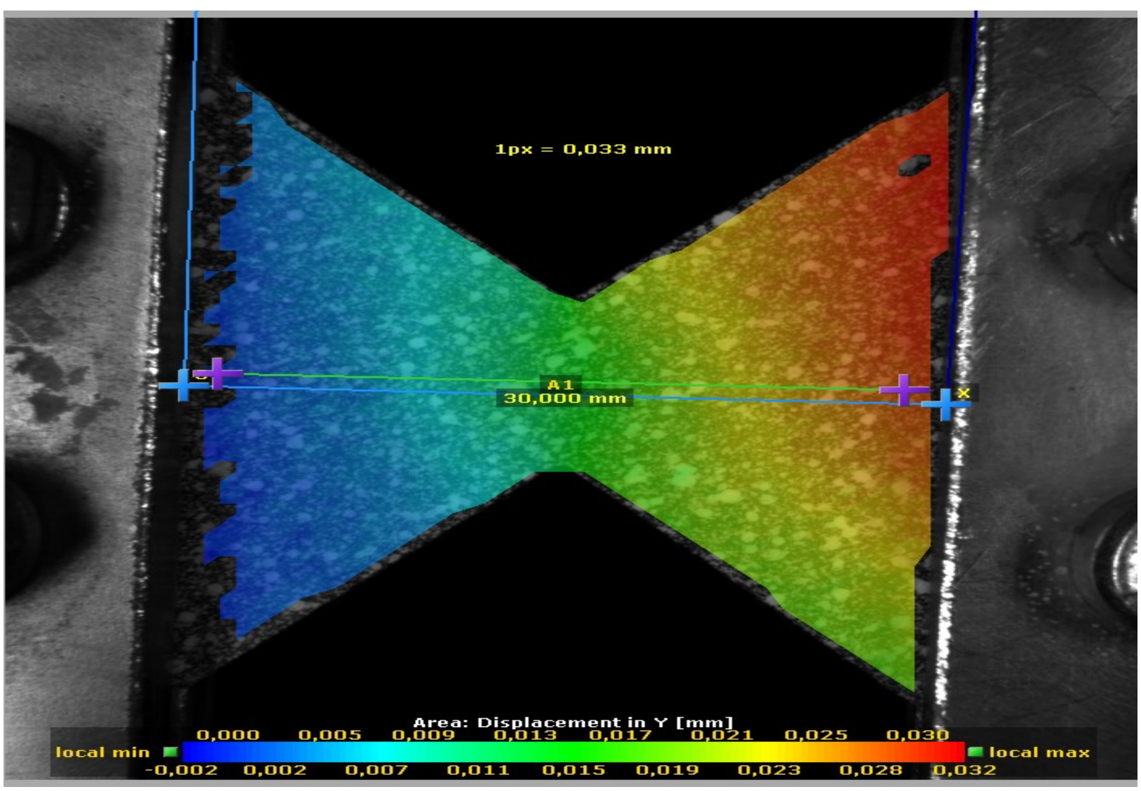

Figure 27 : Experimental displacement contour in the direction of application of load

4.3.3 COMBINED TENSILE AND SHEAR LOADING

The fixture is held in the way that the angle between the specimen and the load cell is placed at an angle of 45° as shown in Figure *28*. It means that the combined tensile and shear load is acting on the specimen. Then the experiment is realized under the speed of 0.1 mm/min.

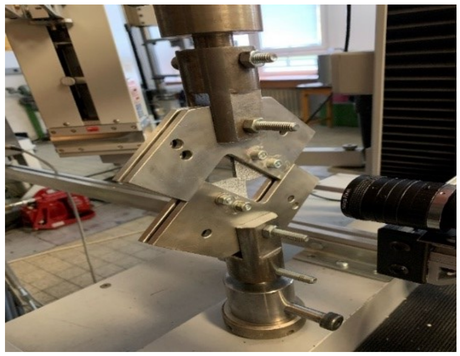

Figure 28 : Combined loading – Shear testing specimen – testing at 45°

The below Figure 29 shows the contour of displacement in the y direction of local coordinate system. The experimental optical measurement contours of XY shear strain is shown in the Appendix 12 .

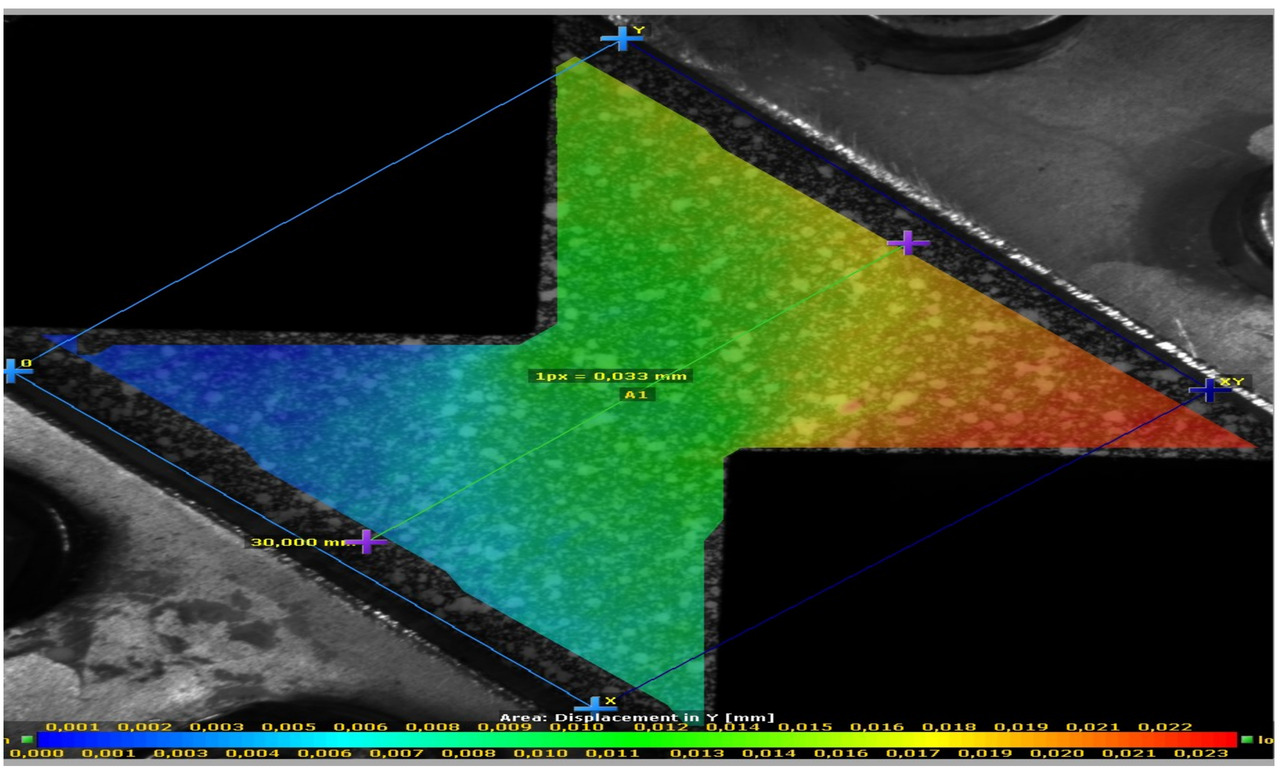

Figure 29 : Experimental displacement contour in the direction of application of load

5 FE SIMULATIONS

The numerical simulation is carried out in Ansys APDL software. The sophisticated features in the ANSYS APDL and the creation of macros are the main advantages to do the simulation effectively within less time. As the specimen with different volumetric fraction of CF, the structure will be more complex and it will be a tedious process in modelling, but using the macro-option we can easily modify the geometry and the mesh and the preprocessing works. The math operations are easily performed in case of plasticity. Numerical simulation is better to perform analysis even on complicated geometries of composites than the experimental approach. The partial differential calculations are programmed such that the process is not so complicated even for composite materials. However, in the case of approximation and reduction mechanisms, the particular knowledge of fibers and matrix and their properties are much important

5.1 MATERIAL MODEL

The finite element model has to be discretized to either linear or quadratic elements. Here, according to the specification of the problem, the SOLID BRICK 8 Node 185 linear Element is chosen for the Onyx and for the CF fiber, the link element 180 is considered. Thus, the model is set so that when meshing, the model can be divided into nodes and elements for doing further partial derivation by numerical iterative method. This Solid brick element can be useful for plasticity and creep simulations, and the link element is used to define the model by a 1D line and assign the value of the area of cross-section so that it will be considered as a 3D model. The CF layers are having circular carbon fiber along with the matrix to form a square cross-section but when pressed by the printer to form the layer, it will be transformed to rectangular to form the layer of CF. The area of CF is 0.112 square millimeters as reported in [21]. The value will be updated in the sections to be considered in the simulation. The material property of Onyx is assumed to be linear elastic isotropic conditions. The orthotropic properties of the CF matrix and the isotropic property of the Onyx will not be considered for simplicity. The material property of Onyx having isotropic property (E=1022 MPa, μ= 0.45) is cited from [9]. The material model of Onyx follows the rate dependent Viscoplastic model (Perzyna model) along with the Chaboche kinematic hardening model, see Nicholas James thesis work [2]. The FEM parameters are explained below in Table *9*. The material property of carbon fiber is having orthotropic material property cited from [12]. However, we can take only the isotropic elastic property in case of link element (E=75918 MPa, μ= 0.4). It will not affect the solution because the stiffness can be found if we know the Young modulus and cross-sectional area.

As we know that the specimen will be having rectangular cross-section and the dimension of the specimen differs for the longitudinal and transverse loading specimen and the dimensions are shown in the Figure 14, Figure 15 as per ASTM standards. The position of the fiber in the layer is to be considered in modelling. Some models will be having symmetrical properties and will be easy to design and mesh a half or quarter specimens so that it will be mirrored by using reflect command or else using symmetrical boundary conditions to solve. The curved portion of the transversal geometry is shown in the Figure 34.

Table 9 : FEM Simulation parametric definition

PARAMETERS			LONGITUDINAL LOADING RECTANGULAR SPECIMEN	TRANSVERSAL LOADING RECTANGULAR SPECIMEN	SHEAR TESTING SPECIMEN [Tensile, Shear, Combined loading]
ELEMENT	ONYX		Solid Brick 8 Nodes	Solid Brick 8 Nodes	Solid Brick 8 Nodes
	CF		Link 3D 180	Link 3D 180	Link 3D 180
MODEL SPECIFICATION			Unit length consideration with symmetrical boundary condition	Unit length consideration with symmetrical boundary condition	Full model
MATERIAL MODEL	ONYX	LINEAR	Isotropic	Isotropic	Isotropic
		NON-LINEAR	Chaboche & Perzyna	Chaboche & Perzyna	Chaboche & Perzyna
	CF	LINEAR	Isotropic	Isotropic	Isotropic
		NON-LINEAR	- (brittle material)	- (brittle material)	- (brittle material)

5.2 MESHING

The Figure 30, Figure 31 and Figure 32 show different meshing strategies used for longitudinal loading, transversal loading and shear testing specimen in performed finite element simulations. Figure *33* shows the mesh of the transversal loading interior curved structure modelled using link element. Figure 34 shows the model of CF filaments in transversal loading. Figure *35* shows the longitudinal loading model and the colored differentiated lines denote the longitudinal CF filaments modelled by using linked elements. and shows the full view of the model of CF filament for 53.1% CF model. Mapped meshing with equal number of elements at the opposite sides of the model has to be defined for getting accurate results in the simulation. Hexagonal mapped mesh is used to discretized the rectangular specimen model. However, for the notch region in the shear testing specimen and the curved portion of CF filament in the transversal loading are mapped meshes as shown in Figure *31* and Figure *32*. The simple 2D mesh is created first and then it is extruded along the z direction as per the material placement. When extruding, the material definition is also done at particular positions. The assignment of material has to be precised as it is a complicated process.

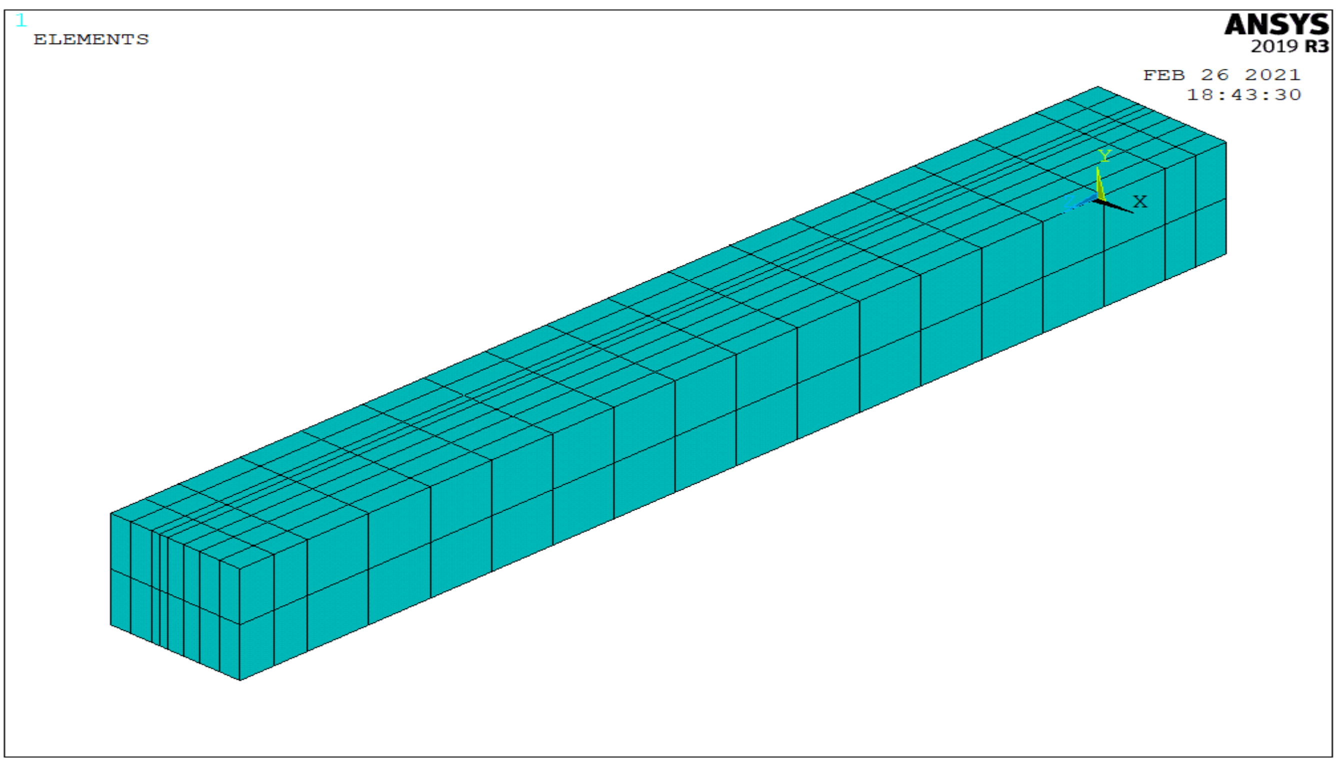

Figure 30: Geometry and Mesh for specimen with 31.7 % VF (Longitudinal Loading) – reduced model of unit length in loading direction

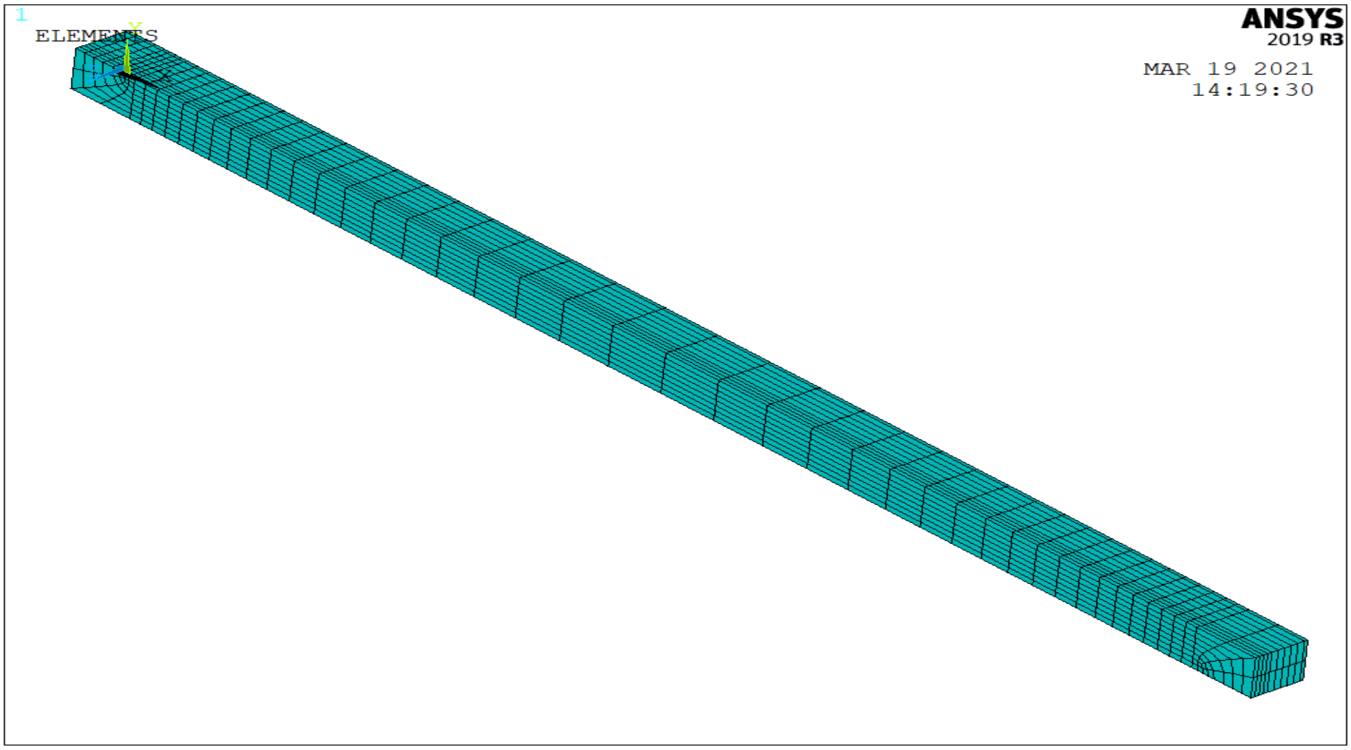

Figure 31:Transverse loading Mesh for specimen with VF 53.6% – reduced model of unit length in loading direction

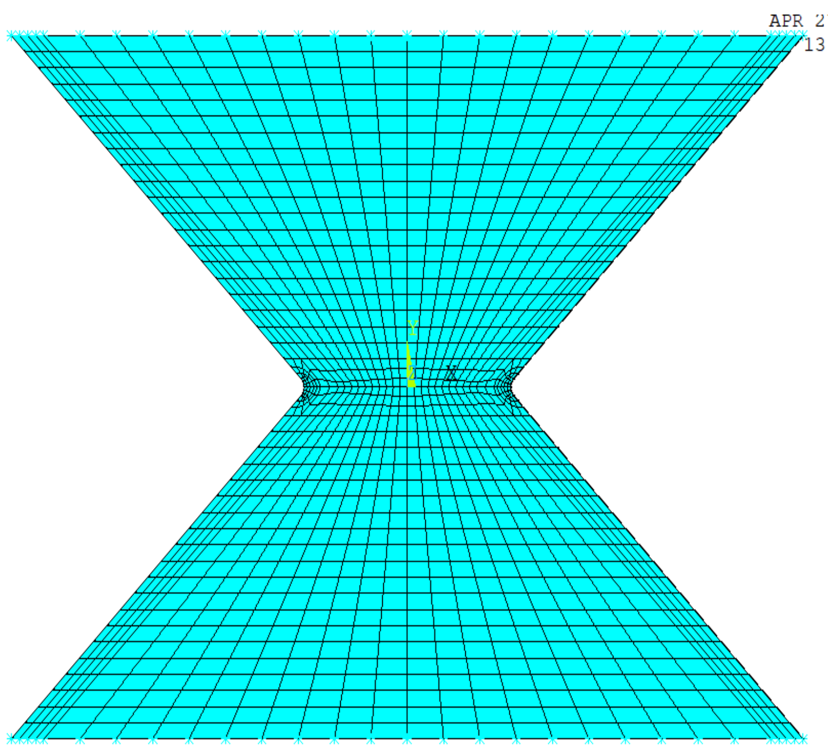

Figure 32 : Mesh of shear testing 3D Composite specimen with two concentric fills of CF

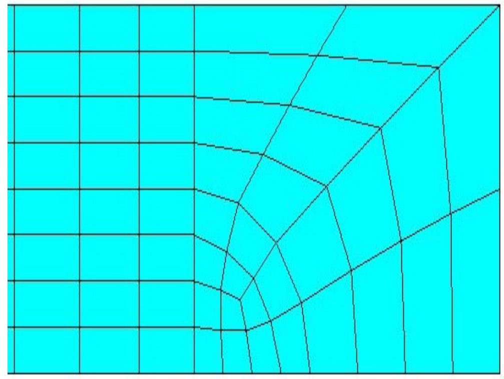

Figure 33 : Transverse loading Mesh for curved surface

For simplicity, we are using the LINK180 element in the case of CF filament assignment as shown below in the Figure *35*. The 3D model is ready for the application of boundary conditions.

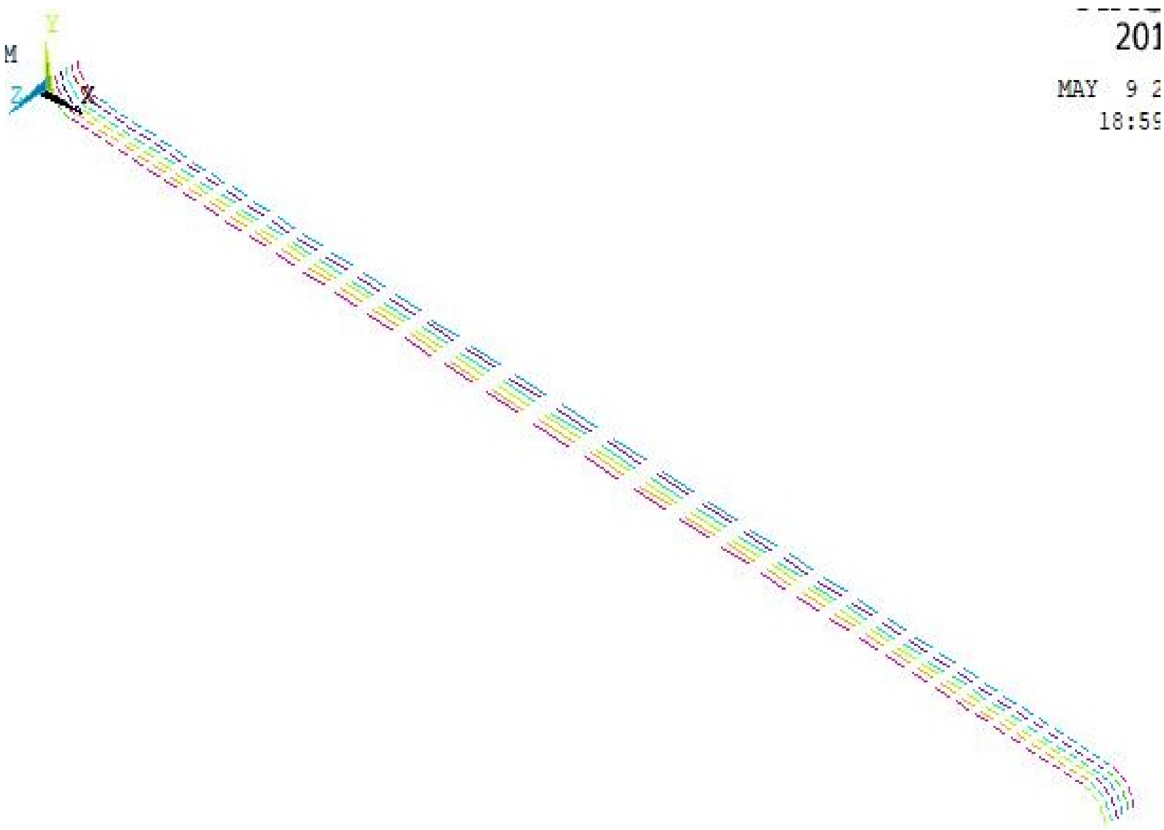

Figure 34 : Transversal loading CF link elements

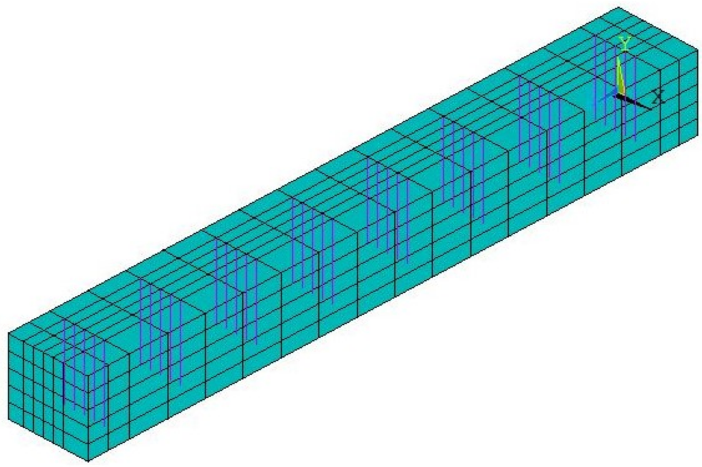

Figure 35 : Longitudinal loading of 53 % CF Model – Unit Length Model

5.3 BOUNDARY CONDITIONS

5.3.1 RECTANGULAR SPECIMEN – LONGITUDINAL AND TRANSVERSAL LOADING

Uniaxial Tensile test is conducted to find the strength and compare other material properties with the experimental part. In this case, we can use symmetrical mode for the rectangular specimen. Because it is hard to model the full model as the composite material is having complex geometry. So, we are reducing the model to unit length only in longer portion and using the hand calculations perform a sketch for the CF Filament position and extrude the elemental model to the finite distance with the material assignment. The Solid model is assigned the material property of ONYX and the CF lines are assigned the linked element as shown in the Figure *35*. In the case of symmetrical condition for transversal and longitudinal loading, the quarter or half of the specimen is modelled and symmetrical displacement boundary conditions are applied on the three sides of the model (as highlighted by "s" symbol in the Figure *36*) and the displacement load is subjected at top end (top area is applied the displacement as shown in Figure *36* as it is the unit length consideration to be acting tensile load).

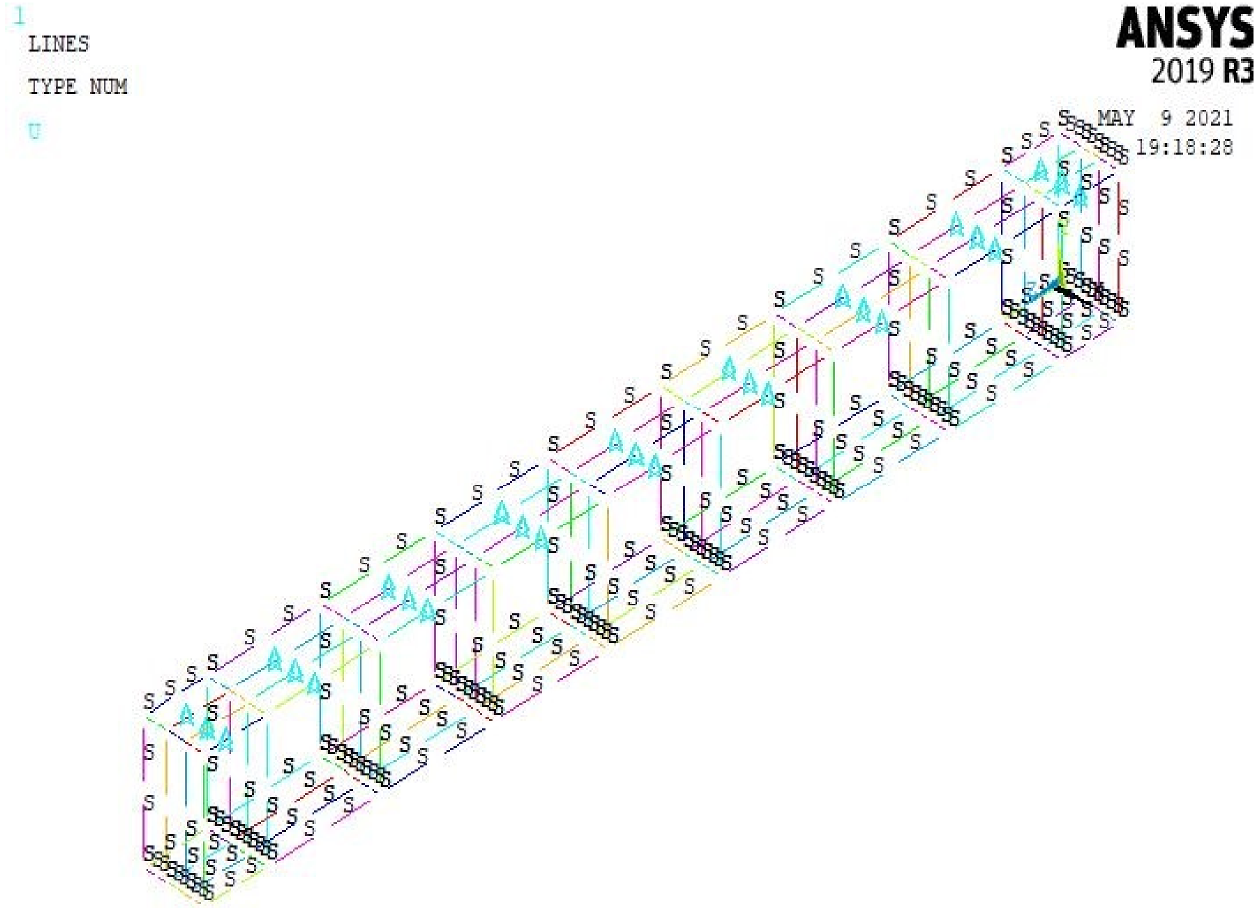

Figure 36 : Boundary condition for Longitudinal loading 21.3 % CF

5.3.2 SHEAR TESTING SPECIMEN

There are three boundary conditions for this specimen as we are doing tensile testing, shear testing and combined shear and tensile testing. The specimen is modelled only at the portion where the surface is allowed to deform, because we are not interested in the gripping area and its evaluation. For this experimental realization, we performed the test with V notch rail fixture. For this numerical simulation, we are performing MPC Algorithm in Ansys APDL to exactly control the stiffness as per the experiment. The aim of this algorithm is to create the pilot node at the coordinate where the load is acting on the testing machine experimentally. These pilot nodes are then connected to the top and bottom surfaces of the specimen where the V notch fixtures are held in the experiment.

- **Tensile Test :** The 3D model is aligned vertically and the lower pilot point, which is connecting the lower area, is restricted with the movement and rotation in all directions (X,Y,Z). Then the vertical displacement speed of 0.1 mm/min is provided at the top pilot node which is connecting the top area (Y direction). It is shown in *Figure 37*.

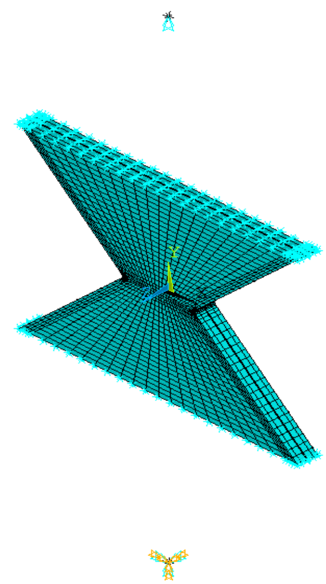

Figure 37 : Boundary condition for Tensile Testing of shear testing specimen

- **Shear Test :** The 3D model is aligned vertically and the left pilot node, which is connecting the lower area, is restricted with the movement and rotation in all directions (X,Y,Z). Then the horizontal displacement speed of 0.1 mm/min is provided at the right pilot node which is connecting the top area (X direction). It is shown in Figure *38*.

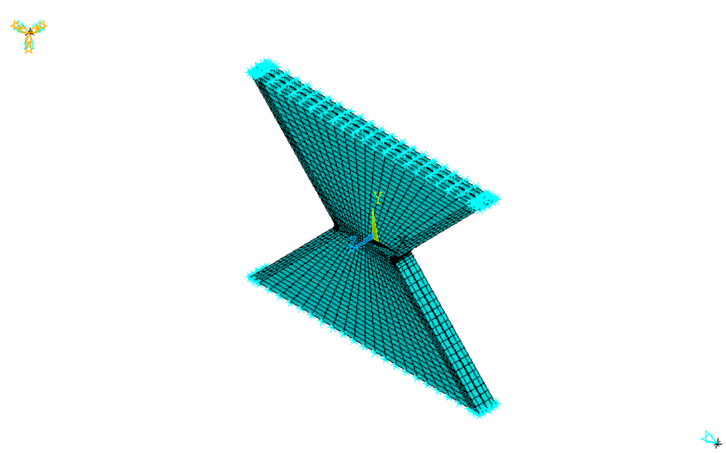

Figure 38 : Boundary condition for Shear Testing of shear testing specimen

- **Combined Test :** The 3D model is aligned vertically and the left corner bottom pilot node at 45°, which is connecting the lower area, is restricted with the movement and rotation in all directions (X,Y,Z). Then, the horizontal displacement speed of 0.1 mm/min is provided at the right corner top pilot point at 45°, which is connecting the top area (45° angle between X & Y coordinate direction). It is shown in Figure *39*.

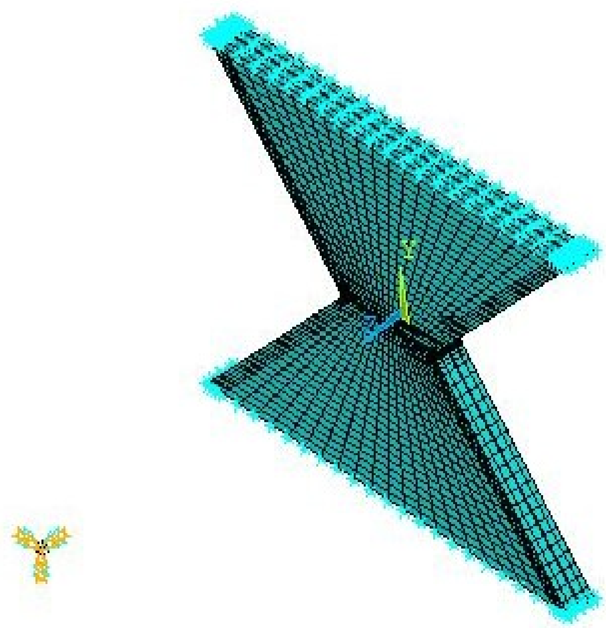

Figure 39 : Boundary condition for Combined Testing of shear testing specimen

5.4 STRAIN RATE SENSITIVITY

Strain controlled testing is nothing but a test conducted on the specimen with a constant strain rate. Tensile testing is commonly conducted to determine the maximum load or stress that the body can withstand for a particular period of time. Based on the strain rate influence followed by the experimental realization, the same strain rate is applied to the finite element simulation to compare the stress-strain curves to compare the results to evaluate the most interesting results and visualize the changes. This practice is applicable for time-dependent inelastic strains. Based on the experimental realization, the DIC optical measurement system reads the deformation, force and time history characteristics of the particular uniaxial loading process. The data are stored as CSV file which can be easily plotted as stress–strain curve in MS Excel to determine the time period at the maximum stress. These values are used in numerical simulations to predict the stiffness. The position rate is maintained for the simulations. However, the sensitivity of analysis to strain rate value is the most significant in the case of transverse loading. That is why two values of strain rate were used in this case: 0.0298%/s (corresponds to 2mm/min) and 0.00727%/s (corresponds to 0.5mm/min).

5.5 SIMULATION RESULTS – STRAIN CONTROLLED TEST

5.5.1 LONGITUDINAL LOADING

Table 10 shows the correlation between the experimental and numerical results. The comparison is very good and the error determination is discussed in the further topic.

Table 10 : Longitudinal loading of composite specimen

COMPOSITE SPECIMEN WITH CF [%]	EXPERIMENTAL ULTIMATE STRESS [MPA]	NUMERICAL SIMULATION		
		ULTIMATE STRESS OF COMPOSITE [MPA]	ULTIMATE STRESS OF CF FILAMENT [MPA]	ULTIMATE STRESS OF ONYX [MPA]
21.3	217.60	210.11	861.67	8.27
31.7	226.72	212.72	603.55	6.11
42.4	389.47	395.69	827.506	7.99
53.1	570.99	650.52	1085.63	9.945
63.7	618.65	725	1214.69	10.32

5.5.2 TRANSVERSE LOADING

The Table *11* shows the ultimate stress comparison between the experimental and numerical results for various specimens under transversal loading. Here the stiffness is similar for every Volumetric fraction of CF filament and the values extracted for 21.3 % and 31.7% numerical result is shown.

Table 11 : Transverse loading of composite specimen

COMPOSITE SPECIMEN WITH CF [%]	EXPERIMENTAL ULTIMATE STRESS [MPA]	NUMERICAL SIMULATION		
		ULTIMATE STRESS OF COMPOSITE [MPA]	ULTIMATE STRESS OF CF FILAMENT [MPA]	ULTIMATE STRESS OF ONYX [MPA]
21.3	20.61	31.16	1.92	26.65
31.7	21.53	27.86	1.72	22.35

5.5.3 TENSILE TESTING OF SHEAR TESTING SPECIMEN

The Figure *40* with plots shows the importance of the concentric fill of CF filament in comparison with pure Onyx material and the influence of the position rate. Those results are only obtained from numerical simulations. It shows the influence of position rate.

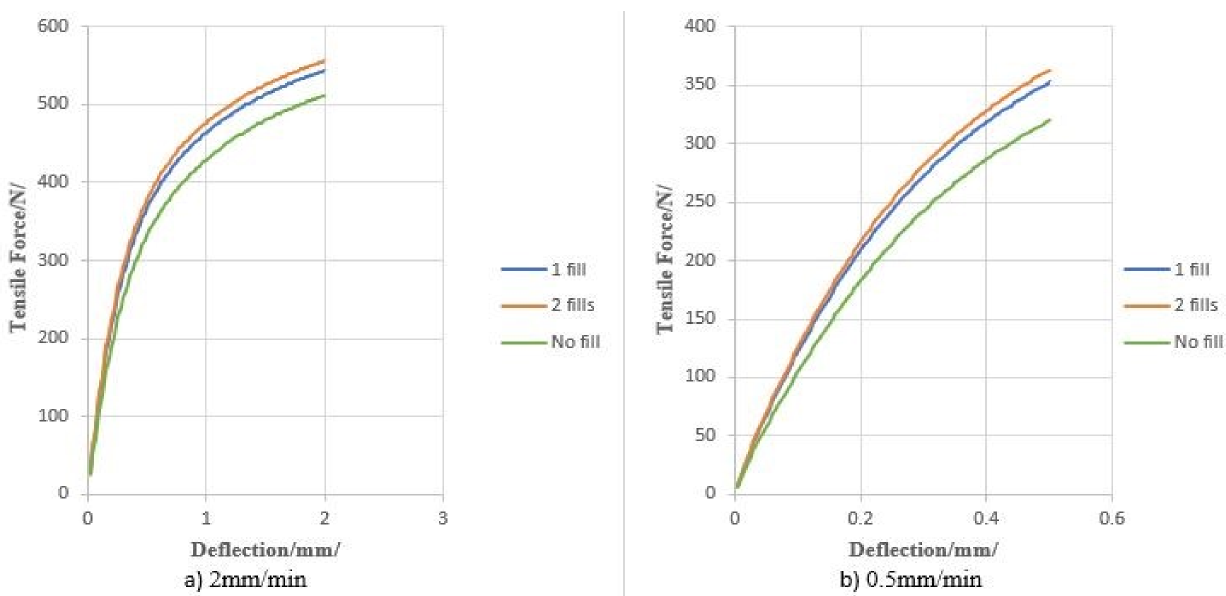

Figure 40: Tensile Force vs Deflection for shear testing specimen at position rates 2 mm/min and 0.5 mm/mm

5.5.4 SHEAR TESTING OF SHEAR TESTING SPECIMEN

The contour in Figure 41 shows clearly how the shear stress is acting on the CF filament in the shear loading mode of shear testing specimen. The opposite direction is showing similar response which is up to the actual assumption. The contour units of stress are in MPa.

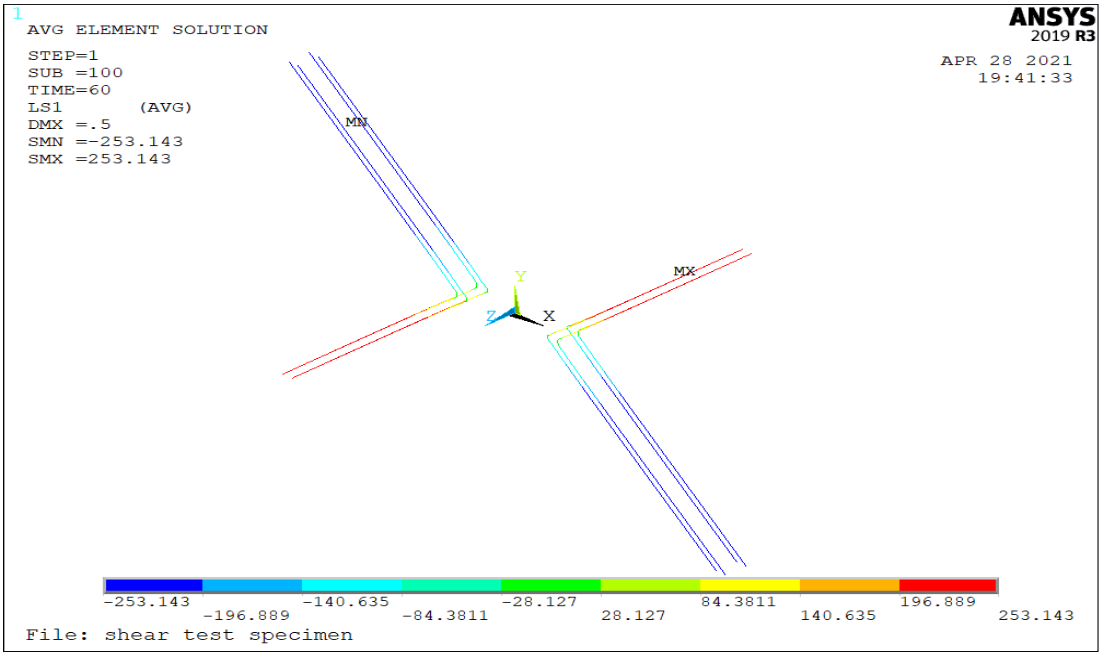

Figure 41: Stress Contour of 2-fill composite specimen under shear loading in x direction

The contours in Figure 42 show clearly how the shear stress is acting on the Composite specimen in MPa. We can exactly visualize that the maximum shear occurs at the middle portion where the thickness is less.

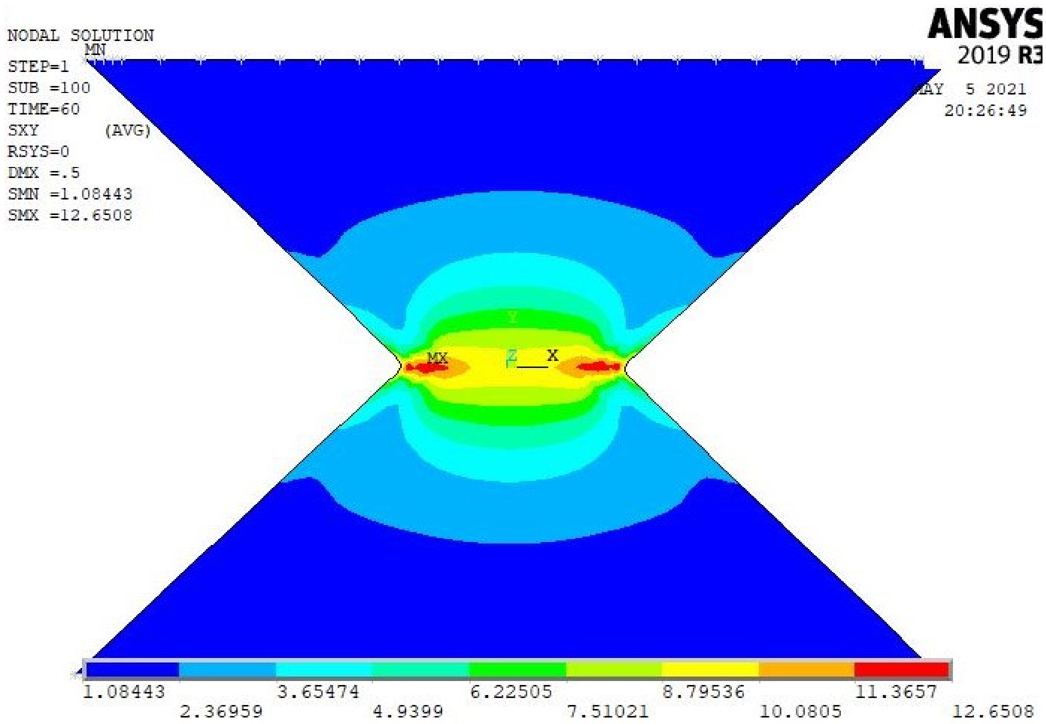

Figure 42: XY shear stress contours obtained for the shear loading case

6 COMPARISON OF EXPERIMENTAL AND NUMERICAL RESULTS – STRAIN CONTROLLED LOADING

The strain-controlled test results for the longitudinal loading in Figure *43* clearly depict low volumetric fraction, i.e. (21.3%, 31.7 %, 42.4 %) are having nice correlation and giving exactly comparable results but the other specimen with more VF is getting deviations when loaded more. The deviations may occur due to the link element consideration in CF Filament material assignment. Instead of this, the beam element consideration is preferable to achieve more accurate results. We can see the stiffness gets increased when we introduce more CF filaments but the expensive of CF will be the thing to be under consideration in this case.

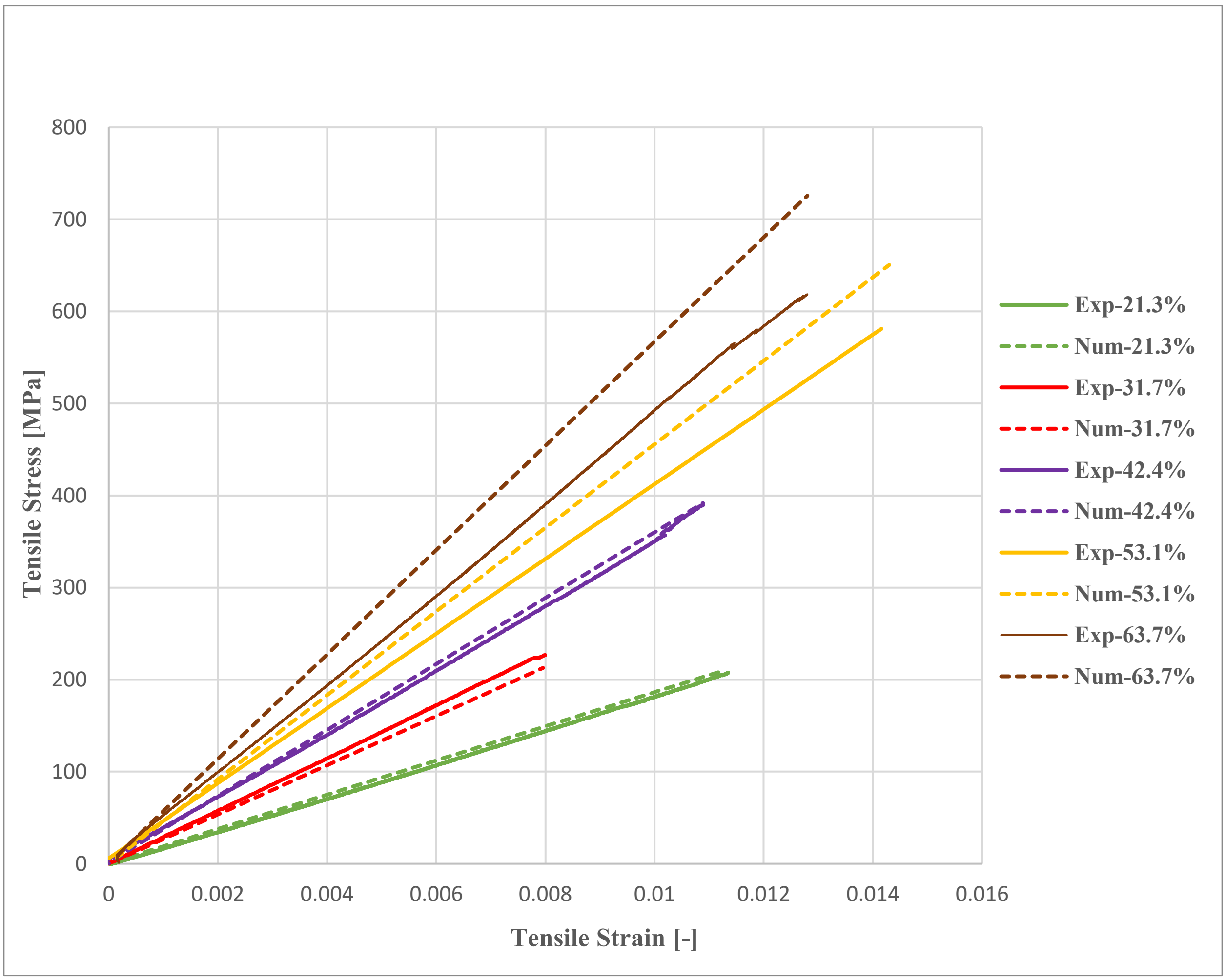

Figure 43: Comparison of experimental and numerical Tensile Stress vs strain for Longitudinal loading Composite (Onyx + CF) Specimen with different volumetric fraction

The difference of numerical and experimental ultimate stress value results is calculated as

$$Difference = \left|\frac{Exp\ Ult\ stress - Num\ ult\ stress}{Exp\ Ult\ stress}\right| \cdot 100 \tag{6.1}$$

The difference of numerical and experimental ultimate stress calculated in accordance with the equation (6.1) is plotted in the graph shown in Figure 44. The error is increasing with the amount of CF filament.

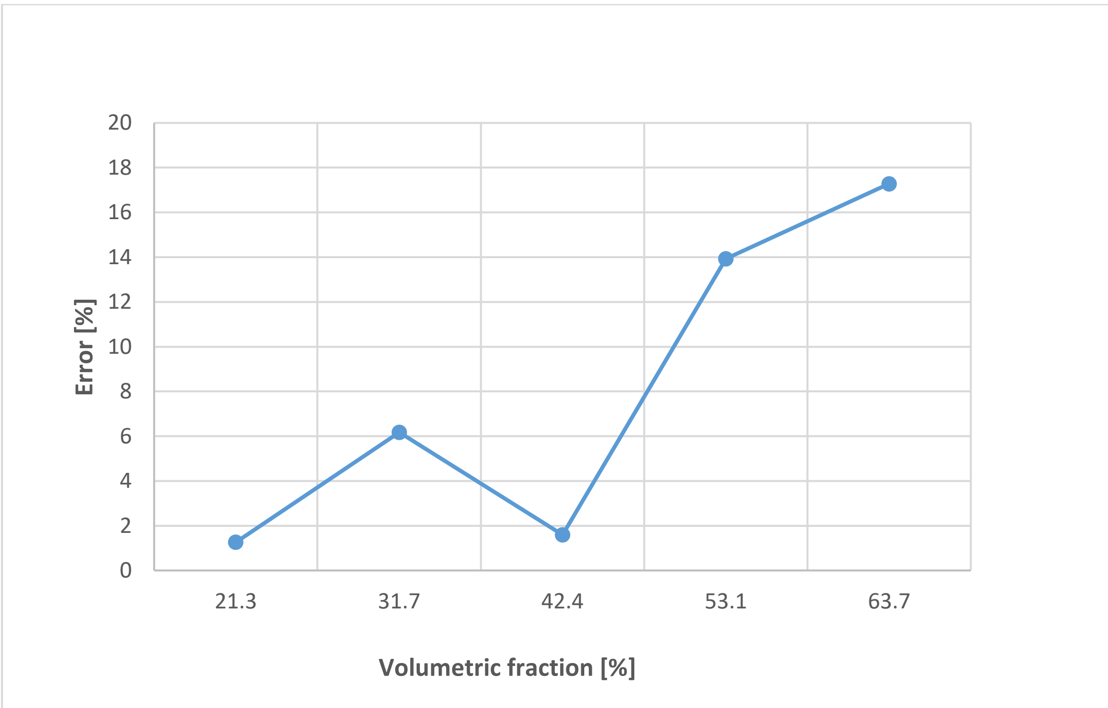

Figure 44 : Difference between Experimental and Numerical Ultimate stress Results for Longitudinal loading

The strain-controlled test results as shown in Figure *45* for the transversal loading. The numerical and experimental results for all volumetric fraction of CF filament gives exactly similar stiffness even though some experimental results are getting diverged after 30% strain due to improper glue between layers. Here the numerical result of only one specimen is compared with the all-experimental results in the Figure *45*. The similar stiffness from the experimental and numerical realization shows the CF filament effect is negligible in case of transversal loading. Also, the position rate influence is negligible in the transversal loading. It depicts the comparable resulting curve and the deviations may occur in the nonlinear part in the transversal loading due to the link element consideration in FEM analysis. Instead of this, the beam element consideration is preferable to achieve more accurate results.

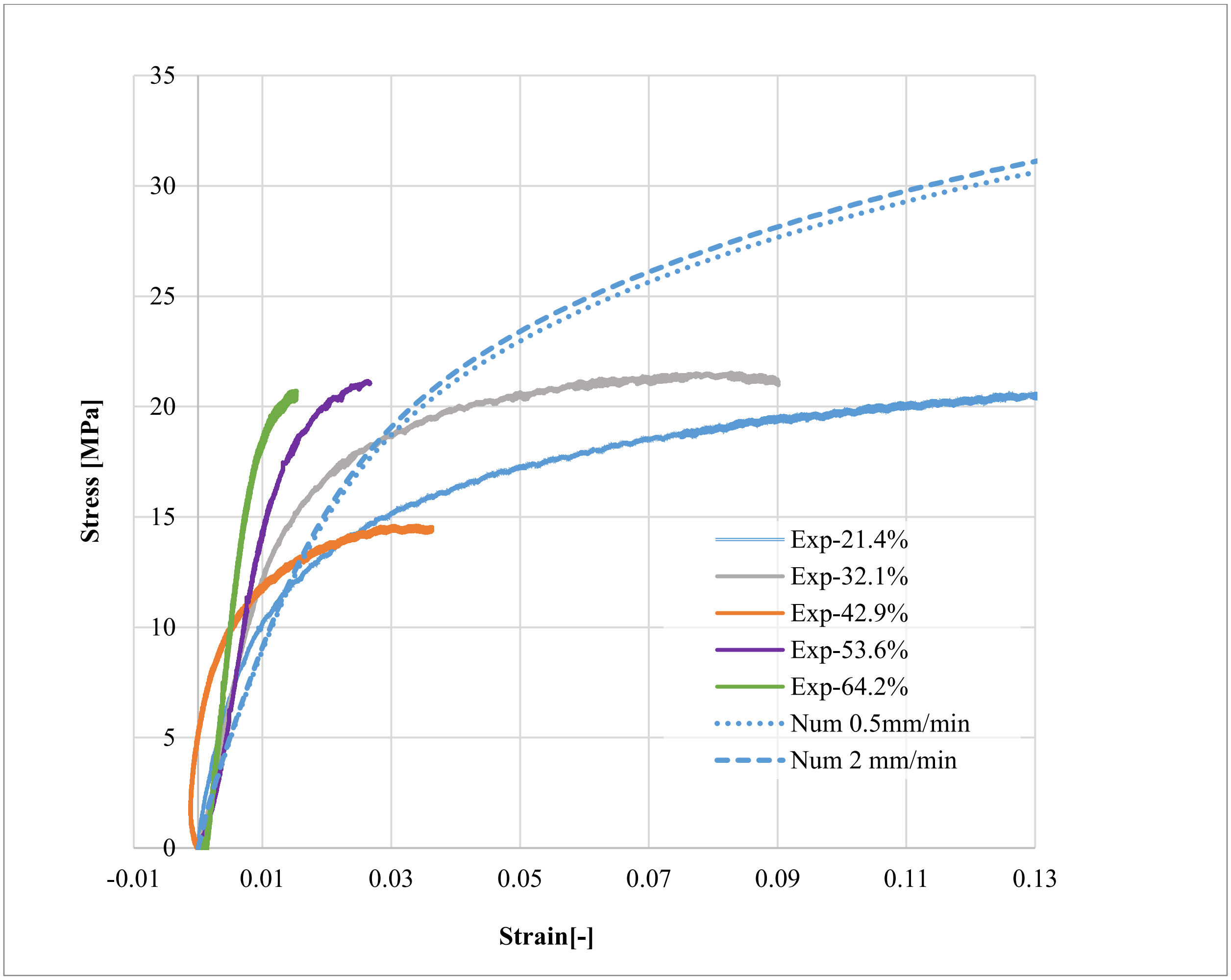

Figure 45: Comparison of experimental and numerical Tensile Stress Vs strain for transversal loading Composite (Onyx + CF) Specimen with different volumetric fraction

Figure 46, Figure 47 and Figure 48 show the comparison of the numerical and experimental results for shear testing specimen which are having nice correlation. The deflection of the specimen in the normal direction of loading is calculated using the path operation in ANSYS APDL as shown in Figure *49*. These results show clearly the predictions are working in simulations. Figure *46* and Figure *48* clearly shows the simulation results are having respectable deviations which can be minimized when considering material model according to datasheet [22] instead of pavlicek model assumption [12]. But the Pavlicek model is working well in the shear loading stiffness prediction as shown in Figure 47. The loading was very low to do not generate any irreversible strain. We can realize more tests with irreversible strain part to visualize more regarding the comparison.

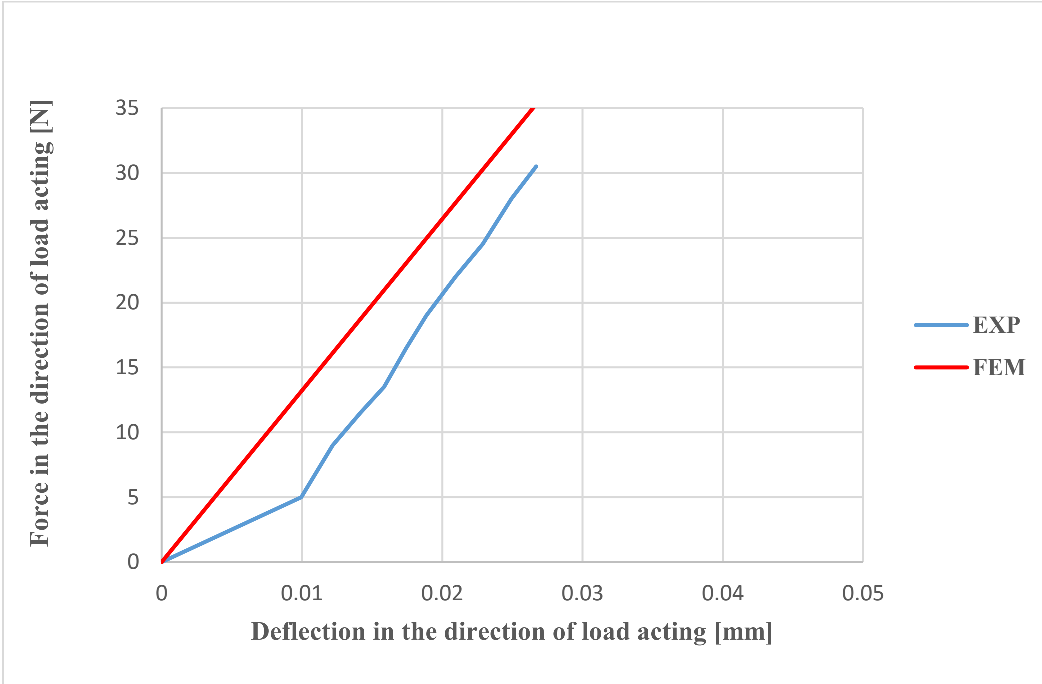

Figure 46 : Experimental VS Numerical simulation comparison of Shear testing specimen – Tensile loading

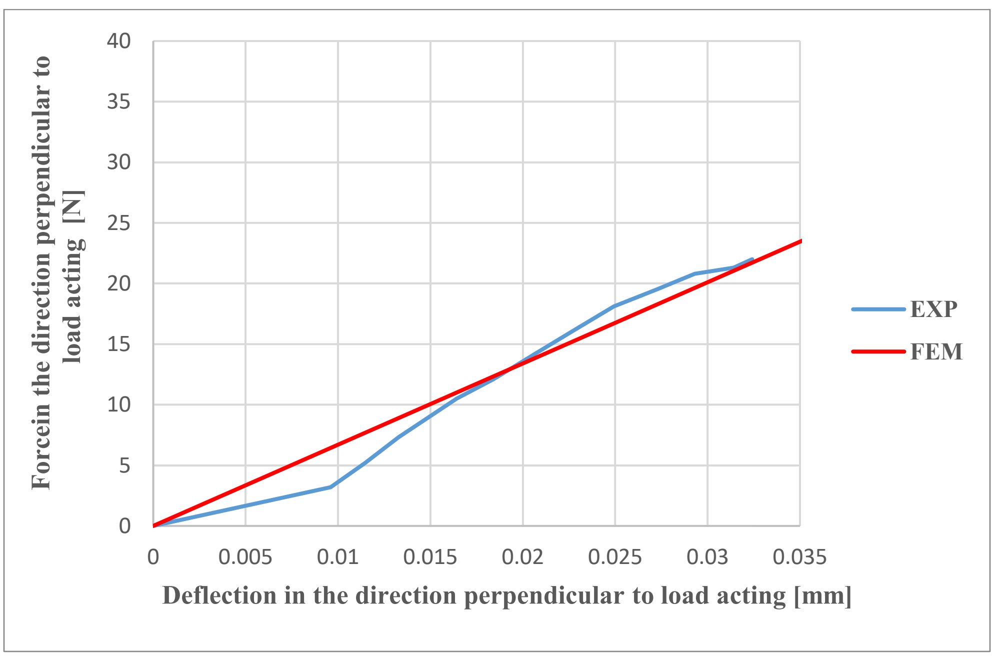

Figure 47: Experimental VS Numerical simulation comparison of Shear testing specimen – Shear loading

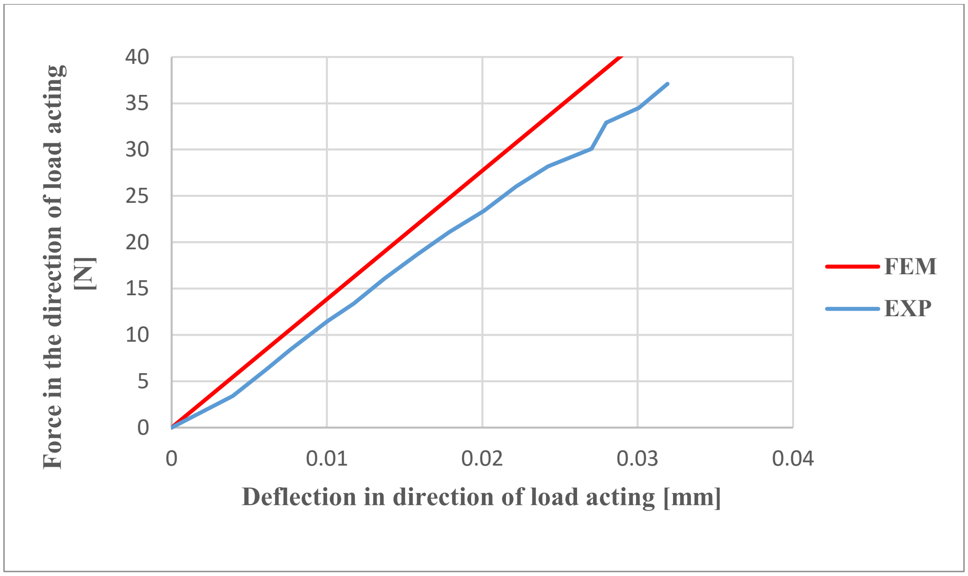

Figure 48 : Experimental VS Numerical simulation comparison of Shear testing specimen – Combined loading

The Path Operation is performed in order to exactly predict the actual deformation undergone in the force application for shear, tensile and combined loading case. The unit mentioned in the Figure *49* contours is in millimeter and it denotes the displacement in Y direction. It shows the distribution of the deformation of the specimen to exactly find out the deflection in Y direction.

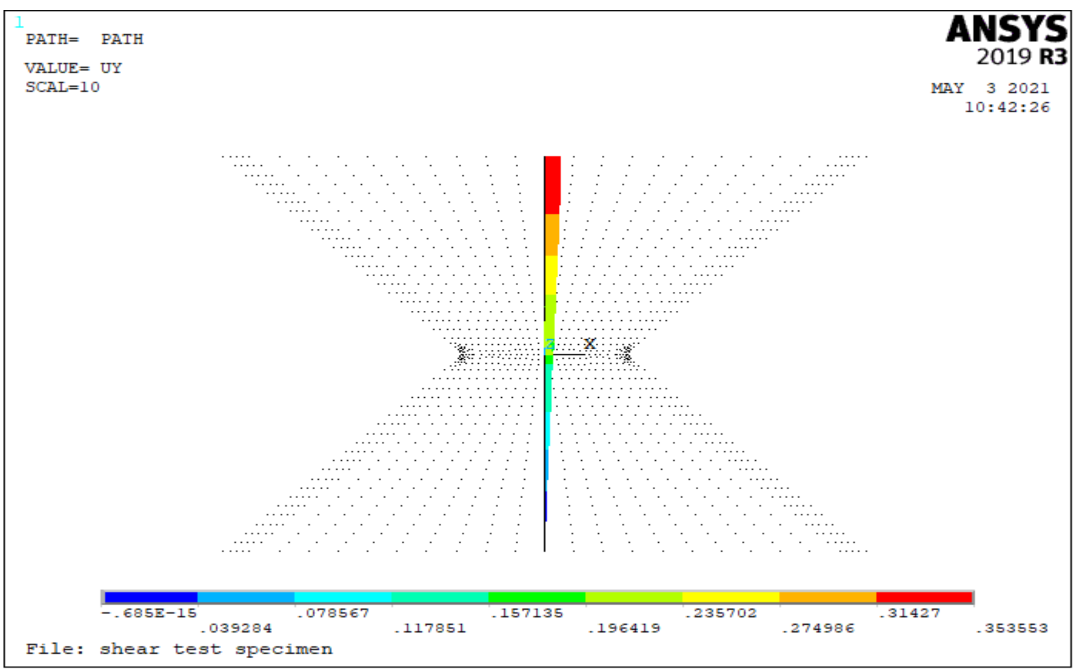

Figure 49 : Distribution of displacement in Y direction

7 ANALYTICAL RESULTS

7.1 LONGITUDINAL LOADING USING ANALYTICAL METHOD

The Table *12* show the material model as per the data sheet [22] . Based on the equation (2.9), we can find the young's modulus in the analytical way as tabulated in the Table *13*.

Table 12 : Material Parameter according to Data sheet [22]

Material	Young's Modulus [MPa]	Symbols
ONYX	1400	E_M
CF	60000	E_F

Table 13 : Young's modulus determination from analytical method for Longitudinal loading

Composite Specimen with CF [%]	Analytical Approach
	Young's Modulus of composite [MPa] E_C
21.3	13881.8
31.7	19976.2
42.4	26246.4
53.1	32516.6
63.7	38728.2

In the FEM simulation done under transversal loading, the fiber with curved part at the bending of CF line to join the other layer is also modelled. So, these results are not enough to get the material strength for individual layer parameters easily. We can use different method of simulation to find out the individual material response.

8 GRAPHICAL COMPARISON OF ANALYTICAL METHOD WITH OTHER METHODS – LONGITUDINAL LOADING

The Figure 50 show the comparison for longitudinal loading between our experimental results averaged value for each speed ratio along with the numerical simulation results (done with the material model according to Pavlicek [12]) and the analytical results obtained from solving the equations as shown in the Table *13*. The correlations are very good and it clearly gives the idea that the material properties are very well predicted and the simulations and experiments are quite predictable in the case of longitudinal loading. The experimental results shown here are the one which obtained by averaging the values for each specimen tested under different position rate. It shows that the simulations are very good and the error will be minimized when considering the material model according to the datasheet [22]. It is recommendable to consider beam element in this case along with the material model according to the data sheet for getting accurate result as compared to experiments.

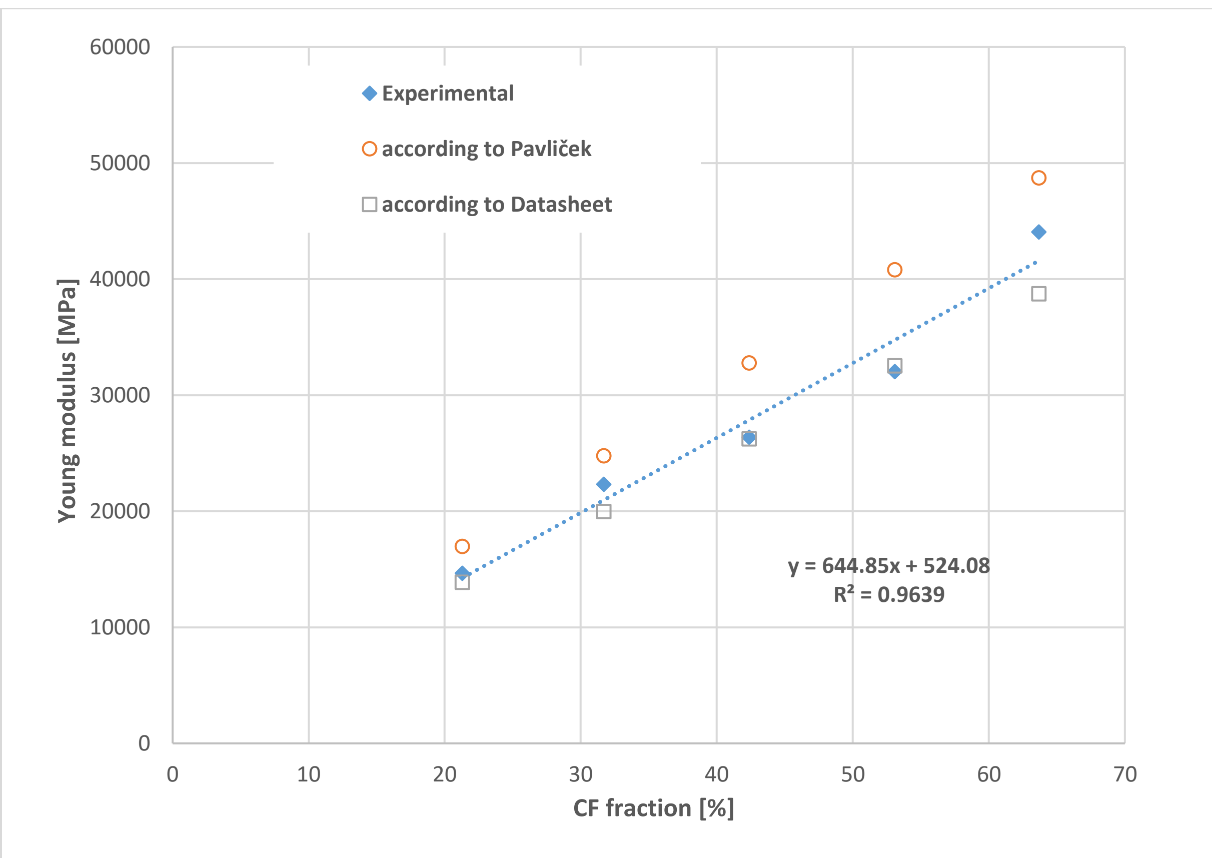

Figure 50: Correlation of five longitudinal specimen for different volumetric Fraction

9 CONCLUSION

The main aim of this diploma thesis is to develop a FE simulation strategy for various tests of the thermoplastic composite material produced by Markforged X7 3D printer (Onyx reinforced with unidirectional CF filament). Even though 3D printed materials are widely popular in the current market, most of the parts are only utilized in prototyping. This disadvantage is taken under consideration in this work to improve the quality of the parts produced by the additive manufacturing technique Chapter 2 deals with the overview of the production techniques of composite materials by additive manufacturing techniques and the mechanism behind printing and predefining the internal structure of the composite using Eiger Software. Moreover, it elaborates the testing methodology and its specification of the tools and fixtures used in the experimental set-up. This part also explains the numerical simulation and analytical methods used for analyzing the composite produced by layer-by-layer fusion. Chapter 3 shows the complete design of the specimen for different loading cases and for different materials. The design is specified based on the literature survey and the dimensions of the specimen are according to ASTM D3039 Standard for composite materials.

Chapter 4 deals with the experimental realization of the tensile testing of a rectangular specimen loaded in the longitudinal and transversal direction of the CF filament and also the tensile, shear, and combined loading of the shear testing specimen produced by Markforged X7 printer. The experimental realization was mainly focused on the elastic domain even though the test is performed until the fracture of the specimen. Every test was performed under strain-controlled loading with DIC optical measurement to predict the strength of the material. Based on the volumetric fraction of the specimen, the ultimate strain varies and it shows the ductility of the material strictly depends on the CF filament. For the shear testing specimen, the V notch rail attached measurements are realized and it gives good correlation between the numerical and experimental results of force vs Deflection curve.Chapter 5 deals with the numerical and analytical study of the specimen which were tested. It utilized finite element simulation with reduced model. The Unit length model is simulated and the errors in comparison with other methods are very less and reliable. In the case of transversal loading, beam element consideration is recommendable than the link element for the CF Filament geometry. These results show that the simulation technique is still possible to predict the behavior of the composites produced by Markforged 3D printer.

Chapter 6 and 7 show the most important results which were obtained during the investigation. The comparison graph for longitudinal loading depicts that the specimen with different volumetric fraction of carbon fiber exactly predicts the response in the simulation compared to another specimen. And it also clearly shows that the influence of ONYX is not so significant for the longitudinal loading. The maximum stress will be acting on the CF filament and the surface which are in contact with the filament. As CF filaments are brittle material, it is the one which is more stressed in the composite. For transversal loading, the curved path covered by the CF filament due to 3D printing will be almost acting normal to the load direction which is stressed more as it is similar to longitudinal loading and it may cause fracture inside the composite. The pilot node consideration in the finite element simulation using MPC Algorithm in Ansys APDL creates the opportunity to predict the stiffness efficiently. The correlation of numerical and experimental results is quite good and this method can be useful for researchers in the future simulations. Considering shear testing specimen with two concentric fills of CF filament, numerically it is proved that more the fills more the strength of composite.

This study shows evidence that increasing the volumetric fraction of CF Filament between ONYX provides better strength for longitudinal loading but for transversal loading, the stiffness is maintained constant for different volumetric fraction of CF filament. The FEM simulations with correct prediction gives good correlation. The material model according to the data sheet [22] gives good correlation of numerical results with experimental value. The influence of position rate is not influenced in longitudinal loading because of the CF filaments which absorb the normal stress but it creates the issue in transverse loading as the filaments is not creating any effect as it is aligned perpendicular to the loading direction. It is recommended to use Onyx in the outer layer and in the middle layer as it will give surface finish to the composite and carbon fiber is the brittle material and it has to be layered between Onyx for better strength. In experimental realization, we can see the non-linear curve response almost for many specimens which is due to the un even starting speed and gripping. Clearly the investigation shows that CF filament are causing great influence with Onyx as a composite produced by 3D printing. As the loading direction creates influence to the filaments, placement of the filament must be in according with the consideration of the phenomenon in which operation and condition, the material is going to be used. The different orientation and positioning of the fiber can be easily done by 3D printing and it will be the best possible way in this case.

10 ACKNOWLEDGMENTS

This research was supported by the Technology Agency of the Czech Republic in the frame of the project TN01000024 National Competence Center-Cybernetics and Artificial Intelligence. The thesis has also been done in connection with project Innovative and additive manufacturing technology— new technological solutions for 3D printing of metals and composite materials, reg. no. CZ.02.1.01/0.0/17_049/0008407 financed by Structural Funds of Europe Union.

11 REFERENCE

[1] A, NIKHIL., 2021. 3D Printing Processes - Material Extrusion (Part 2/8). [online] Engineers Garage. Available at: https://www.engineersgarage.com/tech-articles/3d-printing-processes-material-extrusion-part-2-8/.

[2] RAJKUMAR AROKIARAJ JAMES AKSHAY NICHOLAS, Investigation of stress-strain behavior in ONYX material. Ostrava: VSB Technical University of Ostrava, Faculty of Mechanical Engineering, Department of Applied Mechanics, 2020. Supervisor: Prof. Ing. RADIM HALAMA, Ph.D.

[3] Markforged. 2021. 3D Printing Process. [online] Available at: https://markforged.com/resources/learn/3d-printing-basics/how-do-3d-printers-work/3d-printing-process.

[4] SUPRIYA.S. GADHE, DR. R.R. NAVTHA., 2021.Digital Image Correlation Technique for Strain Measurement of Aluminum Plate [online] in International Journal of Engineering Trends and Technology (IJETT) – Volume 39 Number 6- September 2016. Available at: https://www.researchgate.net/publication/310790368_Digital_Image_Correlation_Technique_for_Strain_Measurement_of_Aluminium_Plate.

[5] Digitalimagecorrelation.org. 2021. [online] Available at: https://digitalimagecorrelation.org.

[6] JOSEPH R. DAVIS, Introduction to tensile testing, Google Books. 2021. Tensile Testing, 2nd Edition. [online] Available at: https://books.google.cz/books?id=5uRIb3emLY8C&printsec=frontcover&hl=cs&source=gbs_ge_summary_r&cad=0#v=onepage&q&f=false.

[7] FIDAN, I., IMERI, A., GUPTA, A., HASANOV, S., NASIROV, A., ELLIOTT, A., ALIFUI-SEGBAYA, F. AND NANAMI, N., 2021. The trends and challenges of fiber reinforced additive manufacturing.

[8] ARIZONA, T. and University, V., 2021. The Finite Element Method and Applications in Engineering Using ANSYS® | SpringerLink. [online] Link.springer.com. Available at: https://link.springer.com/book/10.1007/978-1-4899-7550-8.

[9] GHEBRETINSAE, F., MIKKELSEN, O. AND AKESSA, A., 2019. Strength analysis of 3D printed carbon fiber reinforced thermoplastic using experimental and numerical methods. IOP Conference Series: Materials Science and Engineering, 700, p.012024.

[10] BHUVANESH GOVINDARAJ, Digital Image Correlation and its Application for Accelerated Testing of Specimens Manufactured by 3D Printing. Ostrava: VSB - Technical University of Ostrava, Faculty of Mechanical Engineering, Department of Applied Mechanics, 2020, 68 p. Supervisor: Prof. Ing. RADIM HALAMA, Ph.D.

[11] HART R J, PATTON E G AND SAPUNKOV O 2018 Characterization of continuous fiber-reinforced composite materials manufactured via fused filament fabrication. Technical report, available at: https://apps.dtic.mil/dtic/tr/fulltext/u2/1062410.pdf.

[12] PAVLICEK, P., FOJTÍK, F., FUSEK, M., 2020. Testing Carbon Fibers for 3D Printing. In: Proceedings of 58th International Scientific Conference EXPERIMENTAL STRESS ANALYSIS 2020, October 19 – October 22, 2020, online, Czech Republic, Editors: MARTIN FUSEK, JAKUB CIENCIALA, MICHAL KOŘÍNEK, VOJTĚCH MACHALLA, JIŘÍ ŠMACH, p. 382-386.

[13] ABDUL KAREEM F. HASSAN, OSAMA A. ABDULLAH., New Methodology for Prestressing Fiber Composites 2021. [online] Available at: <https://www.researchgate.net/publication/291820239_New_Methodology_for_Prestressing_Fiber_Composites> [Accessed 26 April 2021].

[14] DR-SEIF.com. Standard Test Method for Shear Properties of Composite Materials by V-Notched Rail Shear Method., 2021. [online] Available at: <http://www.dr-seif.com/content/ME313-HO5.pdf> [Accessed 30 April 2021].

[15] TATIPALLI, V., 2021. Analytical modification of the V-notched rail shear test apparatus for dynamic testing. [online] Semanticscholar.org. Available at: <https://www.semanticscholar.org/paper/Analytical-modification-of-the-V-notched-rail-shear-Tatipalli/b969b4efbc24d8f9ae4371021245d24d92c312bc> [Accessed 1 May 2021].

[16] FATHOLLAH TAHERI-BEHROOZ, HOSEIN SALEHI MOGHADDAM., Nonlinear numerical analysis of the V-notched rail shear test specimen, Reader.elsevier.com. 2021. [online] Available at: <https://reader.elsevier.com/reader/sd/pii/S0142941817314198?token=DFE116D59DDD868D15DAFADFA52B6711558974F2DC406A94E2EA4F0E0A422EBE62C7C65E2772E8A44C2DF5CBFACA7&originRegion=euwest1&originCreation=20210504070029>[Accessed 4 May 2021].

[17] JOHNSON, JEFFREY DOUGLAS, The University of Utah. ProQuest Dissertations Publishing, 2010. 1474674 Search.proquest.com. 2021. Development and evaluation of the Combined Loading Modification to the V-Notched Rail Shear Test method for composite laminates - ProQuest. [online] Available at: <https://search.proquest.com/openview/7cbbef6d86afca2fafbad9c2be54c1a0/1?cbl=18750&diss=y&pq-origsite=gscholar> [Accessed 4 May 2021].

[18] GUDE, M., HUFENBACH, W., ANDRICH, M., MERTEL, A. AND SCHIRNER, R., 2015. Modified V-notched rail shear test fixture for shear characterization of textile-reinforced composite materials. Polymer Testing 43, pp.147-153.

[19] INDIAN INSTITUTE OF TECHNOLOGY, DELHI., Composite Analysis for Modulus and Strength in the Longitudinal Direction, Youtube.com. 2021. Composite Analysis in Longitudinal orientation. [online] Available at:<https://www.youtube.com/watch?v=WhcBM568TlM&list=PL4sLD19zR1iU5YiUD4MawcVW7LSyLivOb&index=3&t=876s> [Accessed 6 May 2021].

[20] INDIAN INSTITUTE OF TECHNOLOGY ,DELHI., Composite Analysis for Modulus and Strength in the transversal Direction Youtube.com. 2021. Composite Analysis in Transverse orientation. [online] Available at: <https://www.youtube.com/watch?v=HGgrOpfpkA&list=PL4sLD19zR1iU5YiUD4MawcVW7LSyLivOb&index=2> [Accessed 6 May 2021].

[21] HE, Q., WANG, H., FU, K. AND YE, L., 2020. 3D printed continuous CF/PA6 composites: Effect of microscopic voids on mechanical performance. Composites Science and Technology, 191, p.108077.

[22] '3D Printing Materials', Markforged. https://markforged.com/materials (accessed Nov. 04, 2020).

LIST OF ANNEXURES

Appendix 1 Longitudinal Loading – 21.3% VF

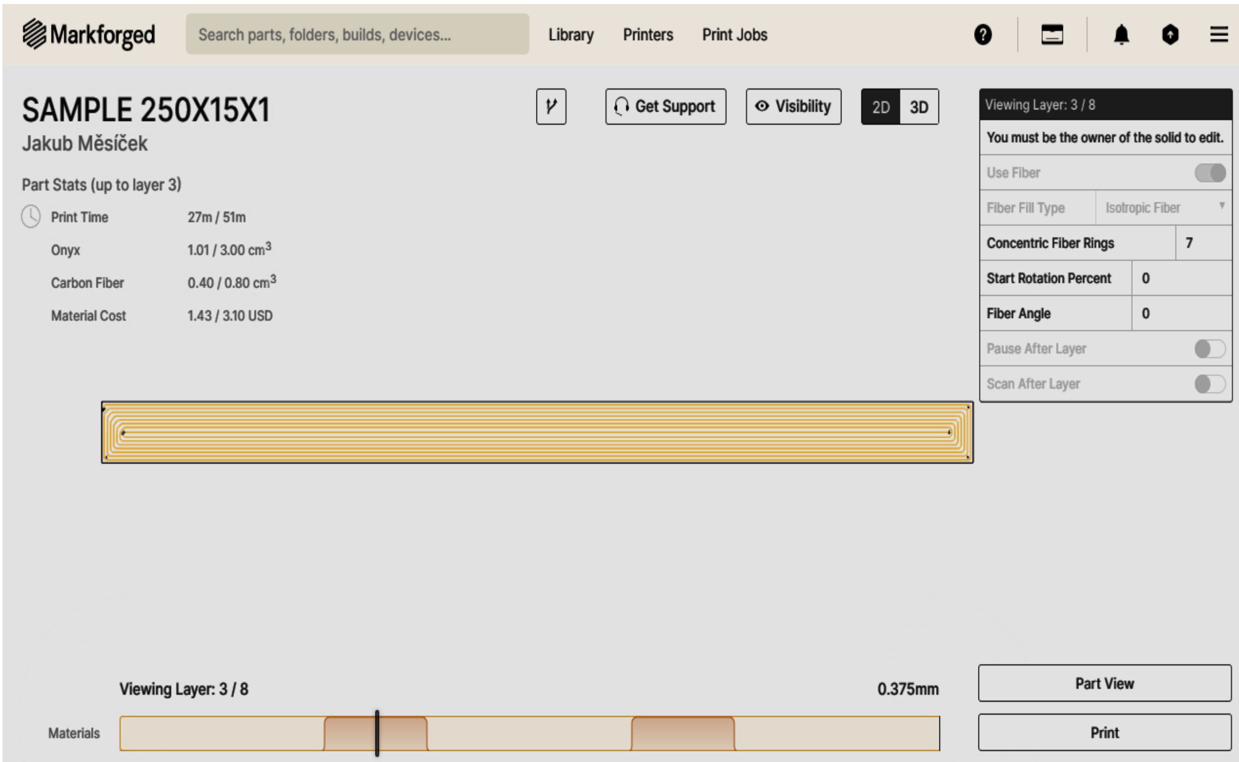

Appendix 2 Longitudinal Loading – 31.7% VF

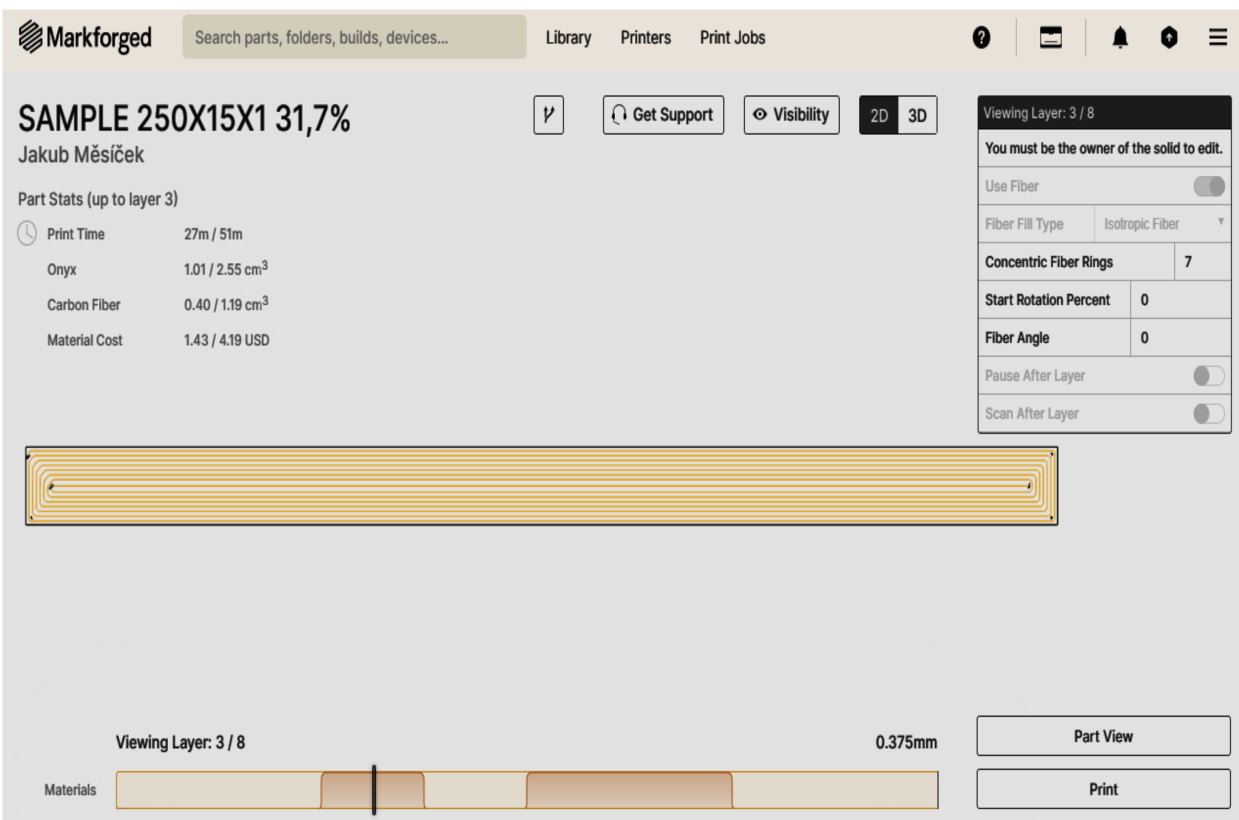

Appendix 3 Longitudinal Loading – 42.4% VF

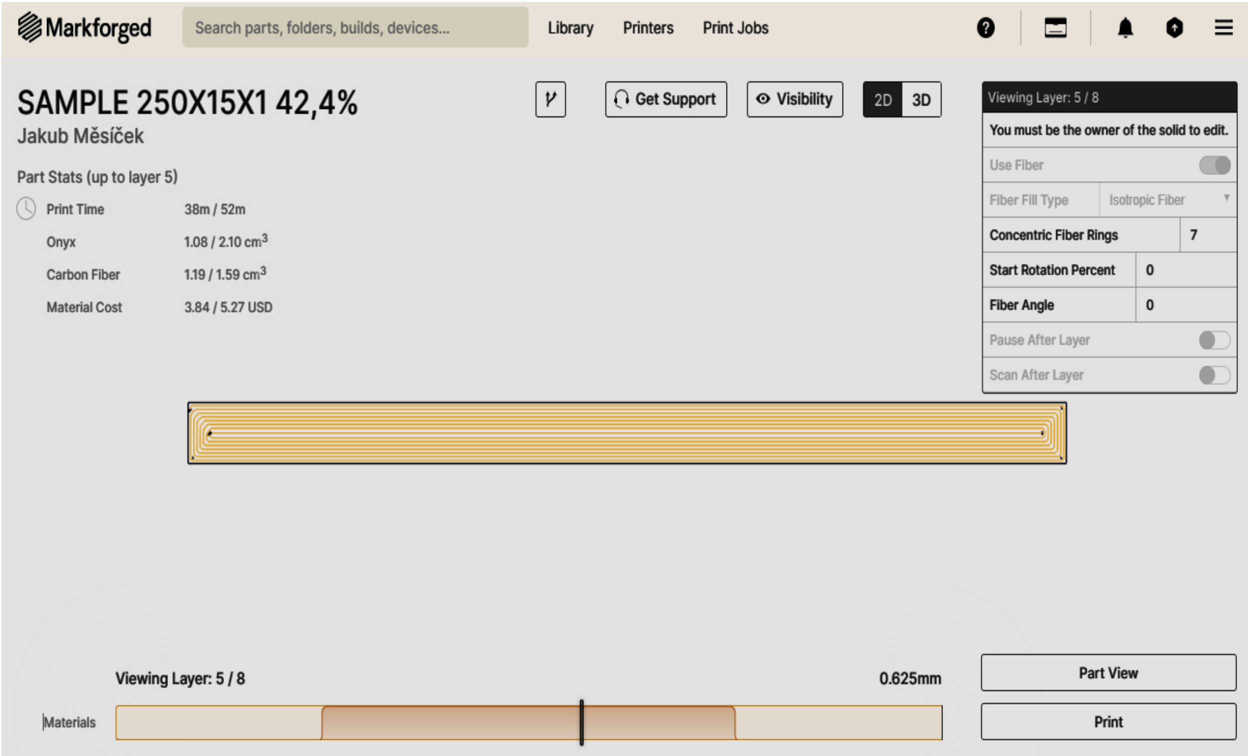

Appendix 4 Longitudinal Loading – 53% VF

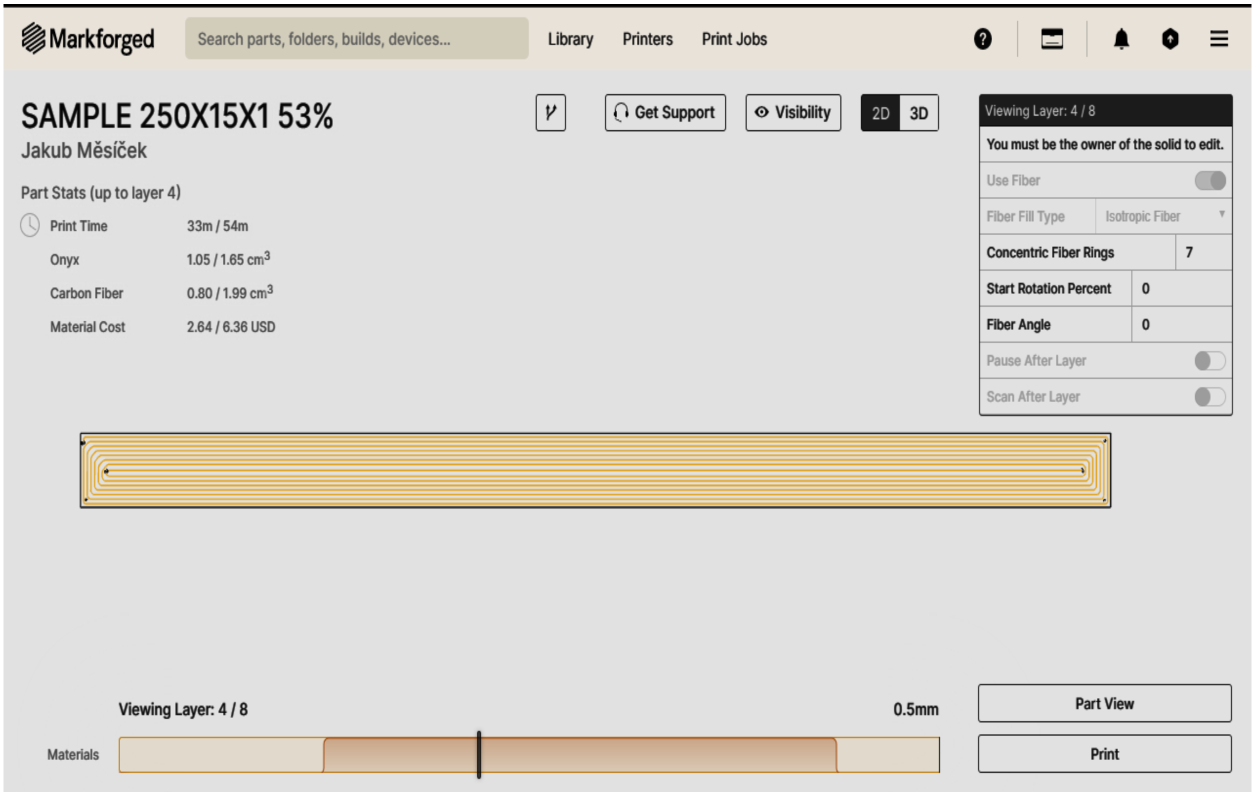

Appendix 5 Longitudinal Loading – 63.7% VF

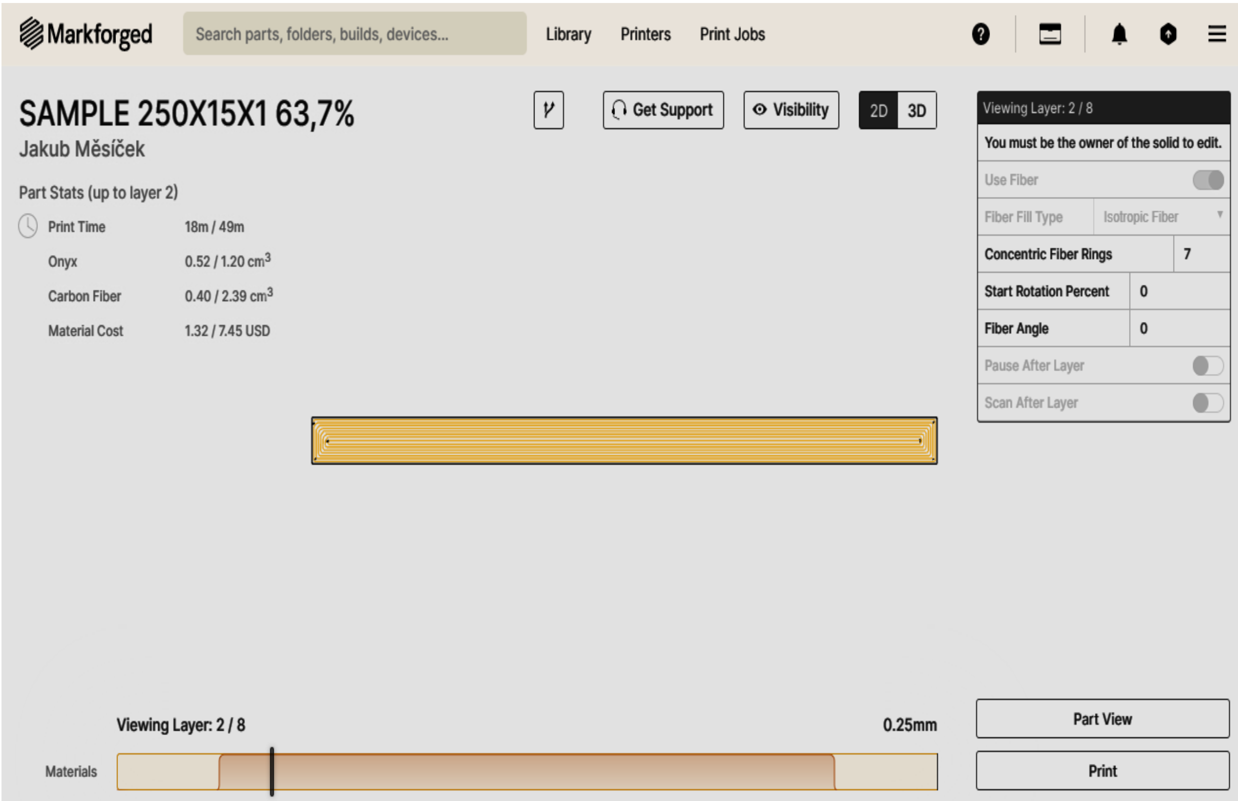

Appendix 6 Transverse Loading – 21.4% VF

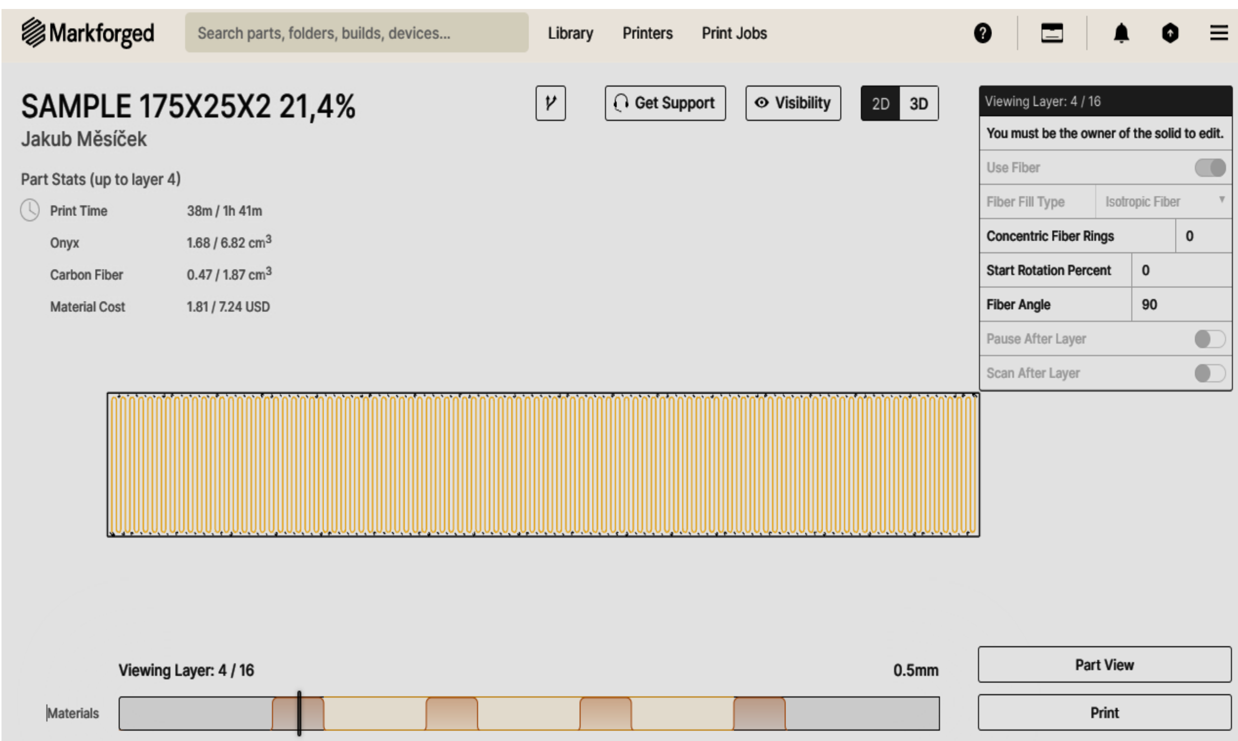

Appendix 7 Transverse Loading – 32% VF

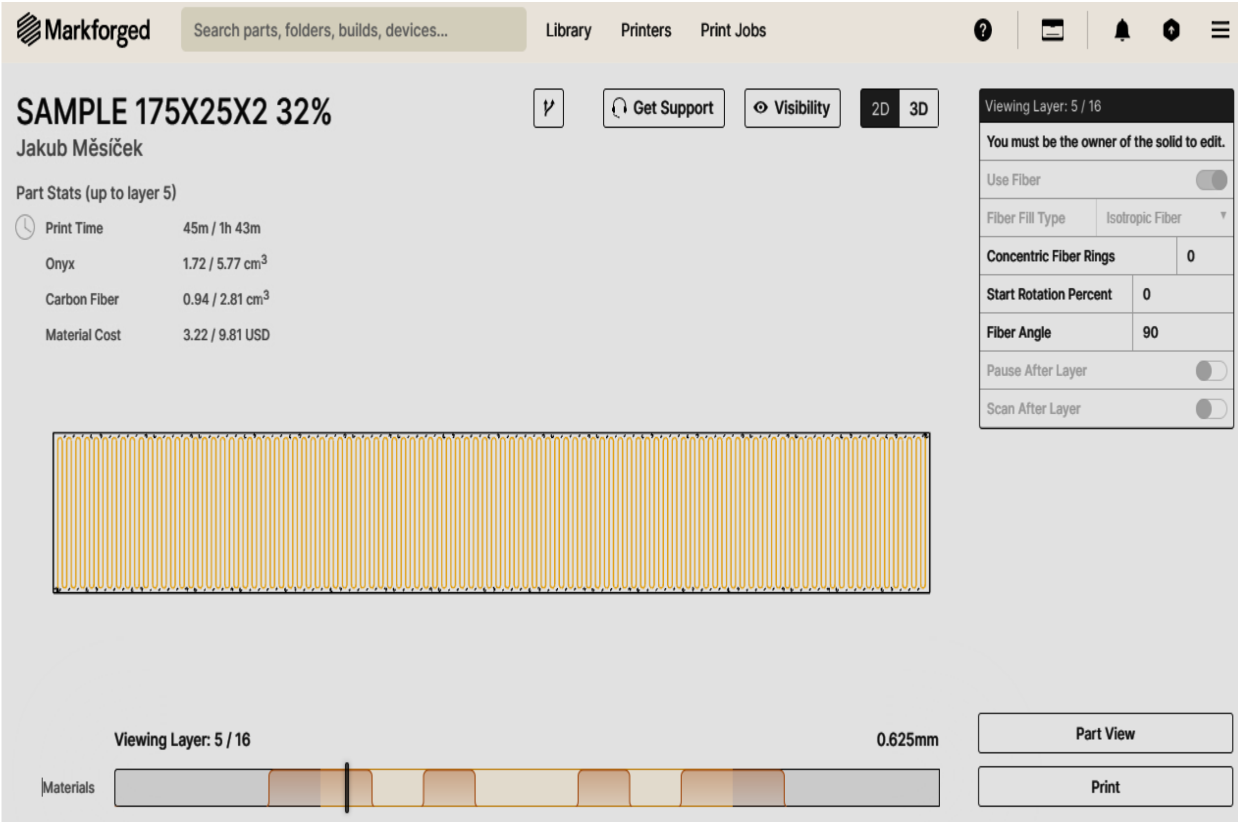

Appendix 8 Transverse Loading – 42.9% VF

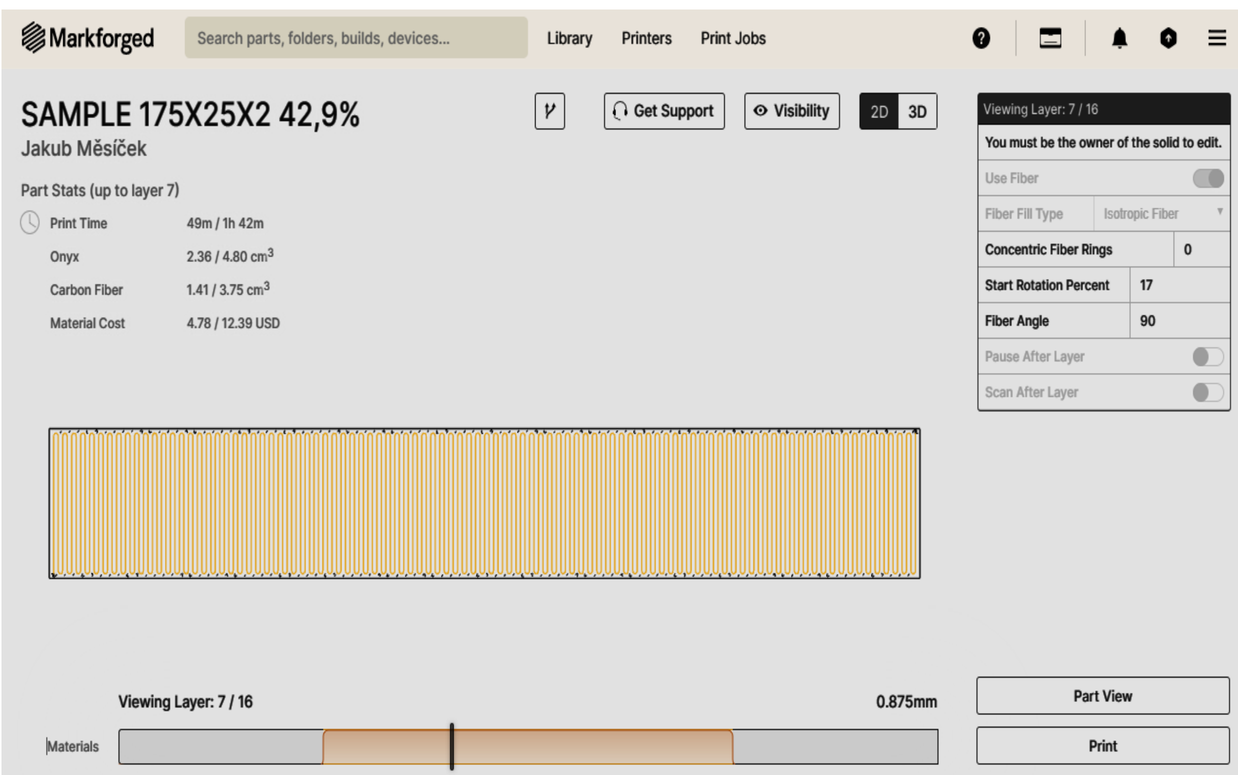

Appendix 9 Transverse Loading – 53.6% VF

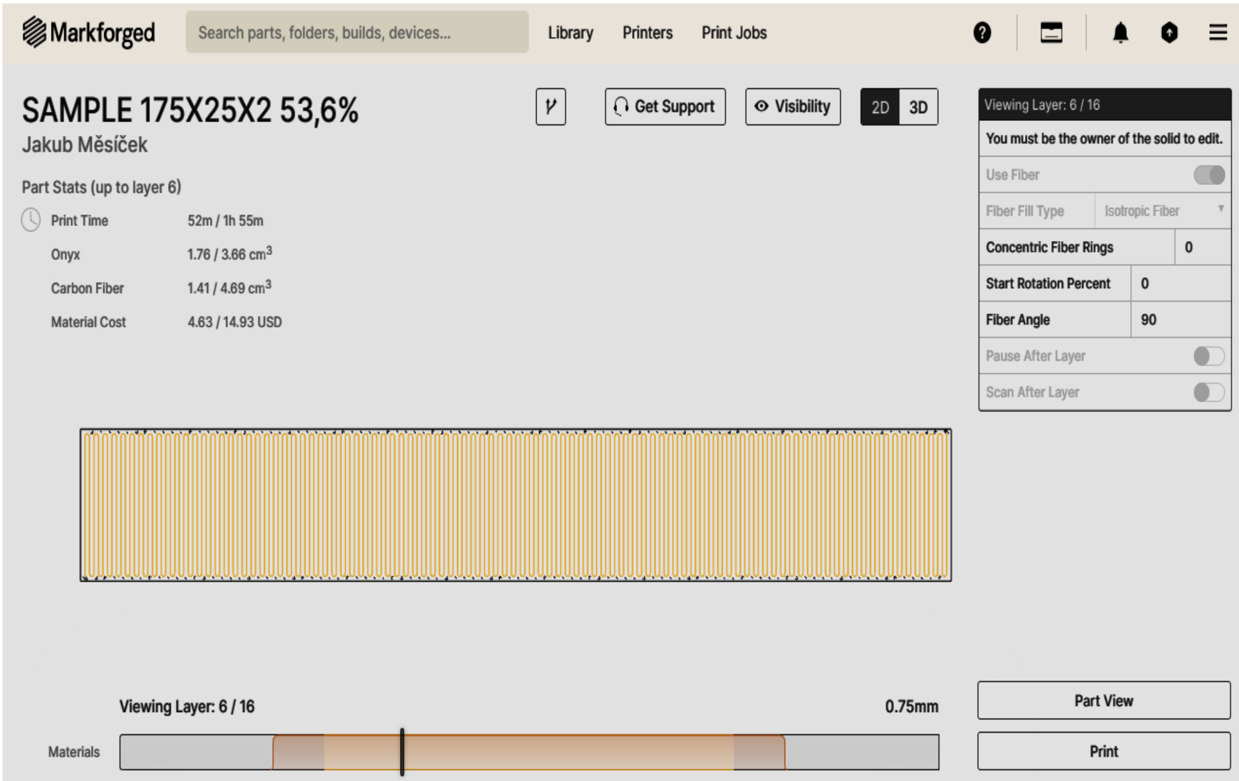

Appendix 10 Transverse Loading – 64.2% VF

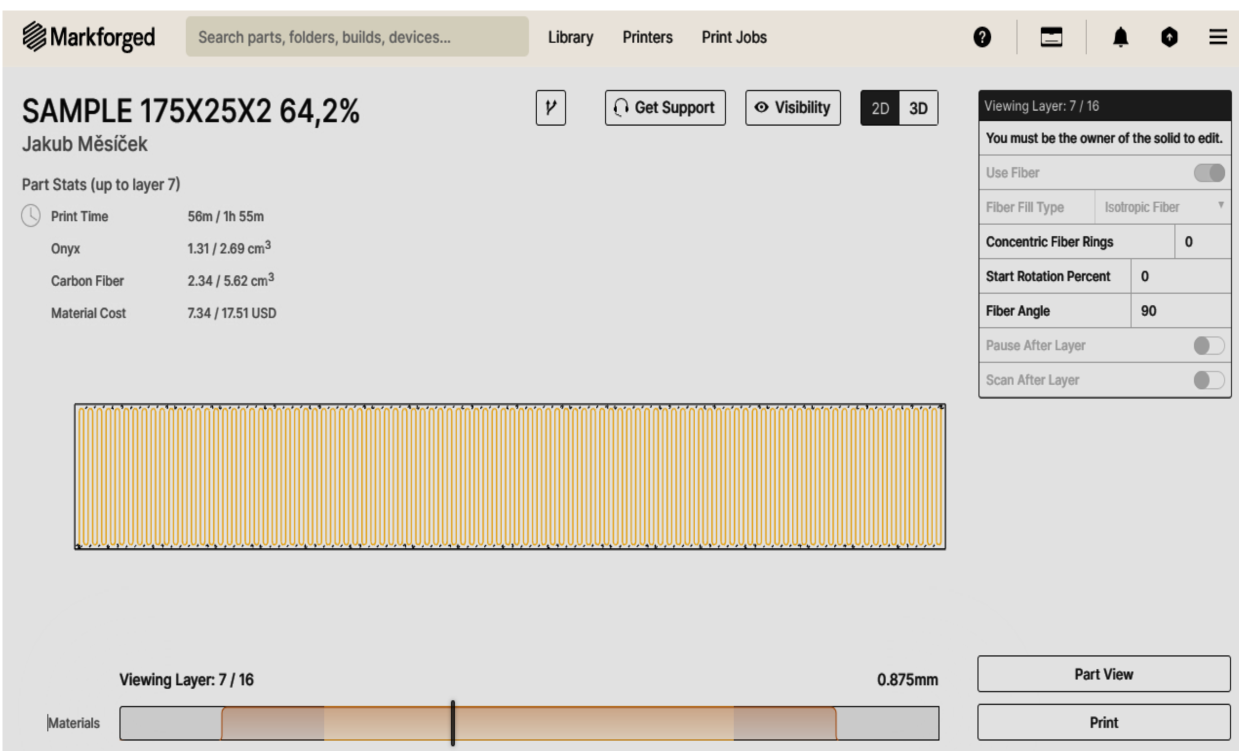

Appendix 11 Shear Testing Specimen with 2 concentric fill of carbon fiber filament

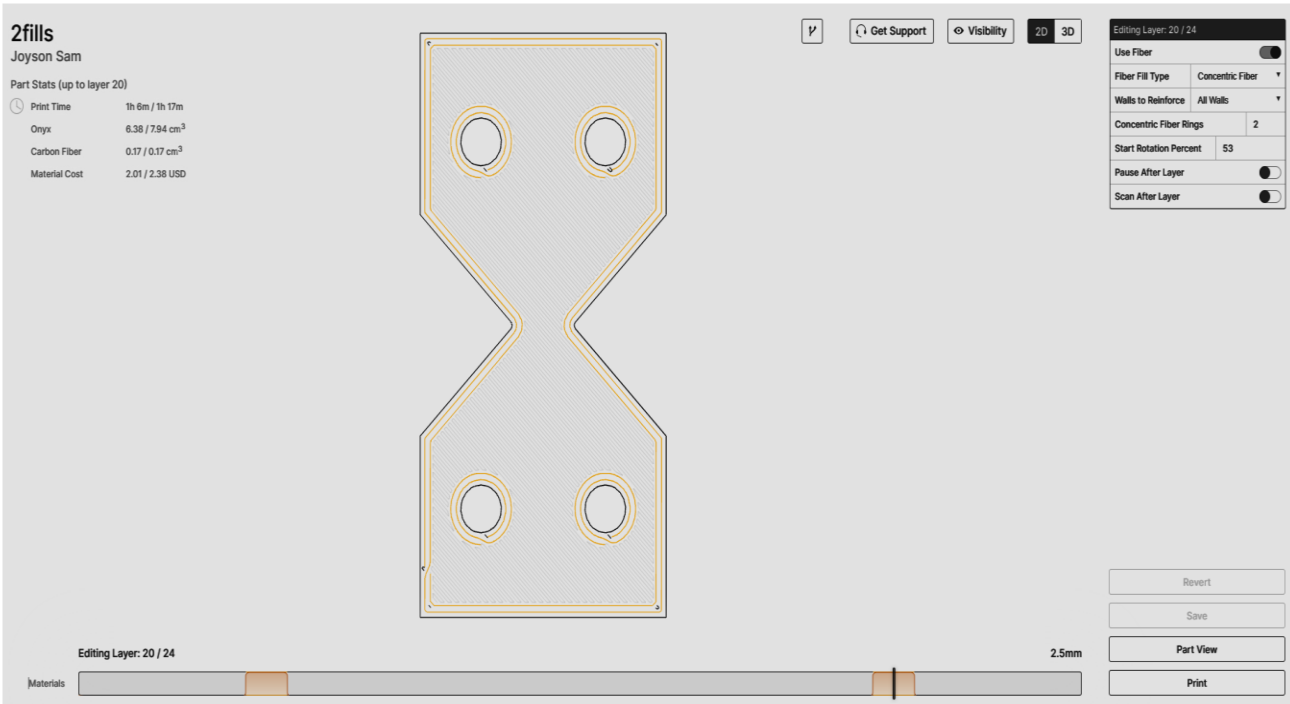

Appendix 12 Experimental Combined loading – XY shear strain